‘QUANTITATIVE ANALYSIS OF THE EFFECT OF LEFLUNOMIDE ON NEURAL CREST CELL GENE REGULATION DURING EARLY EMBRYONIC DEVELOPMENT’

CHRISTOPHER T. FORD BSc (Honours)

SUPERVISOR: DR GRANT WHEELER

A THESIS SUBMITTED FOR THE DEGREE OF

MASTER OF SCIENCE

BY RESEARCH

TO THE UNIVERSITY OF EAST ANGLIA

SCHOOL OF BIOLOGICAL SCIENCES

NORWICH

JULY 2014

WORD COUNT: 25,848

This thesis is dedicated to my parents Paula-Anne and Thomas Ford and to my sisters Louisa-Anne and Ellie-Anne.

And to my first child and my girlfriend Kristin Kreuzer

To be a scientist is merely to seek an answer to a question in which the truth remains elusive. To be a philosopher is having the confidence to venture a thought or idea where no one else has or cares too.

We are all students of life, for life.

Dr Simon B Brown, Edinburgh, 2006

Table of Contents

List of tables

Section 4

Section 5

Section 7

List of Figures

Section 2

Section 5

Acknowledgements

First and foremost, I would like to thank Dr Grant Wheeler for giving me the opportunity to undertake my Master's by Research under his unconditional support and guidance throughout my time within his group. Grant has given me a great deal of encouragement and responsibility and I only hope I have done him proud. I also extend my gratitudes to Professor Andrea Münsterberg, Professor Ian Clark and Dr Victoria Hatch for their unwavering support, generous guidance and invaluable knowledge throughout the duration of my degree.

I am indebted to Kristin Kreuzer as without her support and generosity I would have been unable to undertake my research degree. Grant has also helped where possible by covering the expense of my bench fee and associated costs and in doing so did not financially benefit. Grant also supported my applications to charities for travel and accommodation bursaries in order to attend conferences and meetings. Support for travel and accommodation was provided by Dr Grant Wheeler, the British Society for Developmental Biology (BSDB), the British Society for Cell Biology (BSCB) and the University of East Anglia's School of Biological Sciences.

I am thankful to Dr Rosemary Davidson (School of Biological Sciences, University of East Anglia) for her technical support and expert knowledge. I extend my gratitude's to Dr Alison Davis and her team (Primer Design Ltd, Southampton, UK) for providing excellent support and for awarding me PrimerDesign Silver Student Sponsorship. I would also like to thank Dr Simon Moxon (The Genome Analysis Centre, Norwich Research Park) for providing bioinformatics assistance when accessing the *Xenopus laevis* genome browser to obtain annotated sequence information vital for obtaining real-time PCR primers.

My gratitude's are extended to the University of East Anglia's School of Biological Sciences and the Bio-medical Research Centre for providing an ideal environment to enable me to fulfill my potential.

Lastly, I would like to express my thanks to my friends and family for their never faltering support and encouragement in all that I have accomplished and will go on to achieve. I also thank all my previous supervisors that have helped me to reach this stage in my career as without their support this would not have been possible.

Many thanks.

Disclaimer:
The British Biotechnology and Biological Sciences Research Council (BBSRC) funded work in this thesis under reference BB/I022252/1 to Dr Grant Wheeler, University of East Anglia.

Declaration

I declare that the content of this project is my own work and has not been previously submitted for any other assessment. The report is written in my own words and conforms to the University of East Anglia's Policy on plagiarism and academic dishonesty. Unless otherwise indicated, I have consulted all of the reference cited in this report.

Current Date

31st July 2014

Signature

Christopher T. Ford BSc (Hons)

List of Abbreviations

AFF1: AF4/FMR2 family, member 1

AP: Anterior-posterior

BCIP: 5-Bromo-4-chloro-3-indolyl phosphate

BMP: Bone morphogenic protein

BSA: Bovine serum albumin

cDNA: complementary DNA

Cdk9: Cyclin dependent kinase

Chorulon: Human chorionic gonadotrophin

DEPC: Diethylpyrocarbonate

DSIF: 5,6-Dichloro-1-β-D-ribofuranosylbenzimidazole sensitivity inducing factor

EDTA: Ethylenediamine tetraacetate

ELL: Eleven-nineteen lysine-rich leukemia

FGF: Fibroblast growth factor

GSK3β: Glycogen synthase kinase 3

HEXIM: Hexamethylene bisacetamide inducible

Hsp: Heat shock protein

MAB: Maleic acid buffer

Med26: Mediator 26

MML: Mixed lineage leukemia

MMR: Marc's modified ringer's

NBT: Nitroblue tetrazolium

NC: Neural crest

GS: Goat serum

OD: Optimal density

PCR: Polymerase chain reaction

PolII: Polymerase II

PMSG: Pregnant mare serum gonadotrophin

P-TEFb: Positive transcriptional elongation factor b complex

RNA: Ribonucleic acid

Real-time PCR: Real-time polymerase chain reaction

SEC: Super elongation complex

Ser2: Serine 2

Ser5: Serine 5

St: Stage

TFIIS: Transcription factor II S

TTF: Transcription termination factor

UV: Ultraviolet

WT: Wild type

1. Abstract

The neural crest is a transient population of cells that arises at the border between the neural and non-neural ectoderm. These cells are induced, undergo an epithelial-to-mesenchymal transition, and then migrate along stereotypical pathways to form an array of derivatives such as pigment cells, cranio-facial cartilage and sensory neurons. Neural crest cells have long been studied and much about these cells and their interactions is still not fully understood. The small molecule compound leflunomide inhibits neural crest development. Leflunomide's mode of action is to inhibit pyrimidine biosynthesis, thereby, preventing RNA transcription. Neural crest genes are actively transcribed and like many embryonic stem cells and tumour cells genes undergo an increased level of transcriptional pausing and subsequent elongation making a number of these genes sensitive to leflunomide. It was unclear at what stage of neural crest development leflunomide was acting.

Here, I initially developed a quantitative approach using real-time PCR to measure gene expression in *Xenopus*. Secondly, using real-time PCR I have shown that neural plate border genes are not affected by leflunomide. Thirdly, the neural crest specification genes are affected and the pan neural plate marker Sox2 is not affected by leflunomide. I have confirmed by quantitative real-time PCR that the expression of genes involved in neural crest specification the proto-oncogene cMyc and cMyc responsive genes are affected. cMyc is implicated in embryonic stem cell transcriptional elongation and is well characterised to play an important role in neural crest specification.

1.1 Key words: Neural crest cells, multipotent, leflunomide, transcriptional elongation, cMyc, Sox 10

2. Introduction

2.1. *Xenopus*

2.1.1. *Xenopus* as an animal model to study development

There are more than 20 species of African clawed toed frog. Two species namely, *Xenopus laevis* (*X. laevis*) and *Xenopus tropicalis* (*X. tropicalis*) are widely used in research laboratories as vertebrate animal models for studying early development i.e. cleavage, gastrulation, neurulation and organogenesis. *Xenopus* are a favourable developmental model for scientific use as they can lay hundreds of eggs at once, which will develop synchronously to allow for experiments to be planned and synchronised accordingly (Harland and Grainger, 2011). *X. laevis* eggs are 1.2 - 1.4 mm in diameter and are large enough to be easily manipulated. These embryos are resilient to harsh environments and can withstand microinjection into targeted blastomeres. *X. tropicalis* embryos are more widely used for genetic studies. *X. tropicalis* has had its diploid genome sequenced and annotated, unlike the *X. laevis pseudo*-tetraploid genome that is poorly annotated and is incomplete (Schmitt *et al.*, 2014).

2.1.2. Overview of *Xenopus* development

The *Xenopus* life cycle (figure 2.1) is divided into basic developmental stages using the Nieuwkoop and Faber fate map as a standard example of *Xenopus* developmental stages (Nieuwkoop and Faber, 1967; Schmitt *et al.*, 2014). *Xenopus* embryos at stage 1 where fertilisation has taken place will form the zygote. The zygote is partitioned into two regions, the animal pole, which is pigmented, and the vegetal pole that appears opaque (Wolpert and Tickle, 2010). Sperm enters the unfertilised egg, the oocyte, in the region of the animal pole. The zygote undergoes

cleavage at two hours after fertilisation resulting in two blastomeres of equal size. Cell divisions occur after the first cleavage event every 30 minutes until the embryo reaches the blastula stage at which point many thousands of cells make up the embryo. Embryos at this stage contain a fluid filled cavity named the blastocoel (Wolpert and Tickle, 2010).

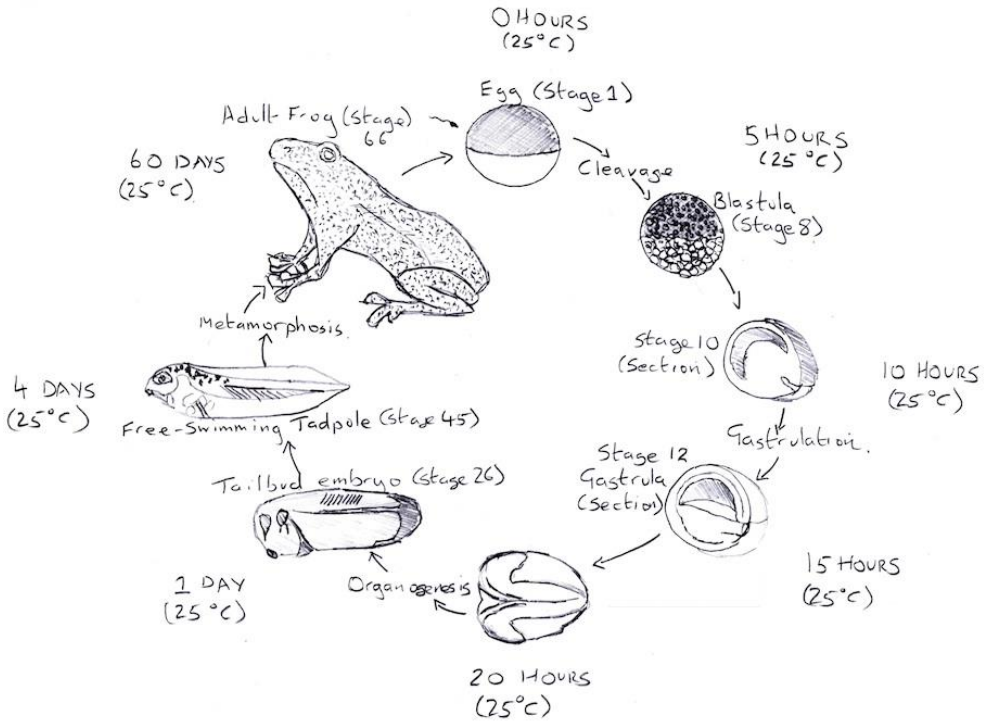

Figure 2.1: The *Xenopus* life cycle
The embryos are staged according to the Niewkoop and Faber fate map (Niewkoop and Faber, 1967). The stages that the *Xenopus* embryo will go through are blastula, gastrula, neurula, tailbud and tadpole developmental stages. The tadpole undergoes metamorphosis into the adult froglet. The timing of *Xenopus* development is temperature dependent.

Once the embryos have matured having reached the blastula stage they will undergo gastrulation. Gastrulation involves the reorganisation of the mesoderm, endoderm and ectoderm classed as the three germ layers. Initially, the blastopore lip forms on the dorsal side of the embryo at the position of the Spemann organiser. The Spemann organiser is needed for dorsal ventral patterning of the embryo. Then the mesoderm and endoderm begin to involute in at the blastopore and the ectoderm will cover the surface of the embryo by a movement

known as epiboly (Wolpert and Tickle, 2010). Post gastrulation the embryos undergo neurulation to form neurula stage embryos (figure 2.2).

2.2. Neural crest development

2.2.1 Overview of neurulation

During neurulation the neural plate rises and folds along the dorsal midline to form the neural tube (figure 2.2). The neural crest cells begin to arise at the border of the ectoderm and the neuroectoderm. Post neurulation the neural tube closes and the neural crest cells undergo an epithelial to mesenchymal transition (EMT) and they migrate away from the neuroepithelium in a rostral to caudal progression to specify a variety of cell lineages. The embryo will undergo a drastic change in body shape as it undergoes convergent extension movements to elongate into a tailbud stage embryo. During convergent extension organogenesis occurs and the embryo will develop its notochord, neural tube and somites that are precursors of muscle (Wolpert and Tickle, 2010). Development continues as the tadpole constructs its facial features such as the eye, ear, mouth and branchial arches. The latter stages of development include construction of the heart to pump oxygenated blood around the body and other vital organs essential for life (Wolpert and Tickle, 2010).

Induction and specification of neural crest cells arises during gastrulation and continues until organogenesis due to a gene regulatory network bridging between the neural plate, non-neural ectoderm and the paraxial mesoderm (Huang and Saint-Jeannet, 2004; Sauka-Spengler and Bronner-Fraser, 2008a). Neural crest cells during neurulation are found within the neural folds and at the dorsal neural tube (figure 2.2).

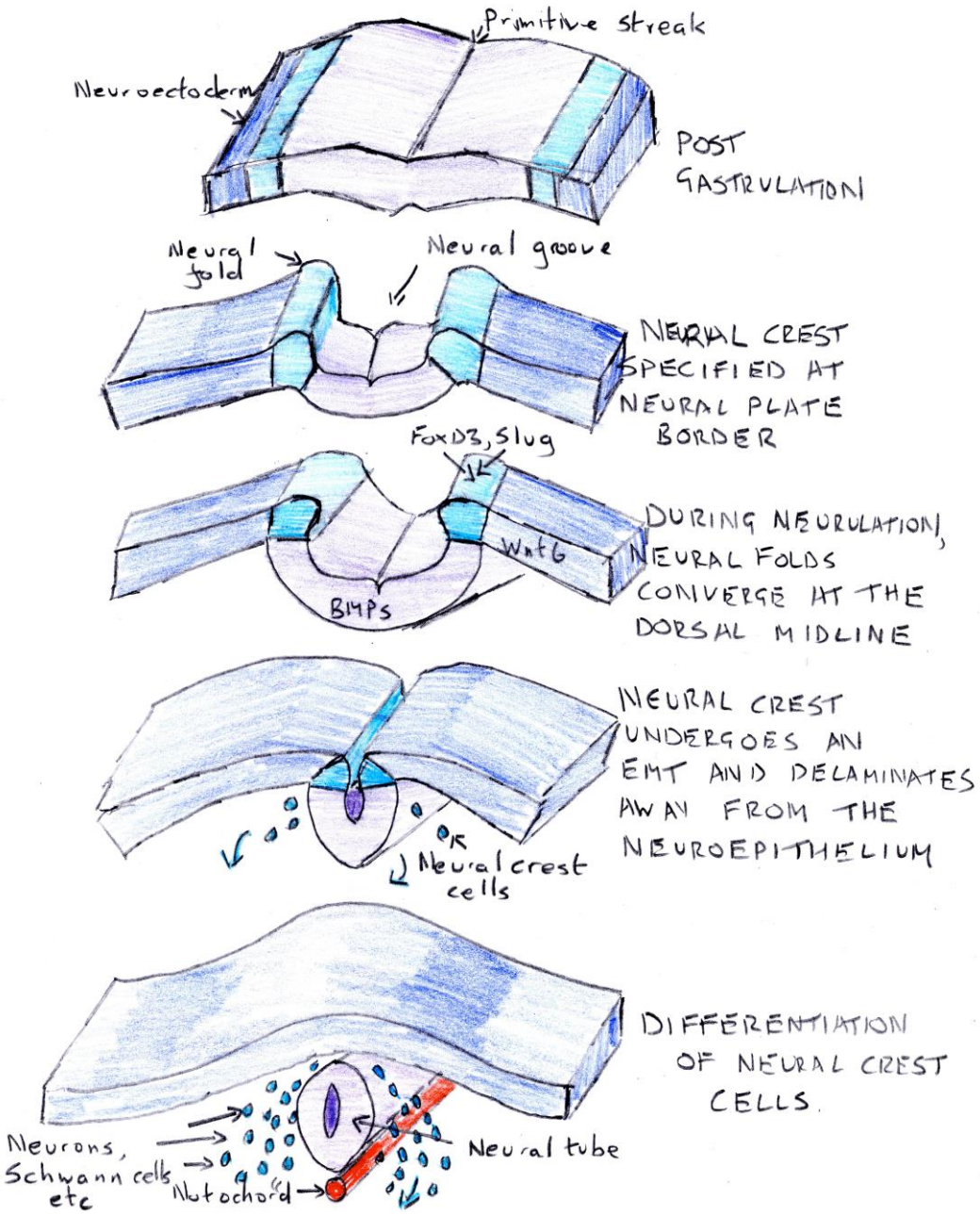

Figure 2.2: Formation of the neural tube by neurulation

The central nervous system arises from a specialised epithelium, the neural plate. This process relies on the inhibition of bone morphogenetic protein (BMP) signalling. Folding of the neural plate to produce the neural groove is initiated by the formation of a distinct hinge point in the ventral region, the floor plate. At the end of neurulation, the lateral edges of the neural plate fuse and segregate from the non-neural epithelium to form a neural tube. The roof plate and floor plate form at the dorsal and ventral midline of the neural tube, respectively. The roof plate becomes a new organising centre that produces BMPs that provides dorsal patterning signals. Neural crest cells derive from the dorsal neural tube and migrate out to form the peripheral nervous system, as well as melanocytes and cartilage in the head. Neural crest cells have been shown to form at an intermediate level of BMP signalling.

The cell-cell adhesion between cells are lost promoting the delamination and migration of neural crest cells that will terminally differentiate when they have stopped migrating once they have moved to their correct temporal and spacial location. Finely tuned gene regulatory networks that receive multiple signals and transcription factors are responsible for neural crest properties such as multipotency, induction, specification, migration and differentiation (Sauka-Spengler and Bronner-Fraser, 2008a).

2.2.2. The Neural Crest

Neural crest cells have been widely studied and continue to be the matter of fundamental advances in areas of developmental biology such as inductive interactions and cell migration over the length of the developing embryo. In the wake of the 21st century studies of neural crest cells have also proven essential in making significant advances in areas such as cancer research, regenerative medicine (including stem cells and their use in tissue engineering), and constructing gene regulatory networks to aid our understanding of the genes that govern neural crest cell development (Sieber-Blum *et al.*, 2006; Song *et al.*, 2008; Zito *et al.*, 2008).

Neural crest cells are highly migratory and form many divergent derivatives including neurons and glia of the sensory, sympathetic, and enteric systems, melanocytes, and the bones, cartilage, and connective tissues of the face (Anderson, 1993; Baker and Bronner-Fraser, 1997; Hall, 1999; Unsicker, 1993). In addition to this neural crest will contribute to C-cells (parafollicular cells) of the thyroid gland and endocrine cells like the chromaffin cells of the adrenal medulla (Le Douarin and Teillet, 1974; Polak *et al.*, 1974). The initiation of neural crest cells is strongly associated to the development of the “new head” (Gans and Northcutt, 1983; Kuratani, 2008). Underlying neural crest

formation is the gene regulatory network that evolved during the early Cambrian period up until the beginning of the vertebrate lineage (Meulemans and Bronner-Fraser, 2005; Sauka-Spengler and Bronner-Fraser, 2006, 2008b; Sauka-Spengler *et al.*, 2007).

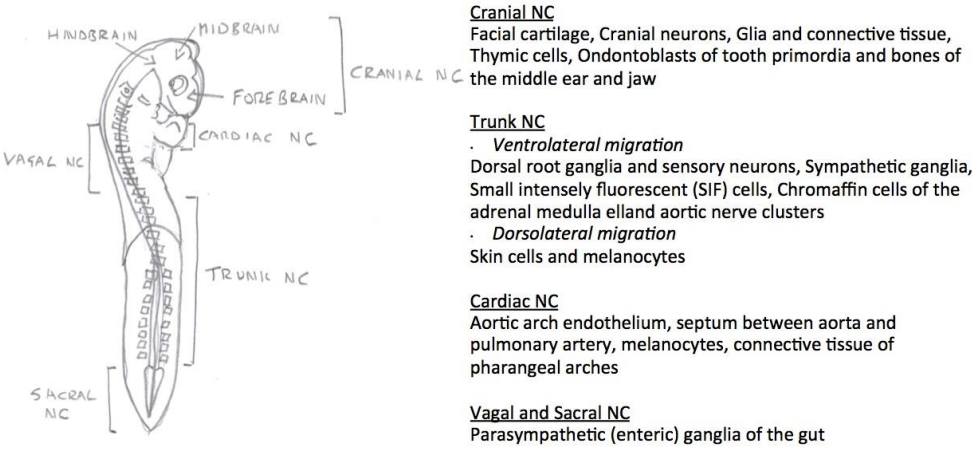

Figure 2.3: Neural crest cell populations in the developing chick embryo

We can divide neural crest cells into subpopulations characterised by their origin and the locations to which they migrate. These neural crest populations can be classed as cranial, trunk, cardiac and vagal neural crest (figure 2.3). Cranial neural crest arises from the presumptive brain and will form cranio-facial cartilage and will contribute connective tissue and nerves that innervate the skull. Cranial neural crest gives rise to bone and cartilage contributing to the skeleton of animals (Cano *et al.*, 2000; Cebra-Thomas *et al.*, 2007; Clark *et al.*, 2001; Freitas *et al.*, 2006; Graveson *et al.*, 1997; Lumsden, 1988; Sanchez-Martin *et al.*, 2002; Smith *et al.*, 1994).

The vagal neural crest cells that come from the neck area of an embryo will migrate to inhabit the intestine. Here, they will give rise to ganglia of the enteric nervous system (ENS). These neural crest derived ganglia create radially symmetrical contraction and relaxation of the gut that propagates a wave in an ante-retrograde fashion to control intestinal peristalsis. If these ganglia fail to innervate the intestine this can cause

megacolon disease referred to as Hirschsprung's disease (Heanue and Pachnis, 2007).

Vagal neural crest have only recently been identified to give rise to cardiac neural crest. Vagal neural crest contributes to musculoconnective tissue of blood vessels and the septum, which is a physical structure that partitions the left side of the heart from the right side to create an outflow of blood into the aorta and pulmonary artery to delivery oxygen-saturated blood to the body and oxygen-depleted blood to the lungs, respectively (Jiang *et al.*, 2002; Le Lievre and Le Douarin, 1975).

2.2.3. The neural plate border and neural crest induction

A series of inductive interactions between border cells and the neural plate, epidermis and underlying mesoderm gradually partition the border region into two spatially and molecularly distinct regions with neural crest forming immediately next to the neural plate and the pre-placodal region. Neural crest progenitors begin to be induced at the neural plate border region earlier than the pre-placodal region, although induction of both populations overlaps temporally (Pegoraro and Monsoro-Burq, 2013). Genes such as Msx1/2 and FoxD3 will localise with Pax3 or Pax7 to the developing neural folds where nascent neural crest cells will form, marked by the expression of Snail and SoxE family genes (Milet and Monsoro-Burq, 2012). At the neural fold stage, neural crest markers and the pre-placodal region are distinct, with neural crest markers expressed in the neural folds and pre-placodal genes expressed more laterally in the ectoderm (Groves and Labonne, 2014). Evidence suggests that mutually repressive interactions occur between transcription factors of the neural crest and placode lineages, just as earlier interactions mark out the boundary between neural and non-neural ectoderm (Groves and Labonne, 2014). To demonstrate this,

Six1 is a pre-placodal gene that is able to repress the neural crest transcription factors Msx1 and FoxD3, whereas Pax7 and Msx1 can repress Six1 (Sato *et al.*, 2010). The tissue interactions that promote neural crest formation are well characterised. Neural crest cells emigrate from the junction of the neural folds with the adjacent ectoderm. It has been proposed that these tissues interact to give rise to neural crest through early signals from the mesoderm and cells derived from the ectoderm that may function to strengthen and maintain a neural crest precursor state.

It has long been reported that gene regulatory networks govern neural crest cell properties such as multipotency, induction, specification, migration and differentiation (Sauka-Spengler and Bronner-Fraser, 2008a). There are three signalling pathways required for neural crest induction, namely, Wnt, fibroblast growth factor (FGF) and bone morphogenic protein (BMP) signalling. The accepted model for neural crest cells arising at the neural plate border in *Zebrafish* and *Xenopus* proposes that BMP4 and BMP7 set up a dorso-ventral gradient that is tightly controlled by the BMP antagonists Noggin, Chordin and Follistatin. These BMP antagonists that are expressed in the underlying dorsal paraxial mesoderm inhibit BMP and therefore initiate neural crest induction; however, more importantly induce neural ectoderm. (Bonstein *et al.*, 1998; Marchant *et al.*, 1998). But, BMP signalling alone without Wnt signalling is not enough to induce neural crest. BMP and Wnt signalling must act in synergy for neural crest induction (LaBonne and Bronner-Fraser, 1998; Mayor *et al.*, 1997).

FGF2 and FGF8 are FGFs that are secreted from the paraxial mesoderm and have been shown to play a crucial role in neural crest cell induction (Monsoro-Burq *et al.*, 2003). Upstream of BMP signalling is the Notch pathway that enhances neural crest development at the lateral border of the neural plate. Notch or Hairy2, which is downstream of the Notch

pathway if overexpressed, has been shown to result in the expansion of neural crest at the neural plate border (Endo *et al.*, 2002; Glavic A Fau - Silva *et al.*). BMP activation is required for the maintenance of neural crest cells that are developing through neurulation (figure 2.4).

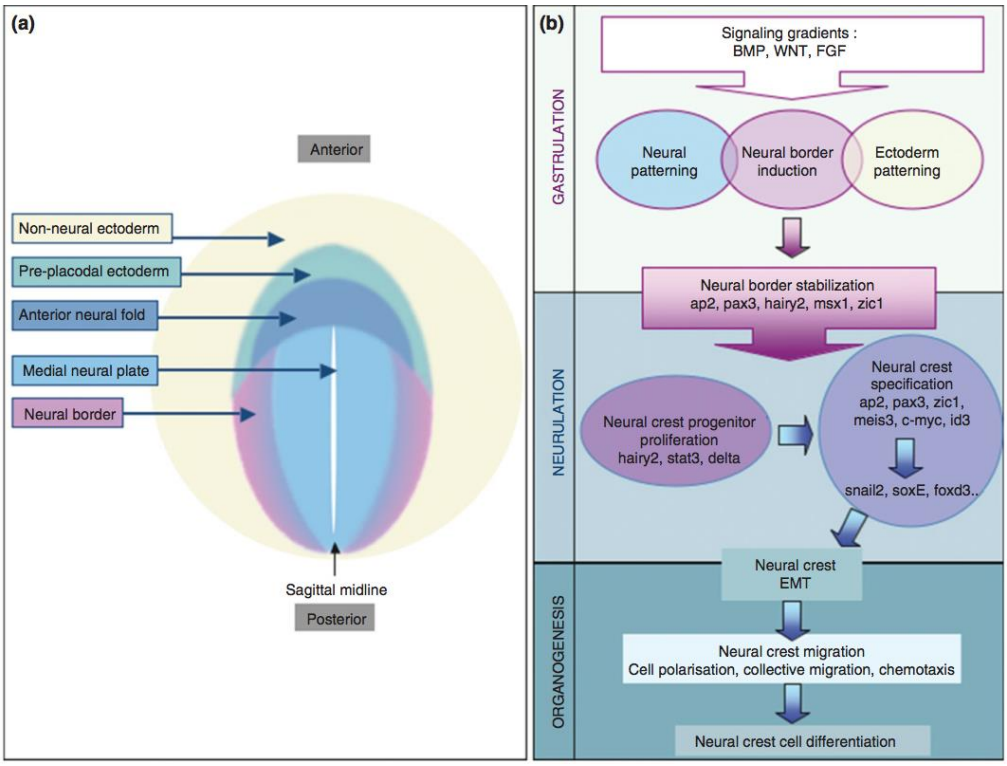

Figure 2.4: Signalling and patterning to define the neural crest (a) Annotation of ectoderm regionalisation at the end of gastrulation. (b) Signals and transcription factors implicated in neural border induction (during gastrulation), neural border stabilisation (end of gastrulation, early neurulation); neural crest proliferation and specification (neurulation) in *Xenopus*. Taken from Monsoro-Burq *et al.*, 2012.

BMP4 from the neural plate border and Wnt signalling arising from the mesoderm next to the neural crest region are essential for maintaining the neural crest (Steventon *et al.*, 2009). The Zic transcription factors, Zic1 and Zic3 and the Pax transcription factors, Pax3 and Pax7 are required for neural crest induction as they specify the neural plate border (Groves and Labonne, 2014). Pax3 (*Xenopus*) and Pax7 (Chick) are expressed shortly after gastrulation at the future neural plate border. (Groves and Labonne, 2014) Both Zic1/3 and Pax 3/7 are up regulated at the border of the neural plate by the loss of BMP signalling.

These transcription factors are referred to as neural plate border specifiers. Neural plate border specifiers increase the expression of FoxD3 and Slug/Snail2 by selectively enhancing Wnt, BMP and FGF pathways that actively regulate their expression (figure 2.4) (Meulemans and Bronner-Fraser, 2004).

In summary, pre-neural ectoderm develops under the guidance of FGFs and the suppression of BMP and Wnt signalling, while non-neural genes are regulated by Wnt and BMP signals. As neural tissue starts to form in response to FGFs and the suppression of Wnt and BMP signalling, neural crest progenitors become specified under the control of FGF and Wnt signals and suppression of BMP signals. At the same time, pre-placodal tissue becomes discernible from non-neural ectoderm under the influence of FGFs and the suppression of both Wnt and BMP signals. Finally, as neurulation starts, Wnts and BMPs expressed at the edge of the neural plate stabilise and maintain a neural crest cell fate, whilst signals along the anterior-posterior (AP) axis induce formation of specific placodes (figure 2.5).

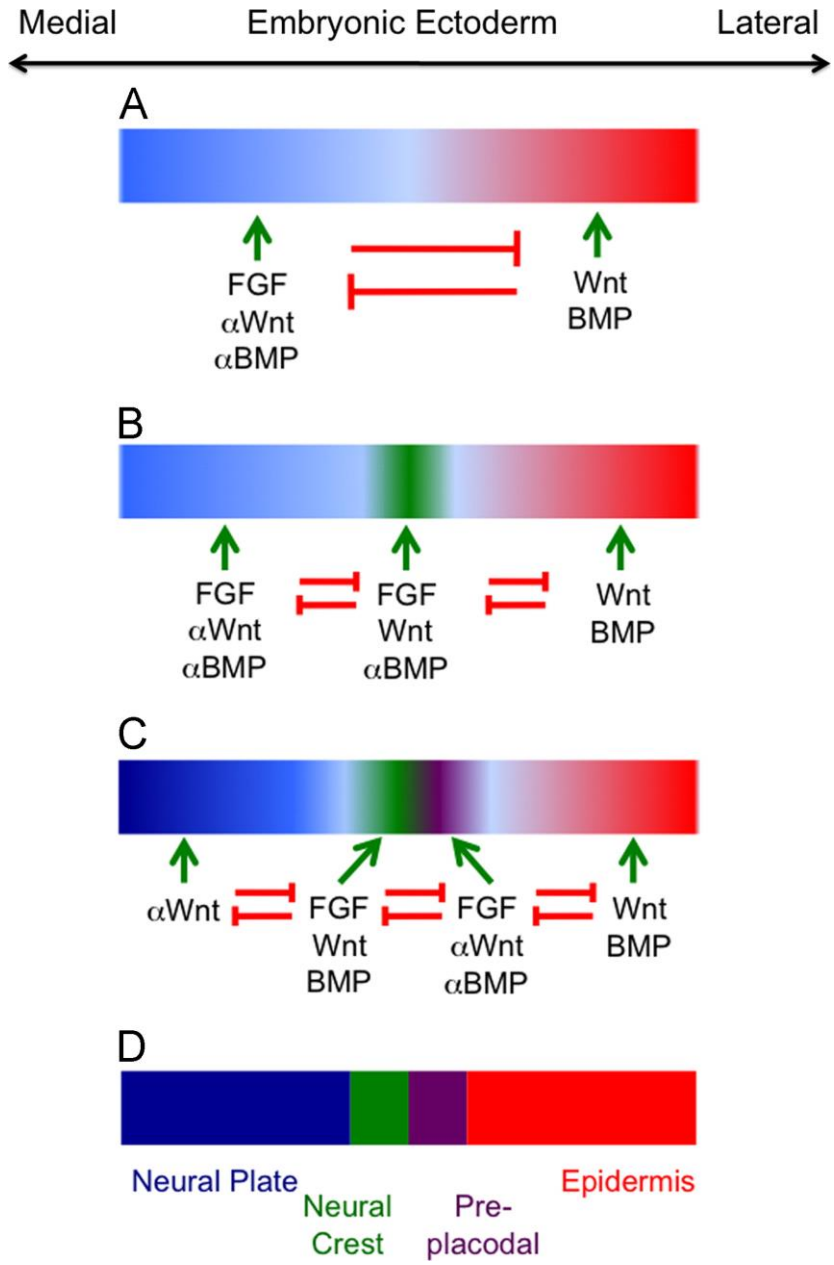

Figure 2.5: A graphical summary of the signals received by embryonic ectoderm during the establishment of the neural plate, neural crest, pre-placodal region and epidermis

(A) Pre-Gastrula. Wnt and BMP signals in the ectoderm initiate differentiation of non-neural ectoderm, while these signals are counteracted by FGFs and BMP and Wnt inhibitors from the organiser or hypoblast. (B) Early Gastrula. Wnt and FGF signals start to induce the first neural crest genes; BMP signaling is not required for this step and may be actively inhibited. (C) Late Gastrula. Pre-placodal genes begin to be induced by FGFs and by an attenuation of Wnt and BMP signals. Wnts and BMPs begin to be expressed at the edge of the neural plate and continueto induce neural crest tissue. (D) Early Neurula. The final resolution of the border region into four distinct regions. Retrieved from Groves and Labonne, 2014.

2.2.4. Neural crest specification through early and late neural crest specifiers

Neural crest cells are specified by well characterised factors including Snail1, Slug/Snail2, Sox9, Sox10, AP2, FoxD3, Twist, Id3 and cMyc (Sauka-Spengler and Bronner-Fraser, 2008a). Neural crest specifiers act cooperatively to regulate their expression (Sauka-Spengler and Bronner-Fraser, 2008a). Slug and FoxD3 expression is controlled by FGF8 from the paraxial mesoderm where it is regulated itself by Msx1. In addition to this, Zic1 and Pax3 expression is essential for Slug and FoxD3 expression via Wnt canonical signalling (Monsoro-Burq *et al.*, 2005; Sato *et al.*, 2005). Wnt-dependent Pax3 regulation is responsible for Sox10 expression which is able to create a positive feedback loop to maintain its own regulation (Honore *et al.*, 2003). The action of Wnt signalling may be important to activate Gbx2 expression, which is the earliest transcription factor for neural crest specification upstream of Pax3 and Msx1. Gbx2 expression is required to posteriorise the neural folds showing that this transcription factor is extremely important for specifying the neural crest (Li *et al.*, 2009).

Genes involved in neural crest specification can be segregated into two sets, i.e. early and late neural crest specifiers, respectively. Early neural crest specifiers are expressed at the neural plate border and they have been characterised as Snail, cMyc and Id3. Late neural crest specifiers are expressed in pre-migratory neural crest and their expression is sustained during migration and they have been characterised as FoxD3, Slug and Sox10. Sox10 belongs to the SoxE super family of genes characterised by a homologous sequence called the high mobility group (HMG-box) (Sauka-Spengler *et al.*, 2007). This HMG box is a DNA binding domain that is highly conserved throughout eukaryotic species. Maintenance of neural crest cell pluripotency and proliferation may be controlled by neural crest speciers cMyc and Id3 to control the cell cycle.

These transcription factors may regulate apoptosis and proliferation when the fate of some neural crest cells is determined (Bellmeyer *et al.*, 2003; Kee and Bronner-Fraser, 2005; Light *et al.*, 2005). Loss of function experiments have shown that losing either cMyc or Id3 that is downstream of cMyc will result in a complete loss of neural crest progenitors. In contrast, if Id3 is overexpressed neural crest cells retain their pluripotent potential and therefore it can be suggested that Id3 is a regulator of cell cycle control to make a decision whether the neural crest cell will proliferate or follow apoptosis (Bellmeyer *et al.*, 2003; Hong *et al.*, 2008; Kee and Bronner-Fraser, 2005; Light *et al.*, 2005). PhB1 is located downstream of cMyc and promotes the expression of Slug/Snail2, Twist and FoxD3 through the reversible repression of E2F1 (Schneider *et al.*, 2010).

2.2.5. The EMT process and migration in neural crest cell development

The neural crest is a textbook example of a cell population that undergoes an epithelial to mesenchymal transition (EMT). Epithelial cells present in the dorsal neural tube undergo reprogramming to transform into a migratory mesenchymal cell population (Nieuwkoop and Faber, 1967; Untergasser *et al.*, 2012). As mentioned previously neural crest cells that arise at the neural plate border and non-neural ectoderm receive signals from both these tissues to activate signalling pathways to specify neural crest (Chavali *et al.*, 2005; Meulemans and Bronner-Fraser, 2004; Thiery and Sleeman, 2006). Cells arising at the neural crest border form the dorsal neural folds and expression of neural crest specifier genes such Sox10, Slug/Snail2, Snail and FoxD3 allow a small number of these cells to become pre-migratory neural crest cells (Meulemans and Bronner-Fraser, 2004; Sauka-Spengler and Bronner-Fraser, 2006). It is these pre-migratory neural crest cells that undergo an epithelial to mesenchymal transition allowing them to migrate away from the neural folds to different regions of the embryo

where they then terminally differentiate into the various cell types already mentioned.

In metazoans, epithelial and mesenchymal cells are the dominant cell types when contributing to the organisation of the various animal body plans, which differ in morphology and function. Epithelial cells display phenotypically characteristic apico-basal arrays, organised cytoskeletons, and attachment to surrounding cells through adhesion junctions allowing them to create uniform layers. In contrast, mesenchymal cells are not polar and do not form intercellular junctions and are generally more migratory.

Mesenchymal cells are able to move throughout the extracellular matrix by secreting matrix metalloproteases (MMPs) (Thiery and Sleeman, 2006). Interestingly, cells displaying either epithelial or mesenchymal cell phenotypes can switch between the two, respectively, during early stage embryonic development. Neural crest cells are able to regulate MMP activity through the release of tissue inhibitors of MMPs (TIMPs) (Chang and Werb, 2001). MMP2 has been implicated in the migration of cardiac neural crest cells and metaloprotease-10 (ADAM10) has been reported to be involved in the development of the cornea (Altschul *et al.*, 1990; Cai *et al.*, 2000). Morpholino knockdown of MMP2 expression in the dorsal neural tube perturbs the neural crest cell EMT (Duong and Erickson 2004). Expression of MMP14 has been found to be important for migrating trunk and cranial neural crest (Harrison *et al.*, 2005). Interestingly, ADAM13 expressed in *Xenopus* is crucial for neural crest cells to detach from the neuroepithelium to undergo migration (Tomlinson *et al.*, 2009).

Levayer & Lecuit (Mayor and Theveneau, 2013) have defined events important for EMT:
1) specification of a sub-population of cells fated to undergo EMT

2) loss of intercellular adhesion mediated by cadherins at adherens junctions
3) loss of polarity markers
4) cytoskeletal reorganisation to drive cell delamination (this is an active process)
5) degradation of the basement membrane.

However, the steps outlined may not occur chronologically and are not all needed to determine if EMT has occurred (Mayor and Theveneau, 2013). It should be considered that while there are many signalling cascades such as Wnt, FGF and BMP there are many molecules involved in neural crest formation and migration.

2.2.6. Differentiation of neural crest cells

Neural crest cells terminally differentiate due to specific groups of neural crest specification transcription factors that regulate specific effector genes, which give the cell its fully differentiated characteristics and properties (figure 2.6). It is widely accepted that neural crest cell differentiation is temporally and spatially regulated. For example, the neural crest specifier Sox10 has an important role in cell differentiation, it will continue to be expressed past neural crest specification in the migrating neural crest cell. Sox10 observed in premigratory neural crest is fated to develop into melanophores and neurons but continues to be expressed in these differentiated cells to upregulate its effector genes. (Sauka-Spengler and Bronner-Fraser, 2008a). To take this example further into melanophores, Sox10 can up-regulate microphtalmia-associated transcription factor (Mitf) which will then regulate the expression of the enzyme dopachrome tautomerase (Dct). Dct is required for melanin synthesis in melanophores (Elworthy *et al.*, 2003; Potterf *et al.*, 2001).

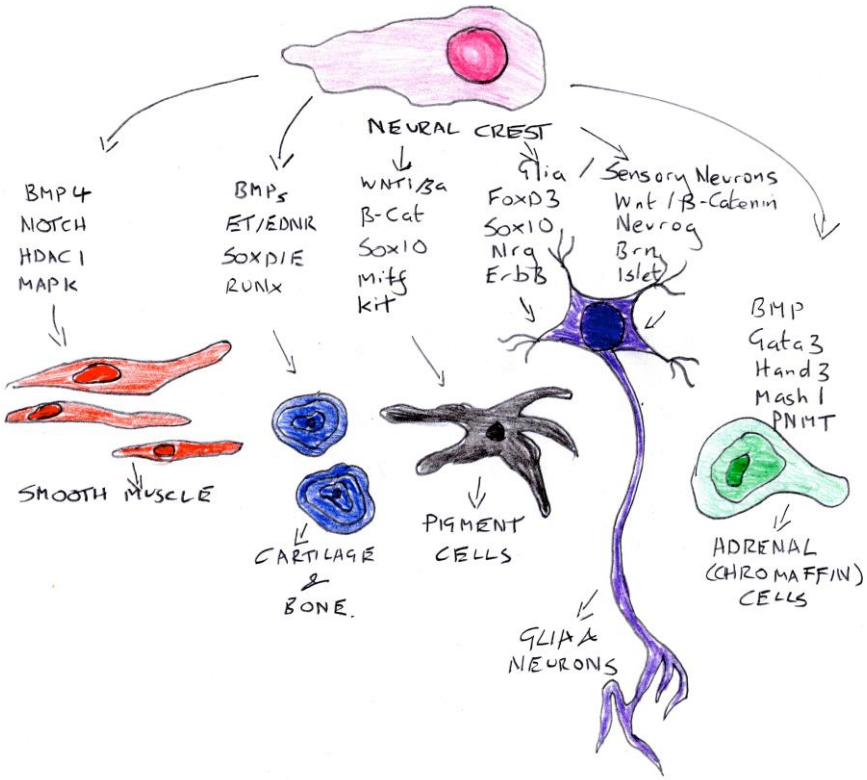

Figure 2.6: Neural crest differentiation
Neural crest cell differentiation is regulated by a network of genes involved in neural crest specification such as Sox10 that promote the expression of effector genes that are able to induce the cells to undergo terminal differentiation. Terminal differentiation of neural crest cells gives rise to a variety of cell types including smooth muscle, cartilage, bone, pigment cells, sensory neurons, glia and adrenal cells. Based on Mayor and Theveneau, 2013.

In contrast, certain transcription factors are absolutely essential for repressing the expression of genes involved in neural crest cell lineages to promote cells going down a different lineage. A good example of this is FoxD3 can repress Mitf in melanophores to cause a lineage switch, resulting in them changing their lineage to give rise to glial cells (Thomas and Erickson, 2009). The differentiation of other cell types is down to comparable temporal and spatial regulation by gene regulatory networks. Neural crest cells during development terminally differentiate and in order to do this specific ligands must be present, for example, in mammals; melanophores must maintain their terminally differentiated state and survive. The cell surface ligands these melanophores express must dimerise with the c-kit receptors and

Endothelin B receptors expressed on the surface of surrounding cells (Tachibana, 2000). Neural crest cell differentiation is a highly regulated process and requires the timely expression of different transcription factors to give rise to various cell lineages.

2.2.7. Melanophores

Neural crest cells can give rise to pigment cells or melanophores in the skin, which function to protect animals from DNA damage caused by high-energy penetrating ultraviolet radiation (Cooper and Raible, 2009). Melanophores make and transfer melanin to neighbouring cells resulting in uniquely identifiable pigmentation patterns. Pigmentation phenotypes in amphibian and fish can change rapidly in response to their environment for protection, by means of mimicry, camouflage or warning colouration or to encourage sexual selection (Cooper and Raible, 2009). Melanogenesis requires Mitf expression that can be identified in melanoblasts during migration from the neural tube (figure 2.7).

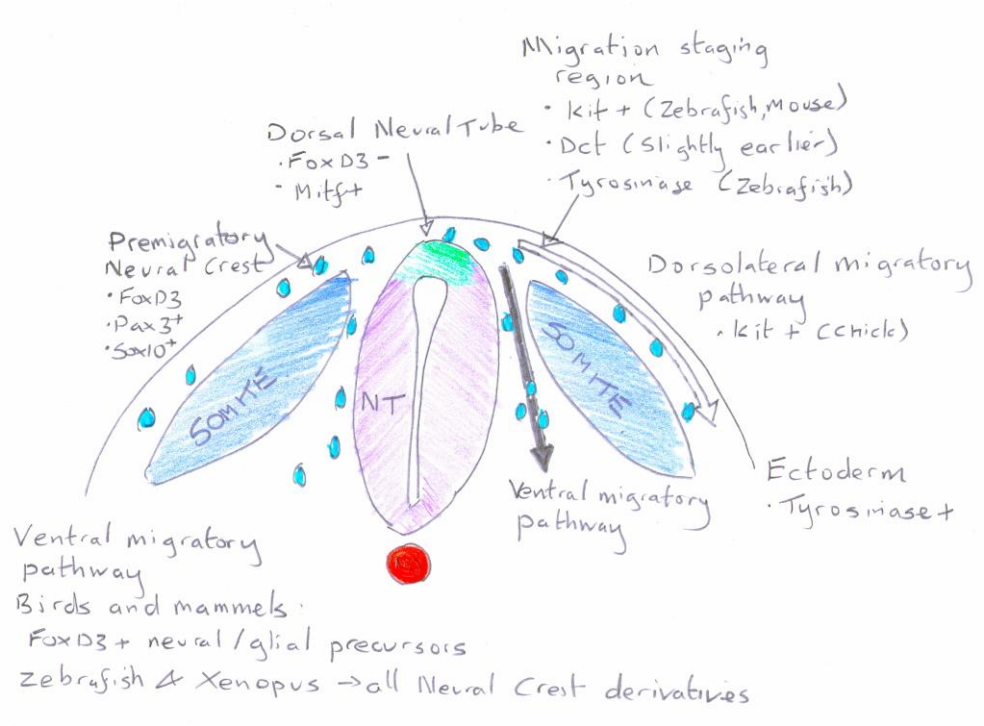

Figure 2.7: Melanophore development
Neural crest cells migrating along ventral (black) and dorsolateral (white) pathways are specified by many transcription factors. Melanophores are formed from neural crests migrating along the dorsolateral pathway and are specified by transcription factors illustrated here. Based on Thomas and Erickson, 2008.

Chick and mouse mutants of Mitf possess defects in their pigmentation or patterning. Mitf has been shown to up regulate tyrosinase and tyrosinase related protein 1 (Tyrp-1) during melanogenesis (Thomas and Erickson, 2008). Wnt3a activation of melanophores increases Mitf expression in the dorsal neural tube during migration of neural crest cells. Another important signal in melanophore development is that of the kit receptor and its ligand KitL. Mutations of either the kit receptor or KitL result in pigmentation defects (Thomas and Erickson, 2008). Heterozygous Kit mutations are the cause of piebaldism in humans. Kit receptor activation by KitL results in signalling cascade activation that phosphorylates Mitf, increasing its transcriptional activity (Thomas and Erickson, 2008).

Endothelin signalling has a role in melanophore development and migration. It is currently thought that Edn-3 signalling interacts with the Kit receptor signal cascade in mammals to promote melanoblast differentiation (Thomas and Erickson, 2008). In chick EdnrB1 has been shown to be expressed in early neural crest (Lecoin *et al.*, 1998). When these differentiate into melanophores this EdnrB1 expression is replaced by EdnrB2 expression. It has also been demonstrated that the Edn3 ligand that binds specifically to EdnrB2 is expressed in the ectoderm at the same stage of pigment cell development (Elworthy *et al.*, 2003; Lecoin *et al.*, 1998). Experiments in chick have shown that knocking down EdnrB2 significantly reduces the number of melanophores present (Shin *et al.*, 1999).

2.2.8. Melanoma and the neural crest

Melanoma is a rare and potentially aggressive type of skin cancer that can metastasise from the skin to other organs in the body. Melanoma arises from the neural crest derived melanophores that are located in the epidermal base layer of the skin. Melanoma can arise in areas of non-sun exposed skin as well as in areas of sun-exposed skin. Melanoma has a low mortality rate if excised when it is slow growing and has not yet penetrated the basal layer of skin. Once the melanoma has penetrated into the dermal layer of the skin it can then invade and metastasise, thereby, significantly increasing the mortality rate (Iyengar and Singh, 2010; Uong and Zon, 2010). The mortality rate for melanoma is very high due to its propensity to metastasise and to chemotherapy resistance. Melanoma is treatable in the early stages, however, once the cancer has metastasised treatment is limited and prognosis is poor. Both genetic and environmental factors are contributing factors to developing melanoma, but individuals who are Caucasian and exposed to the UV radiation from sun exposure are referred to as high-risk candidates for skin cancers. A number of genes implicated in neural crest and melanophore development have been identified in melanoma to be mis-regulated (Uong and Zon, 2010).

The B-raf oncogene gene mutation that encodes B-RAF protein is the most commonly mutated gene that has been identified in melanoma. This mutation makes up for 60 % of all known melanoma gene mutations. A substitution in valine (V) to glutamate (E) at codon 600 (BRAF-V600E) results in a 700 fold increase in BRAF kinase activity, which deregulates activation of the downstream MEK/ERK effectors and drives cell proliferation (Uong and Zon, 2010). p53 loss of function experiments in *Zebrafish* expressing the BRAF-V600E mutation using a Mitf promoter give rise to melanomas similar to those identified in patients that present in the clinic (Patton *et al.*, 2005). The BRAFV600E

mutation, therefore, is linked to the formation of melanoma observed in 60 % of melanoma patients. A number of neural crest cell genes have been identified to play a role in melanoma formation such as Mitf, Slug/Snail2 and Endothelin receptor B (EndrB). Mitf promotes cell cycle progression and tumour survival and growth when overexpressed (Garraway *et al.*, 2005). In early tumour formation knock down of Slug/Snail2 in melanoma cell lines has shown a slower rate of cell migration making this neural crest gene a player in melanoma metastasis (Gupta *et al.*, 2005; Uong and Zon, 2010). Overexpression of EndrB has been identified to lead to increased BRAF activity in melanoma and has been found in a small number of melanoma patients (Uong and Zon, 2010). EndrB may increase endogenous levels of Snail expression resulting in more aggressive tumour penetration deep into the skin until it reaches the stratum basale where it can find a blood supply in order to metastasise (Bagnato *et al.*, 2004). Sox9 and Sox10 are two neural crest specifiers identified in end stage melanoma. Their expression may be used as markers for how aggressive the melanoma is in individual patients (Bakos *et al.*, 2010). Pax3 specifies the neural crest and its expression in melanophores may contribute to melanoma formation in response to environmental stimuli (Medic and Ziman, 2010). In summary, melanoma is a multifactorial disease and compounds that act in synergy to target different pathways may provide better prognosis for patients and reduce chemotherapy resistance.

2.2.9. Neural crest diseases/Neurocristopathies

Failure of neural crest development in humans results in a number of genetic diseases that are known as neurocristopathies. Examples include, but are not limited to: Waardenburg syndrome, Hirschsprung disease, piebaldism, congenital central hypoventilation syndrome, pheochromocytoma, paraganglioma, Merkel cell carcinoma, multiple

endocrine neoplasia, neurofibromatosis type I, CHARGE syndrome (Coloboma of the eye, Heart defects, Atresia of the nasal choanae, Retardation of growth and/or development, Genital and/or urinary abnormalities, and Ear abnormalities and deafness), familial dysautonomia, DiGeorge syndrome, Axenfeld Rieger syndrome, Goldenhar syndrome (hemifacial mi crosomia), craniofrontonasal syndrome, Noonan syndrome, LEOPARD syndrome, cardiofaciocutaneous syndrome and Costello syndrome (congenital melanocytic nevus, melanoma and certain congenital heart defects of the outflow tract) (Mayanil, 2013). Here, I will briefly introduce two neurocristopathies.

Hirshprung's disease is one disease where the major symptom is aganglionic megacolon that results from the loss of neural crest derived enteric neurons. Mutations in the RET gene is known to cause Hirschprung's disease (Badner *et al.*, 1990; Romeo *et al.*, 1994). Waardenburg syndrome (WS) is another example of a neurocristopathy that can be subdivided into four syndromes depending upon a number of symptoms with different levels of severity. All neural crest derived cell types can be affected in Waardenburg syndromes. In all cases of Waardenburg syndrome a loss of skin pigmentation as caused by a loss of melanocytes and often deafness is observed in individuals (Read and Newton, 1997). The least severe Waardenburg syndrome is WS2 as individuals only have defects in pigmentation. WS2 is often linked with mutations in MITF, although Sox10 mutations can cause the same phenotype (Bondurand *et al.*, 2007; Tassabehji *et al.*, 1994). Individuals who have WS1 display a loss of skin pigmentation and dystopia canthorum, which is lateral displacement of inner canthi in the eye giving the physical appearance of a wider nasal bridge. However, those who have WS3 in addition to the phenotypes observed in WS1 also have limb deformities. Therefore, individuals with WS1 and WS2 demonstrate that the formation of neural crest cell derived craniofacial

cartilage and melanocytes are affected. Mutations in Pax3 are known to cause these Waardenburg syndromes (Tassabehji *et al.*, 1992). The last syndrome to be described is WS4, which is a combination of symptoms from Waardenburg syndromes and Hirschprung's (Omenn and McKusick, 1979). Mutations in several genes have been associated with this syndrome including endothelin B receptor (EDNRB), its ligand endothelin 3 (EDN3), and Sox10 (Edery *et al.*, 1996; Kuhlbrodt *et al.*, 1998).

2.3. Chemical genetics

2.3.1. Chemical screens and compound identification

Chemical genetic screens utilise novel small compounds (< 2000 Da) to alter the function of specific genes and so determine their role in developmental processes. Chemical genetic screens are easy to set-up and can target a specific gene at a specific time point by adding or taking the compound away. Chemical genetic screens can utilise freely available compound libraries and have the advantage of being inexpensive to set-up and free to run in house. This type of screening using compounds from libraries is extremely useful for high-throughput phenotypic studies to uncover novel compounds that have the potential of being therapeutic drugs to treat disease. Current chemical genetic screens that utilise small vertebrates such as *Xenopus* and *Zebrafish* is advantageous over the use of mammalian models as they provide an inexpensive way to find new drugs, their targets and to assay compound toxicity (Wheeler and Brandli, 2009; Zon and Peterson, 2005). Amphibians can be used in chemical screens due to their opaqueness, which makes phenotypic analysis easier, quick development time and production of thousands of eggs at any one time, which makes the process high-throughput due to their ability to absorb compounds from the surrounding media (Wheeler and Brandli, 2009).

Xenopus embryos have been used in chemical screens for these reasons mentioned. The large number of *Xenopus* embryos that can be collected are small enough to develop in a 96-well plate. The compounds can be added to salt media and the embryos can be left to develop in optimal conditions as the compound is absorbed across the permeable vitelline membrane through the embryo epidermis (Tomlinson *et al.*, 2005; Wheeler and Brandli, 2009). We use *Xenopus* embryos in our laboratory to carry out in-depth analysis of several compounds. Currently, our most promising compound is leflunomide, which will be discussed next.

2.3.2. Leflunomide

Leflunomide is currently marketed under the trade name Arava® for the treatment of rheumatoid arthritis in the UK. It is an inhibitor of dihydroorotate dehydrogenase (DHODH) and was identified in a chemical genetics screen in my laboratory in collaboration with colleagues at Harvard Medical School to alter pigment development in *Xenopus laevis* and *Zebrafish* (*Danio Rerio*). During this screen of 2000 compounds, NSC210627 was identified to inhibit pigment cell development in *Xenopus* and *Zebrafish*. The chemoinformatic Discovery Gate algorithm was used to identify compounds with a high level of structural similarity (figure 2.8).

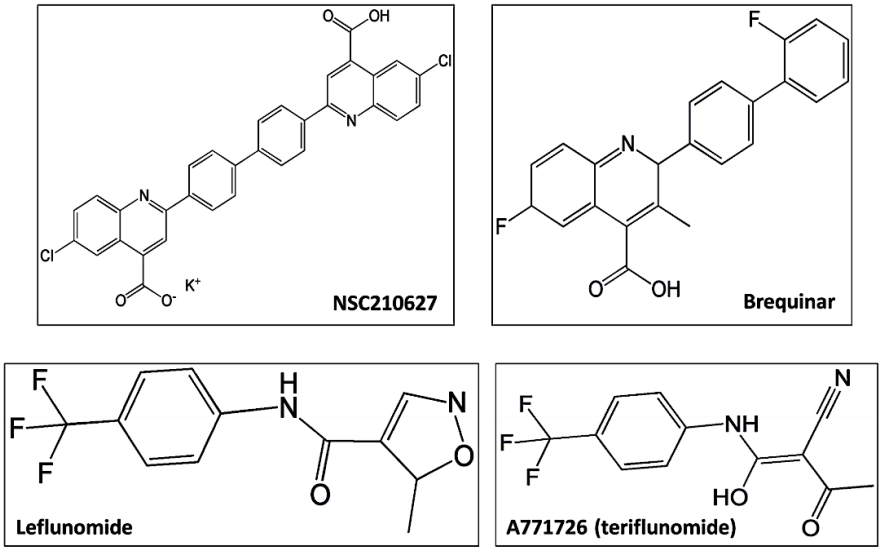

Figure 2.8: Chemical structures of DHODH inhibitors
Top Left: NSC210627. Top Right: brequinar. Bottom Left: leflunomide. Bottom Right: A771726 (teriflunomide).

The compound brequinar was identified, an inhibitor of DHODH. Leflunomide is structurally dissimilar to brequinar but also inhibits DHODH and phenotypically mimics the effect of NSC210627 (White *et al.*, 2011). The enzyme P450 converts leflunomide to its active metabolite teriflunomide. Leflunomide is an already prescribed drug that has been approved both by the United States Food and Drug Administration (FDA) and the UK Medicines and Healthcare products Regulatory Agency (MHRA) to treat rheumatoid arthritis. Leflunomide is inexpensive and along with its approved drug status it was selected for further experiments. DHODH is an enzyme responsible for pyrimidine biosynthesis and is therefore required for RNA transcription and DNA replication. Leflunomide is therefore thought to act by inhibiting the transcription of genes involved in melanophore development (Loffler *et al.*, 1997; White *et al.*, 2011).

Leflunomide in *Zebrafish* causes complete abrogation of melanophores and iridophores at 38 and 72 hours post fertilisation, respectively (figure 2.9). Interestingly, leflunomide treatment results in significant down regulation of neural crest cell genes such as Sox10 and

Slug/Snail2 and of Dct and Mitf that are genes expressed to regulate pigmentation development in melanophores (figure 2.9). Gene expression in blood and notochord remains unaffected by leflunomide treatment (White *et al.*, 2011). Unpublished data from the Wheeler laboratory has shown that neural crest genes in *Xenopus* embryos can be specifically affected by leflunomide (Hatch and Wheeler, IN PRESS). Leflunomide has been shown to reduce the number of neural crest cells in cell culture further suggesting this drug specifically affects the self-renewal of this multipotent cell type (White *et al.*, 2011). Melanoma tumours have been documented to adopt a similar genetic signature to that of the neural crest by expressing many of these genes involved in normal neural crest development and melanophore specification. Leflunomide, therefore, may be used to treat patients with melanoma (White *et al.*, 2011). Using a combination of leflunomide and a BRAFV600E inhibitor (PLX4720) administered into mouse melanoma xenografts has been shown to completely prevent tumour formation *in vivo* (White *et al.*, 2011).

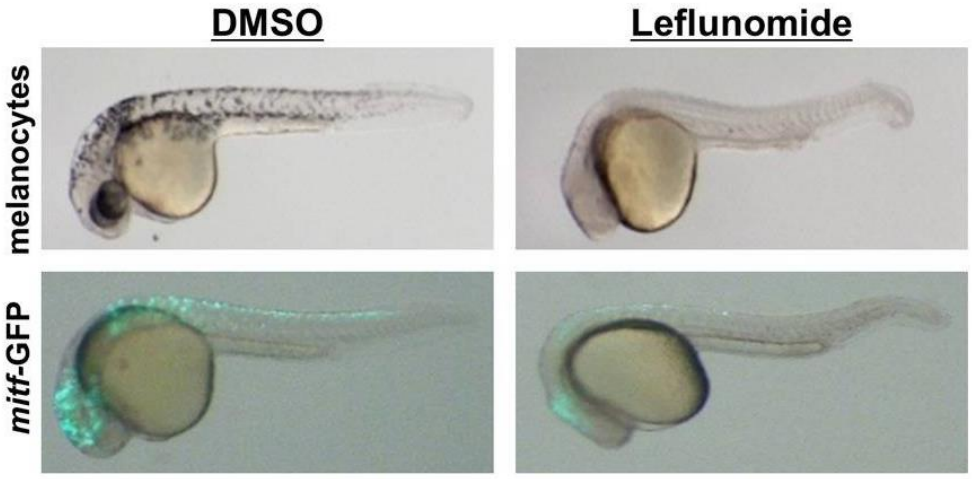

Figure 2.9 The effect of leflunomide on Zebrafish
Top two images show that post leflunomide treatment zebrafish loose melanophores, a neural crest derivative, entirely when compared to the DMSO control. The bottom two images show neural crest progenitors using GFP regulated by a Mitf promoter. Post leflunomide treatment there is a loss of these progenitors shown by the loss of GFP expression. Retrieved from White *et al.*, 2011.

Leflunomide is thought to carry out its function through the inhibition of transcriptional elongation by preventing the synthesis of pyrimidines. This will deplete the pool of cellular pyrimidines available for RNA synthesis and DNA replication. It has been shown in *Zebrafish* that leflunomide treatment phenotypically mimics spt5/spt6 *Zebrafish* mutants. Spt5 mutants also elicit an almost complete overlap of genes affected to that of leflunomide treated embryos. This includes a reduction of the expression of neural crest genes Sox10, Crestin and Mitf as shown by microarray. Experiments performed using human melanoma cell lines showed leflunomide to specifically inhibit the transcriptional elongation of Myc target genes. This is of strong interest to us as Myc is implicated to play roles in both neural crest specification and transcriptional pause release in embryonic stem cells. (Bellmeyer *et al.*, 2003; Hong *et al.*, 2008; Rahl *et al.*, 2010).

2.4. Transcriptional regulation

2.4.1. RNA polymerase pausing and transcriptional elongation

For cells to proliferate, differentiate and grow they must regulate their genes through transcription. Transcription requires RNA polymerase II (RNA pol II) recruitment to the promoter region by DNA-binding transcription factors (Hochheimer and Tjian, 2003). Following on from this, RNA pol II regulates gene expression in various cell types. Temporally regulated genes require promoter proximal pausing of Pol II. Promoter proximal pausing is where Pol II stops transcribing a gene and is held in a poised state at the 5' end of the gene within 50 nucleotides of the transcriptional start site (TSS) (Core and Lis, 2008). A gene is held in a poised state by the recruitment of pause factors; negative elongation factor (NELF), DRB-sensitivity inducing factor (DSIF) and transcription factor IIS (TFIIS) (Wada *et al.*, 1998; Yamaguchi *et al.*, 1999). NELF strongly associates with the clamp

domain of RNA pol II through its subunit NELF-A. DSIF is made up of two constituent subunits, Spt5 and Spt6. If either of these subunits is mutated, transcriptional elongation can be inhibited (Keegan *et al.*, 2002; Missra and Gilmour, 2010). Transcriptional elongation requires the positive transcription elongation factor, p-TEFb, that forms a part of the super elongation complex (SEC) machinery. Cyclin dependent kinase 9 (CDK9) and cyclin T1 are recruited to form the p-TEFb complex in eukaryotic cells (Bres *et al.*, 2008; Kohoutek, 2009) (figure 2.10).

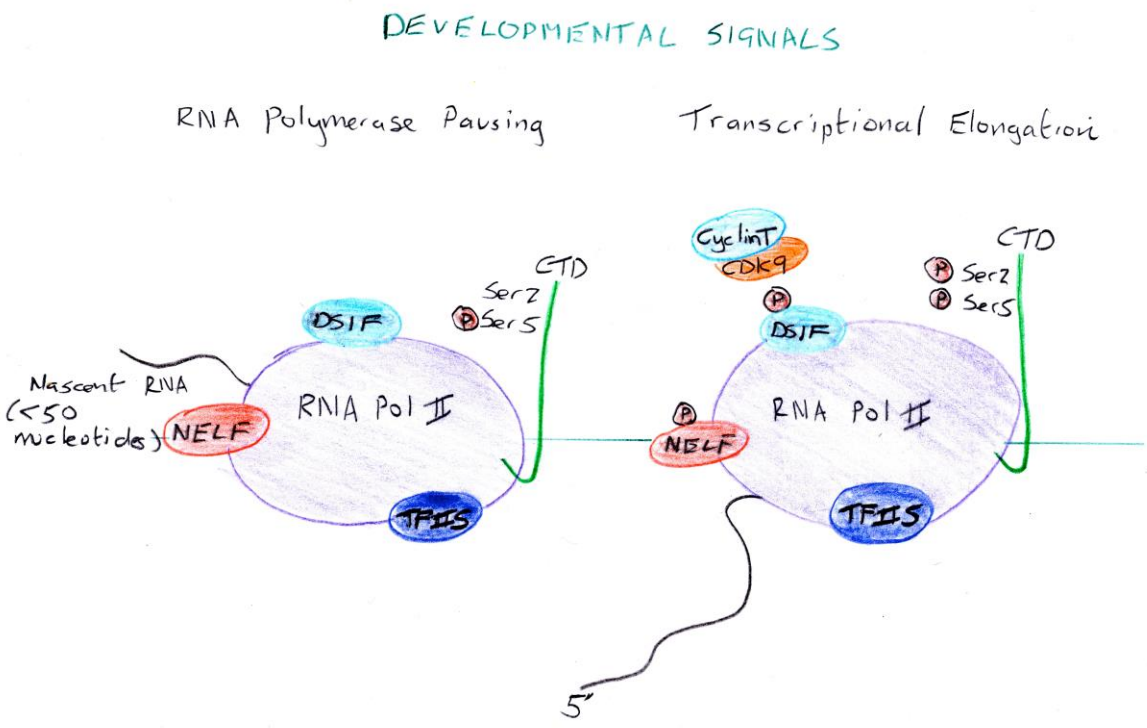

Figure 2.10: RNA polymerase pausing and transcriptional elongation RNA polymerase (Pol) II can stall after transcription initiation approximately 50 nucleotides downstream of the transcriptional start site. Release from polymerase pausing is initiated by developmental and environmental signals. In the paused state Pol II associates with both DSIF and NELF and the C-terminus is phosphorylation on serine 5 residues. The P-TEFb complex can induce pause release by phosphorylating on the serine 2 residue and also DSIF and NELF. NELF will dissociate from the complex and transcriptional elongation will commence.

Poised RNA pol II is associated in a complex with both DSIF and NELF. To initiate transcriptional elongation, phosphorylation of serine residues in locations 2 and 5 of the "**YSPTSPS**" motif in the C-terminal domain (CTD) of the large subunit of Pol II must take place. Phosphorylation of PolII at CTD and phosphorylation of the Spt5 subunit of DSIF is performed by p-TEFb to allow for transcription and the synthesis of full-length gene transcripts. Once phosphorylation of both RNA pol II and Spt5 occurs NELF will dissociate from the complex. DSIF will remain associated with RNA pol II to switch its function to promote transcriptional elongation (Fujita *et al.*, 2009). Pause release mechanisms in eukaryotes also involve other transcription factors such as transcription factor IIF (TFIIF) and TFIIS (TFIIS). Pausing and elongation during transcription is widely recognised as transcription elongation checkpoint control (TECC) (Luo *et al.*, 2012).

Transcriptional pausing may maintain stem-cell pluripotency and therefore prevent the transcription of genes involved in differentiation as approximately 30 % of genes in embryonic stem cells are held in a poised state with no elongation. The literature also reports that not only can RNA pol II transcribe genes in a sense direction; transcription can occur in an antisense direction (Rahl *et al.*, 2010; Seila *et al.*, 2008).

2.4.2. The p-TEFb complex

Recruitment of the positive elongation factor complex (p-TEFb) is essential for transcription after polymerase has been released from its poised state. The p-TEFb complex located in the nucleus is conserved across eukaryotes. The p-TEFb complex comprises enzymatic subunits CDK and cyclin that undergo a conformational change to initiate kinase activity (Zhou *et al.*, 2012). CDK9 is a core protein involved in all p-TEFb complexes, which is *hyper*-phosphorylated at Thr186 (T-loop) (Li *et al.*, 2005). P-TEFb enzymatic activity is tightly regulated by

phosphorylation to control transcription of genes held in a poised state. P-TEFb can reversibly bind 7SK small nuclear ribonucleoprotein particle (snRNP) to regulate transcription and can be identified in an inactive or active phosphorylation state within the nucleus (figure 2.11). P-TEFb is inactive if bound to 7SK snRNP and will become active when rapid transcription is needed to occur by its recruitment into the super elongation complex (SEC) (Peterlin and Price, 2006; Zhou *et al.*, 2012).

P-TEFb when inactive is bound to the inhibitory domain of RNA binding proteins hexamethylene bisacetamide (HEXIM) 1 or 2, which are in turn bound to 7SK snRNP. HEMIM 1 and 2 have been found to compensate for each other both *in vitro* and *in vivo*. They act by inhibiting the p-TEFb function and so are thought to be entirely novel CDK inhibitors (CDKI) as no other CDKIs interact with RNA to mediate inhibition (Barboric *et al.*, 2005; Byers *et al.*, 2005; Michels *et al.*, 2004; Nguyen *et al.*, 2001; Yik *et al.*, 2005; Zhiyuan *et al.*, 2001). La-related protein 7 (LARP7) and methyl phosphate capping enzyme (MePCE) bind to the 7SK snRNP complex to aid its binding to p-TEFb (He *et al.*, 2008; Krueger *et al.*, 2008; Xue *et al.*, 2010).

The inhibitory complex formed between p-TEFb and 7SK snRNP means that p-TEFb activity is carefully regulated and its activity can be narrowed down to precise genes when it is needed. This can stop the release of poised genes before they are needed (Zhou *et al.*, 2012). Knoweldge of how p-TEFb can target specific genes is still unknown. It is thought that p-TEFb can be directed by different transcription factors that bind to it in response to signalling cascades allowing it to incorporate into many diverse forms of the super elongation complex increasing the specificity between P-TEFb and its target genes. Incorporation into the super elongation complex has been shown to heighten p-TEFb's enzymatic activity (Luo *et al.*, 2012).

2.4.3. The super elongation complex (SEC)

The super elongation complex (SEC) is composed of active p-TEFb and a number of different regulatory proteins and their subunits (figure 2.11). As well as the super elongation complex accommodating the active p-TEFb complex it also associates with eleven-nineteen lysine rich leukaemia 1 and 2 (ELL1 and ELL2, respectively), AF4/FMR2 family member 1 (AFF1) and AF4/FMR2 family member 4 (AFF4) (Lin *et al.*, 2010; Yokoyama *et al.*, 2010). Interestingly, super elongation complexes vary in these additional constitutive proteins depending upon the gene that they are transcribing. ELL proteins (ELL1 and ELL2) are known to compensate for each other and the same has been demonstrated for AFF proteins (AFF1 and AFF4) (Biswas *et al.*, 2011). AFF proteins hold the complex together to support the formation of the SEC complex (Luo *et al.*, 2012) (figure 2.11).

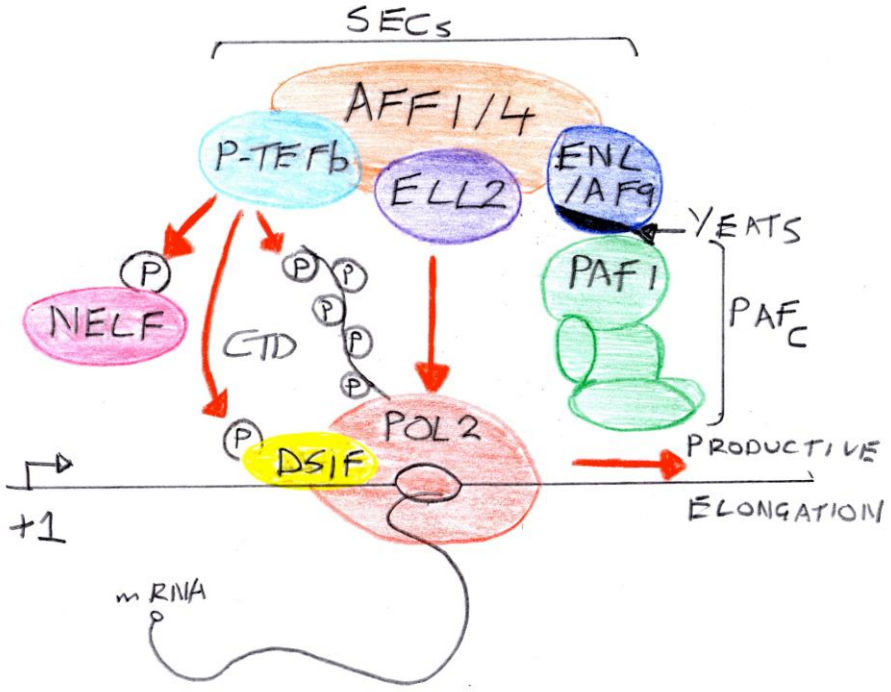

Figure 2.11: The super elongation complex (SEC)

In mammals the SEC is comprised of the positive transcription elongation factor b complex (p-TEFb), AFF family member 1 or 4, one of the eleven-nineteen lysine-rich leukemia (ELL) proteins, ENL and AF9. These proteins are also associated with RNA polymerase associated factor c (PAFc) via the YEATS domain of AF9. When associated with the SEC, p-TEFb is active and phosphorylates the C terminal domain of RNA Pol II, DSIF and NELF allowing NELF to dissociate and positive transcription elongation to occur. Based on Li *et al*., 2005.

SEC complexes are located at promoter regions of genes when active transcription is necessary to respond to Wnt and FGF signals, for example, or to acute changes in temperature. It is for this reason that heat shock and rapid response genes are predominantly regulated by RNA polymerase pausing (Fuda *et al.*, 2009; Luo *et al.*, 2012). The main function of SEC that will be described here is within a developmental context. Published articles suggest SEC recruitment to poised genes is not only essential for rapid gene induction but to allow synchrony amongst genes in development, specifically during early development.

Experiments involving *Drosophila melanogaster* (fruit fly) have described that during embryonic development particular sets of genes can be coined "synchronous" genes. These synchronous genes have a paused pol II at the promoter. These genes such as *short gastrulation* (*sog*), tended to be found in complex gene regulatory networks. Other genes did not show this necessity for paused pol II. These genes were termed "stochastic" genes and they demonstrated erratic and unpredicatable gene expression, for example *thisbe* (*ths*) (Boettiger and Levine, 2009). Studies have shown that pausing is important and present on genes that are rapidly induced and also on those that are considered master regulator genes whose expression is tightly regulated. Gilchrist recently has shown that genes known to be rapidly induced such as antibacterial genes do not have a paused pol II. Conversely, genes involved in regulating the fly's innate immune system can undergo pausing. Therefore, the types of genes which pausing is crucial for the expression of remains unknown (Gilchrist *et al.*, 2012).

Chromatin immunoprecipitation (ChIP) sequencing is a widely used method to analyse protein interaction with DNA. Much of the evidence for a paused RNA pol II has come from ChIP seq experiments carried out in embryonic stem cells. The first of these experiments showed that a paused polymerase associated with the components of the SEC can be recruited consistently to embryonic stem cell genes (Lin *et al.*, 2011). The embryonic genes cMyc and the heat shock protein hsp70 have been shown to have a poised RNA polymerase bound to them. The recruitment of SEC to these genes occurs via the N terminal domain of a mediator protein subunit (Med26) (figure 2.12). Loss of Med26 results in reduced SEC associated RNA polymerase II spanning the length of cMyc and hsp70 in ChIP sequence experiments using human cell lines. Another group has shown that SEC associated proteins and Med26 are located at the promoter of hsp70 before heat shock and loss of Med26 results in reduced phosphorylation of serine 2 of pol II on cMyc and hsp70 genes indicating that Med26 is required not only for the recruitment of SEC but to regulate and maintain the positive transcription of these genes (Takahashi *et al.*, 2011).

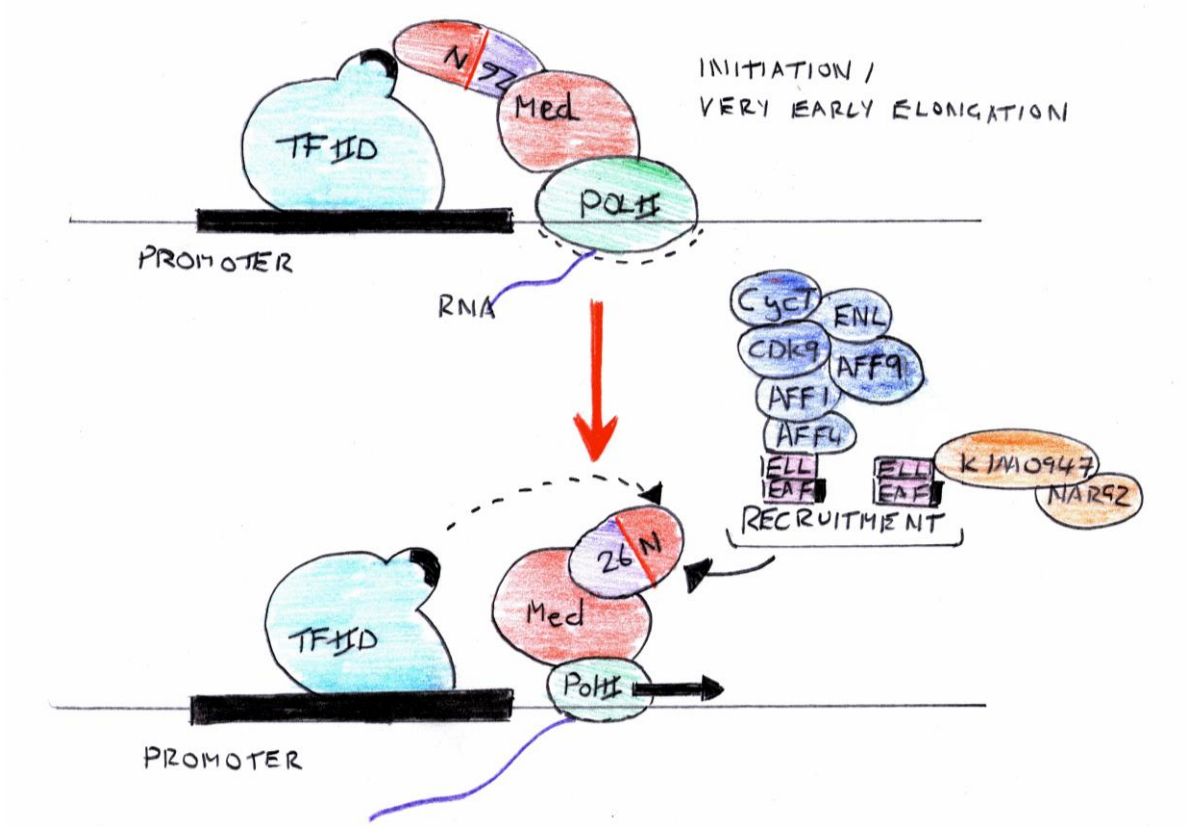

Figure 2.12: Med26 recruits the SEC to RNA polymerase II
The N-terminal domain of the mediator subunit Med26 interacts with TFIID associated with poised RNA polymerases at the promoter region. Induction of some signals promotes the release of Med26 from TFIID allowing it to associate with the SEC via EAF. This allows positive transcription elongation to occur. Based on Jang *et al*., 2005.

Components of the SEC and novel proteins regulating polymerase activities are still being discovered. One such protein is transcription termination factor TTF2 that has been shown to co-localise with an exonuclease protein Xnr2 at the starting position of poised genes. Loss of both TTF2 and Xnr2 shown by ChIP sequencing has revealed an extension of paused transcript from the transcription start site extending along the exon of the gene (Brannan *et al.*, 2012). These experiments reveal a possible function for TTF2 and Xnr2 to promote early termination of gene transcription (Brannan *et al.*, 2012).

2.4.4. Regulating productive elongation

Triggering p-TEFb activation results in phosphorylation of DSIF and NELF resulting in dissociation of NELF from RNA pol II allowing transcriptional elongation to follow. DSIF remains associated with the RNA pol II complex and switches from productive elongation phase to promotion (Rahl *et al.*, 2010). After p-TEFb has phosphorylated CDK and cyclin proteins, it can return to its inactive state. Subsequent to this, elongation occurs and is controlled by TFIIS and the rate of elongation is mediated by TFIIF (Fish and Kane, 2002; Zhou *et al.*, 2012). Poised Pol II can be rescued by TFIIS by promoting cleavage of halted RNA transcript therefore permitting the formation of a new 3' end that is incorporated into the RNA pol II active site allowing transcription to continue (Fish and Kane, 2002).

Histone modifications are essential for productive elongation to occur to allow access to regions that are inaccessible to RNA pol II. We know that RNA pol II associates with RNA polymerase associated factor c (PAFc), which methylates H3K4 and H3K79, that arises from a complex between PAFc and SEC. Methylation of H3K4 and H3K79 are molecular beacons for genes undergoing active transcription (Sims *et al.*, 2004). Components of PAFc have been identified to be Rtf1, Paf1, Ctr9, Leo1 and Cdc73 (Krogan *et al.*, 2002; Sims *et al.*, 2004). PAFc requires Rad6 and SET for ubiquitination and trimethylation of histones, respectively, since PAFc has not been found to possess any enzymatic activities (Briggs *et al.*, 2002; Dover *et al.*, 2002; Krogan *et al.*, 2003a; Krogan *et al.*, 2003b; Wood *et al.*, 2003). PAFc has been found to be an essential adaptor complex to cross link RNA pol II and methyltransferases. PAFc has been described to form a complex with SEC, p-TEFb and factors associated with Pol II for example TFIIS and DSIF (Chen *et al.*, 2009; He *et al.*, 2011; Kim *et al.*, 2010). In summary, transcriptional control is a

tightly regulated process to prevent premature transcription and the timely transcription of embryonic genes.

2.4.5. Role of cMyc in transcriptional elongation

Recently the transcription factor cMyc has been implicated to play a role in proximal pause release in embryonic stem cells. cMyc has always been associated with both the self-renewal of embryonic stem cells and multipotent neural crest cells. (Rahl *et al.*, 2010). A study has previously reported that Myc is able to associate to the p-TEFb complex and is subsequently involved in RNA polymerase pause release. (Bellmeyer *et al.*, 2003; Gargano *et al.*, 2007; Kanazawa *et al.*, 2003). cMyc expression in embryonic stem cells is now hypothesised to regulate transcriptional pause and release of embryonic genes through recruiting p-TEFb to RNA polymerase II (RNA pol II). Loss of cMyc expression results in reduced phosphorylated levels of serine 2 RNA pol II with a marked decrease in elongation of genes. However, RNA pol II polymerase pausing is not affected, as the endogenous level of Ser5-phosphorylation associated with initiation remains unchanged. Genes that are primarily regulated by cMyc expression under go an increased level of pausing and elongation (Rahl *et al.*, 2010). It may be assumed that cMyc is involved in transcriptional elongation in other types of proliferative cells. The upturn in proliferation genes observed in a variety of cancers may be partially due to elevated cMyc expression. Therapeutics that affect cMyc but are not direct Myc targets may be useful cancer drugs, such as leflunomide, since an increase in genes associated with proliferation is observed when cMyc is upregulated (Rahl *et al.*, 2010; White *et al.*, 2011).

cMyc is believed to undergo RNA polymerase pausing (figure 2.13). In studies were the SEC subunits Paf1 and Med26 have been knocked down to display a loss of SEC components along the gene body of cMyc

and other paused genes. RNA pol II has been found in ChIP-seq experiments to accumulate at the promotor region of paused genes. This result in there reduced transcription and consequently, overall mRNA present in these cells is much less. As a consequence of pausing a reduction in Ser2 phosphorylation is observed that is associated with positive transcription elongation. This study strongly suggests that transcription of cMyc requires transcription of Med26 and Paf1 to enlist the SEC to its promoter site (Takahashi *et al.*, 2011).

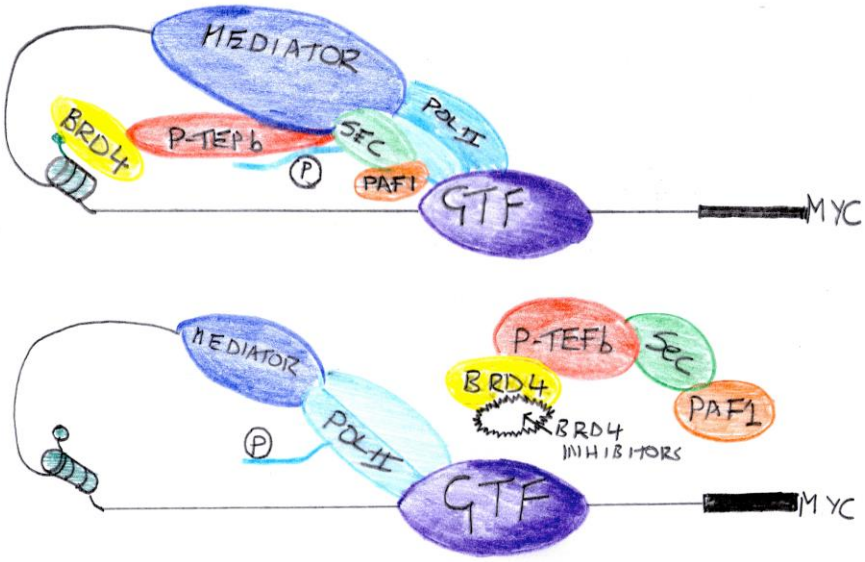

Figure 2.13: Myc undergoes RNA polymerase pausing
(top) For the myc gene to be transcribed it must associate with the active form of p-TEFb in association with the SEC. This occurs as Brd4 will also associate with p-TEFb and attach to the chromatin at the myc promoter region. (bottom) A possible therapeutic target of myc overexpressing cancers is Brd4. Inhibitors of Brd4 have been shown to downregulate myc gene expression. Based on Guo *et al*., 2000.

Interestingly, Brd4 knock down has been shown to result in reduced cMyc expression. Brd4 present in another active p-TEFb complex is normally associated with basal level transcription. In human acute myeloid leukaemia (AML) cells Brd4 knock down resulted in reduced cMyc expression and were found to lower cancer cell self-renewal (Zuber *et al.*, 2011). Bdr4 was reported in this study to associate with

the chromatin at the promoter site of cMyc. AML cells that were treated with I-BET151, an inhibitor of Brd4, caused it to dissociate from the SEC resulting in a loss of cMyc expression (figure 2.13) (Zuber *et al.*, 2011). To conclude, inhibition of Myc expression by preventing the function of the SEC may be a potential target for many cancers that overexpress Myc protein.

3. Aims

Using the pyrimidine biosynthesis inhibitor leflunomide as a tool to prevent transcriptional elongation I aim to confirm the importance of this process during neural crest specification. Our laboratory, in collaboration with the Zon laboratory, has shown that leflunomide's action inhibits the transcriptional elongation of cMyc target genes in *Zebrafish* (*Danio Rerio*), *Xenopus* and melanoma cell lines (White *et al.*, 2011). cMyc has been shown to play an important role in initiating the transcription of genes required for neural crest specification (Bellmeyer *et al.*, 2003). I aim to show quantifiably that administering leflunomide on *X. laevis* embryos can prevent the expression of neural crest specifying genes such as Slug, Sox10 and cMyc. Results gained will implicate the importance for a regulator of transcriptional elongation during neural crest development. Unpublished data from my host laboratory strongly suggests this would be the case as transcriptional pausing and subsequent elongation has very recently been shown to regulate genes associated with embryonic stem cell pluripotency (Rahl *et al.*, 2010). Our laboratory hypothesises that this level of transcriptional control is also the case for neural crest cells as they share a stem cell like multipotent potential. Candidate genes involved in neural crest cell specification must be tightly regulated to prevent inappropriate differentiation, therefore, transcriptional pausing would prevent the transcription of genes keeping their multipotent potential. I aim to investigate this process in neural crest cells by identifying neural crest cell genes sensitive to leflunomide by developing a quantitative method using real-time PCR in *Xenopus*. Results gained will complement unpublished data in my host laboratory to investigate the effect of inhibiting transcriptional elongation on neural crest specific genes to show that transcriptional regulation is important for neural crest specification.

4. Research Methods and Materials

4.1. Obtaining *Xenopus laevis* embryos

4.1.1. *Xenopus* source

The adult *Xenopus laevis* used in this thesis were obtained from the University of Portsmouth in the European Xenopus Research Centre (Portsmouth, UK) originally sourced from Nasco. *Xenopus laevis* were maintained in a temperature-controlled room at the Controlled Environment Facility (University of East Anglia, UK) for the subsequent production of eggs and sperm for experiments.

4.1.2. Male dissection and testis isolation

The dissections of males for testes were carried out following the legislation in the Animals (Scientific Procedures) Act 1986. Male frogs were anaesthetised by immersion in a solution of ethyl 3-aminobenzoate methanosulfonate salt (Sigma, A5040-25G) (0.5 g in 300 mL of dH_2O) for 2 hours at 4°C or until the heart has stopped beating as advised by the Named Animal Care & Welfare Officer (NACWO). The depth of anaesthesia was assessed by the absence of a withdrawal reflex by checking for autonomic responses. Male frogs were exsanguinated and testes were removed post-mortem and cleared of attached blood vessels and connective tissue. Testes were placed in ice-cold testes storage buffer and stored at 4°C and used the following day. The male carcass was stored for 1 month at -18°C and then disposed of by incineration.

- Testes storage buffer: 80% foetal calf serum, 20% 1.0 x MMR, 1:1,000 U gentamycin sulphate
- PMSG: 100 U/mL PMSG was prepared in PBS and stored at 4°C.

4.1.3. Induction of egg production

To induce ovulation, pigmented adult female *Xenopus laevis* frogs were primed by injection with 100 U of pregnant mare serum gonadotropin (PMSG) intervent into the dorsal lymph sac. Primed frogs were kept at 18°C for 4 – 7 days without feeding. 14 hours prior to the first egg harvest the primed frogs were induced with 500 U of human chorionic gonadotropin (HCG) – Intervent and placed at 16°C.

4.1.4. *In vitro* fertilisation

Embryos were collected from induced female frogs into 9 cm Petri dishes. Excised sections of male testes were macerate in a 1.5 mL eppendorf tube using a pestle in 1 mL of 1.0 x MMR to release sperm. The testes 1.0 x MMR solution was evenly distributed onto the eggs using a 3 mL pipette for 5 minutes at 18°C. The use of a high salt solution (1.0 x MMR) prevents sperm entry and allows maximal dispersion of the sperm over the eggs prior to sperm entry. The eggs were then immersed in 0.1 x MMR for 20 minutes at 18°C allowing fertilisation. Eggs can then be visually assayed for cortical rotation, an indication of successful fertilisation, where the plasma membrane and cortex rotate relative to the inner cytoplasm.

- 0.1 x MMR: 10 mM NaCl, 0.2 mM KCL, 0.1 mM $MgCl_2$, 0.2 mM $CaCl_2$, 0.5 mM HEPES (pH 7.5)
- 1.0 x MMR: 100 mM NaCl, 2 mM KCL, 1 mM $MgCl_2$, 2 mM $CaCl_2$, 5 mM HEPES (pH 7.5)

4.1.5. De-jellying of fertilised embryos

Post fertilisation the eggs were stripped of their jelly coat to allow experimental manipulation. The eggs were immersed in excess 2%

cysteine (pH 8.0) dissolved in 1.0 x MMR and transferred to a 250 mL glass beaker. Embryos were then gently swirled until de-jellying is complete as observed by the tight stacking of the embryos. The embryos were then washed in 0.1 x MMR to remove trace amounts of cysteine and any debris. Embryos were to develop until they reach the required stage of development according to Nieuwkoop and Faber (Nieuwkoop and Faber, 1967).

4.1.6. Fixing embryos

Once embryos reach a stage that is required as depicted by Nieuwkoop and Faber, they were fixed (Nieuwkoop and Faber, 1967). Embryos were fixed using MEMFA (3.7 % formaldehyde, 1.0 x MEM salts made up to the required volume using DEPC dH_2O). They were then left for 1 hour at room temperature, washed 3 times in PBST and dehydrated in 25 %, 50 %, 75 % methanol and stored in absolute methanol at 4°C.

4.2. *In situ* hybridisation probe synthesis

4.2.1. Preparation of competent cells

A 5 mL culture of DH5α *Escherichia coli* (*E.coli*) was incubated overnight in Lysogeny Broth (LB) at 37°C with shaking at 200 *rpm*. 200 mL of LB media was inoculated with primary culture and was incubated at 37°C with shaking at 200 *rpm* until the optical density (OD) at 600 nm reached 0.3 to 0.4. When the OD is reached the culture is split into 4 x 50 mL falcon tubes and incubated on ice for 15 minutes. The cells are spun down at 2,000 *rpm* at 4°C for 10 minutes. The supernatant is discarded and the bacterial pellet was re-suspended in 16 mL of filter sterilised TB I buffer. The cells were placed on ice for 15 minutes and then spun at 2,000 *rpm* at 4°C for 10 minutes. The supernatant is discarded and the pellet is re-suspended in 4 mL of filter-sterilised TB II

buffer. 1 mL aliquots were then stored at -80°C until required for transformations.

Solutions

- TB I pH 5.8: 0.1 M $RbCl_2$, 0.068 M $MnCl_2H_2O$, 0.01 M $CaCl_2$, 1 M KAc pH 7.5, 37.5 mL glycerol was added to adjust the total volume to 250 mL and pH using 0.2 M HAc.
- TB II: 0.5 M MOPS pH 6.8, 0.01 M $RbCl_2$, 1.04 M $CaCl_2H_2O$, 37.5 mL glycerol was added to adjust the total volume to 250 mL. Aliquots were stored at -80°C.

4.2.2. Transformation

1 µL of plasmid DNA was ligated into 100 µL of competent DH5α *E. coli* cells and left on ice at 4°C for 30 minutes. Competent cells underwent heat shock at 42°C for 2 minutes to allow the cells to ingest the plasmid DNA. Heat shock was followed by 5 minutes incubation on ice. 300 µL of SOC media was added to the competent cells after incubation and a further incubation on ice for 5 minutes. 1 hour at 37°C was required to allow growth of the bacteria. 200 µL of ligated cells were plated out onto agar and LB plates containing the correct antibiotic. The inoculated plates were left at 37°C overnight to allow colony formation.

4.2.3. DNA midi prep

Transformed cells that formed colonies were removed by a sterile pipette tip and incubated in 50 mL LB media supplemented with carbicillin overnight at 37°C with rocking at 200 *rpm*. The DNA plasmid was then isolated using the Qiagen™ Hi-speed plasmid purification kit (Qiagen, 12643) according to manufacturers instructions. 1 µL of the final product was run on a 1% agarose gel at 65 V until the migration of the bands was sufficient to identify the different sizes of DNA 1 kb

ladder (New England Biolabs, N3232L). 1 µL was placed on a nanodrop™ spectrophotometer to determine the DNA concentration of the purified DNA plasmid.

4.2.4. Restriction digest

Clones within plasmid constructs were linearised by restriction digestion using an appropriate restriction enzyme. 2 – 10 µg of plasmid was added to 2 µL of the required restriction enzyme. 5 µL of buffer was added and made up to 50 µL with RNase free water. This was incubated at 37°C for a minimum of 2 hours or alternatively overnight. The linearised plasmid was visualised on a 1 % agarose gel.

4.2.5. Ethanol precipitation

Digests were purified using ethanol precipitation. 1:10 v/v of 0.3 M sodium acetate and 250 µL of ethanol were added to a 50 µL digest and left overnight at -20°C to precipitate. After overnight precipitation the sample(s) were then centrifuged at 16,700 *rpm* for 15 minutes. The supernatant was discarded and the DNA pellet washed with 70 % ethanol prepared using RNase free water and centrifuged at 16,700 *rpm* for 5 minutes. The ethanol was aspirated off and the pellet was left to air dry at room temperature. The pellet, once dried, was re-suspended in 20 µL of RNase free water and stored at -20°C.

4.2.6. Agarose gel electrophoresis

Agarose gels are prepared at a 1 % concentration. 0.5 g of agarose was dissolved in 50 mL of 1 x TAE buffer by heating to 80°C. Ethidium bromide was added to the agarose once cooled to 60°C at a concentration of 0.5 µg/mL to visualise the DNA using a UV trans illuminator following electrophoresis. DNA sample(s) were mixed with

$^{1}/_{10}$ volume of 10 x DNA loading dye before loading in the well(s). Electrophoresis was carried out at 70 V for 65 minutes.

4.2.7. Probe synthesis and purification

Plasmids that contain the gene of interest were linearised using the appropriate restriction enzymes to digest at restriction sites to give sense and anti-sense RNA probes. Linearised DNA was purified prior to probe synthesis. Probe synthesis required the following components to be included in the reaction mixture made up to 20 µL with RNase free water; 4 µL 5x transcription buffer, 2 µL DTT, 1 µL DIG labelled UTPs, 1 µL RNAsin, 1 µL linearised DNA, 2 µL RNA polymerase. The reaction mixture was incubated for 3 hours at 37°C. Adding 30 µL of RNase free water to the reaction mix and centrifuging it through a G50 column according to manufacturers instructions purified the probe. 5 µL of probe was run on a 1 % agarose gel and visualised by a UV trans illuminator to verify probe quality. 5 µg of purified probe was then added to 10 mL of hybridisation buffer and stored at -20°C. Plasmids used to make probes are shown in the table 4.1.

Clone name	Sense RE	Antisense RE	Sense polymerase	Antisense polymerase	Source
Sox10	Xho1	EcoR1	T7	T3	Dr Victoria Hatch (University of East Anglia)

Table 4.1: *In situ* hybridisation probes

4.2.8. Whole mount *in situ* hybridisation (WISH)

Embryos for WISH were rehydrated from absolute methanol by using 75 %, 50 %, 25 % methanol prepared in phosphate buffered saline

supplemented with 0.1 % Tween-20 (PBST) for 10 minutes each followed by x 2 PBST washes for 5 minutes with rocking at room temperature. Embryos were treated with 10 µg/mL Proteinase K for 5 to 10 minutes depending the embryonic stage of development i.e. stage 18 for 10 minutes, stage 15 for 8 minutes and stage 12 for 5 minutes. *Xenopus* embryos were washed twice in PBST for 10 minutes and incubated in 3.7 % formaldehyde/PBST for 30 minutes with rocking at room temperature. Embryos were washed 3 times in PBST for 10 minutes and incubated in hybridisation buffer at 60°C for 6 hours. The embryos were placed in fresh hybridisation buffer with the appropriate probe and incubated overnight at 60°C with rocking.

The probe was removed after overnight heating and stored at -20°C. Embryos were washed with fresh hybridisation buffer for 20 minutes and underwent 3 washes in 2 x sodium chloride and sodium citrate solution (SSC) for 30 minutes and 2 washes in 0.2 x SSC for 30 minutes, all at 60°C. Embryos were washed twice in Maleic acid buffer with 0.1 % Tween (1.0 x MABT) for 30 minutes at room temperature and then placed into a 1.0 x MAB and 2 % Boerhinger Mannhein Blocking (BMB) solution for 1 hour at room temperature with rocking. BMB solution was replaced with antibody solution containing anti-deoxygenin (1:2000) and incubated overnight at 4°C with rocking.

Antibody solution was removed and embryos were washed in 1.0 x MABT 5 times for 30 minutes at room temperature with rocking and incubated in a MABT wash overnight at 4°C with rocking. The colour reaction was then carried out by washing the embryos in fresh alkaline phosphate buffer twice for 10 minutes at room temperature with rocking. Embryos were placed in nitro blue tetrazolium / dimethylformamide (NBT/BCIP) in alkaline phosphate buffer (67.5 µL NBT, 52.5 µL BCIP made up to 15 mL with alkaline phosphate buffer) until the preferred colour intensity was observed. Embryos were put in

5.0 x TBST solution overnight to remove background colour and then imaged with a Zeiss stmi SV6 microscope.

Solutions

- Alkaline Phosphatase Buffer: 100 mM Tris (pH 9.5), 50 mM $MgCl_2$, 100 mM NaCl, 0.1 % Tween 20
- Antibody solution: 2 % BMB, 20 % goat serum, anti-DIG Fab fragment, (1:2000 dilution) in 1 x MAB
- BCIP: 50 mg/mL in 100 % DMF
- Blocking solution: 2 % BMB in 1 x MAB
- BMB (Boehringer Mannheim Blocking agent) 10 %: 10 % (w/v) in BMB preheated (50 °C) 1 x MAB, stirred until dissolved and then autoclaved, aliquoted and stored at –20°C
- Hybridisation buffer: 50 % formamide, 5 x SSC, 1 mg/mL Torula RNA, 100 μg/mL Heparin, 1 x Denharts solution, 0.1 % Tween 20, 0.1 % CHAPS, 10 mM EDTA
- MAB 1 x (Maleic Acid Buffer): 100 mM Maleic acid; 150 mM NaCL (pH 7.5)
- MEMFA: 10 % MEM salts, 10 % formaldehyde
- MEM salts: 0.1 M MOPS, 2 mM EGTA, 1 mM $MgSO_4$, pH7.4
- NBT (Nitro Blue tetrazolium): 75 mg/mL in 70 % dimethylformamide (DMF)
- PBS 10 x: 2.5g $NaH_2PO_4.H_2O$, 11.94g $NaHPO_4.H_2O$, 102.2g NaCl, 400 mL DEPC dH_2O. pH adjusted to 7.4 and volume to 1 L
- PBST: 1.0 x PBS, 0.1 % Tween 20
- Proteinase K (10 μg/ml): 1 μL proteinase K, 1 mL PTw
- SSC 20X: 175.3g NaCl, 88.2g sodium citrate. pH adjusted to 7.0 and volume to 1 L with DEPC H_2O

4.2.9. Bleaching pigmented *X. laevis* embryos

Embryos' for WISH were bleached to observe *in situ* staining. Embryos were placed in a solution of 5.95 mL DEPC H_2O, 3.3 mL 30 % H_2O_2, 0.5 mL formaldyhyde and 0.25 mL 20 x SSC and incubated on a light box until pigment was removed. Post-bleaching the embryos were washed three time in PBS for 15 minutes and fixed in MEMFA overnight at 4°C.

4.3. Real-time PCR

4.3.1. Quantitative PCR methodology

Real-time PCR has standardised the detection of DNA and RNA transcript in biologically important samples. A single copy of a unique sequence can be amplified and detected. In theory, there is a quantitative relationship between the initial amount of cDNA generated and the amount of transcript post-amplification. The use of real-time PCR has eliminated the variability previously associated with touchdown PCR by allowing the quantification of PCR product to now be both routine and reliable.

Real-time PCR is a sensitive and reproducible method for quantifying RNA target concentration in *Xenopus* and in other biological systems by using polymerase chain reaction. SYBR green is a dye used to detect double stranded DNA and is the chosen reporter for real-time PCR assays in this thesis. The process of amplifying target cDNA generated from a reverse transcriptase reaction is described as follows:

1. When SYBR Green dye is added to a sample it immediately binds to all double-stranded DNA present in the sample.

2. During the PCR, DNA Polymerase amplifies the target sequence, which creates the PCR products, or "amplicons."

3. The SYBR Green dye then binds to each new copy of double-stranded DNA.

4. As the PCR progresses, more amplicons are created. Since the SYBR Green I dye binds to all double-stranded DNA, the result is an increase in fluorescence intensity proportionate to the amount of PCR product produced.

SYBR Green was the chosen real-time PCR chemistry for assays in this thesis as it can monitor the amplification of any double stranded DNA sequence in real time. Since no probe is required, the major advantage was that many genes could be analysed at a reduced cost if we are to compare the cost of oligonucleotide primers *vs.* Taqman probes. The disadvantage of using SYBR green is that it may generate false positive signals by binding to non-specific double-stranded DNA sequences.

Real-time PCR reactions are characterised by the moment in time during cycling that amplification of a PCR product is detected rather than the amount of product that has accumulated after 40 cycles, for examples. The greater the amount of template DNA at the start of cycling the sooner a significant increase in fluorescence is recorded. The detection of a fluorescent signal is recorded autonomously on an amplification plot in real time. The amplification plot is the florescent signal intensity *vs.* the cycle number. An increase in florescence above a baseline (background signal) indicates the detection of accumulated PCR product. The parameter cycle threshold (C_t) is defined as the cycle number at the point the florescence detected passes the fixed threshold. Comparing the C_t scores generated from untreated *vs.* treated samples

is used to determine the fold change in gene expression as performed in this thesis.

4.3.2 General guidelines

Bacteria and RNases are potentially contaminants in the working place that can cause some major problems, including the degradation of RNA and the amplification of non-specific PCR products. The bench and routinely used equipment, such as the pipettes, were regularly cleaned with detergent and RNase Zap® (Ambion). Sigma water (Sigma) was used in all reagents and procedures required for the following molecular biology protocols. Additional Sigma water (Sigma) autoclaved with 0.1 % diethylpyrocarbonate (DEPC) (Sigma) was also prepared for work associated with RNA. All glass and plastic ware was either autoclaved or manufacturer-certified sterile prior to use.

4.3.3. RNA extraction

X. laevis embryos (*n*=10) were placed in a 1.5 mL eppendorf tube and all liquid was removed and replaced with 1 mL TRIzol™ reagent (Ambion®, 15596-026) before flash freezing in liquid nitrogen at -196°C for 15 minutes. Embryos that were not to be used after flash freezing were stored at -80°C until required. Harvested embryos in TRIzol™ were thawed on ice at 4°C and vortexed until all material was masticated leaving a homogenous solution. RNA is stable in TRIzol™ as the reagent deactivates RNAses to allow for long-term storage. 500 µL of chloroform was added to the homogenous mix of embryos in TRIzol™ and inverted 5 to 10 times and incubated at room temperature for 10 minutes to permit complete dissociation of nucleoprotein complexes. The eppendorf tube(s) were spun at 16,400 *rpm* (24 x 3,75 *g*) for 10 minutes in a cooled centrifuge at 0°C. At this stage, if the centrifugation had not been sufficient, the DNA-containing interphase would appear

turbid due to poor compaction. An additional chloroform step would resolve this. After centrifugation the eppendorf(s) are placed on ice at 4°C and the upper phase is placed into a new tube. Care is taken at this stage to avoid aspirating the DNA-containing white interphase as this will lead to DNA contamination in the RNA preparation. 500 µL of ice-cold isopropanol and 1 µL of Glycoblue™ (Invitrogen, AM9516) were added to precipitate the RNA. The eppendorf tube(s) were then vigorously vortexed and incubated at room temperature for 10 minutes before centrifugation at 0°C for 30 minutes at 16,400 *rpm*. The supernatant was removed and discarded leaving behind the RNA pellet, which was a visible blue colour. The RNA pellet is washed with 70 % ethanol (prepared using RNase free water) and centrifuged at 0°C for 10 minutes. The ethanol was removed and the RNA pellet was left to air-dry at room temperature before being re-dissolved in 45 µL of RNase free water in preparation for DNase treatment.

4.3.4. DNase treatment

10 x DNase I buffer was added to each RNA sample to a final concentration of 1 x 6 µL of DNase I was added to each sample and incubated at 37°C for 30 minutes. 1 µL of 250 mM EDTA stock was then added to prevent chemical scission during heat inactivation of DNase I at 75°C for 10 minutes. RNA was precipitated using 500 µL absolute isopropanol and 1 µL Glycoblue™ to remove EDTA, which may inhibit downstream reactions by chelating Mg^{2+} ions and was then re-suspended in 20 µL of RNase free water once the pellet had air dried at room temperature.

4.3.5. Determining RNA concentration by spectrophotometry and denaturing gel electrophoresis

To determine the amount of RNA extracted from *X. laevis* embryos (*n*=10) after TRIzol™ extraction and DNase I treatment, it is a requirement to use a nanodrop both to determine the amount of RNA present and to detect DNA or phenol/chloroform contamination. Absorbance measurements will detect any molecules absorbing at a specific wavelength post-purification resulting in a signal for nucleotides, RNA, ssDNA and dsDNA that will absorb at 260 nm and contribute to the total absorbance. The ratio of absorbance at 260 nm and 280 nm is used to quantitate the purity of RNA used for subsequent real-time PCR experiments. A ratio of ~ 1.8 is accepted as "pure" for DNA; a ratio of ~ 2.0 is accepted as "pure" for RNA. If the ratio is substantially lower in either case, it may indicate the presence of protein, phenol/chloroform or other contaminants that absorb strongly at 280 nm. The nanodrop used to determine RNA concentration in this thesis is the NanoDrop® ND-1000 spectrophotometer that gives a consistent 260/280 ratio. The second measure of RNA purity is the 260/230 ratios. The 260/230 values for "pure" RNA are higher than the 260/280 values and are within the range of 2.0 to 2.2. Again, if this ratio is substantially lower then, it may also indicate the presence of contaminants that absorb at 230 nm. The RNA extraction protocol previously described the use of Glycoblue™ that absorbs at both 260/280 and 260/230. This does affect the nanodrop quantification but is not significant. The expected Glycoblue™ 260/280 and 260/230 values are 1.71 and 0.84, respectively.

To confirm that the RNA extracted has not degraded due to RNase activity, gel electrophoreses using a 1.5 % denaturing formaldehyde gel in MOPS buffer can be used. 1 g of agarose powder in 72 mL of dionised water was stirred and heated to 80°C. 10 mL of 10 x MOPS buffer was

added and stirred. Once the agarose mix had cooled to 60°C 18 mL of fresh formaldehyde (37 %) was added and stirred. The mix was then poured into a northern blot tank and allowed to cool at room temperature. Once set, the gel was immersed in 1 x MOPS buffer. The RNA sample(s) were heated at 70°C for 10 minutes with 2 x RNA loading dye (Thermo scientific, R0641) for visualisation under a UV trans illuminator. Electrophoresis was carried out at 70 V for 65 minutes. Intact total RNA run on a denaturing gel will have sharp 28S and 18S rRNA bands. Completely degraded RNA will appear as a very low molecular weight smear.

- 10 x MOPS buffer: 0.4 M MOPS (pH 7.0), 0.1 M sodium acetate, 0.01 M EDTA (pH 8.0)

4.3.6. cDNA preparation

First strand cDNA Synthesis Using SuperScript™ II reverse transcriptase enzyme (Invitrogen, 18064-014) was used to make cDNA from template RNA in the range of 1 ng - 5 µg in a 20 µL reaction volume. Using nuclease-free micro centrifuge tube(s) 1 µL of random hexadeoxynucleotides (Promega, C1181), 1 µL of 10 mM deoxyribonucleotides [dATP, dCTP, dGTP and dTTP] (Promega, U1410) and 1 µg of total RNA (x µL) were added and made up to a 20 µL volume with RNase free water. The mix was then centrifuged for 1 minute to settle contents and incubated at 65°C for 5 minutes and placed back on ice at 4°C. 4 µL of 5 time First strand buffer, 2 µL of 0.1 M DDT and 1 µL of RNasin (Promega, N2611) was vortex and centrifuged at 16,700 *rpm* for 30 seconds before incubation at 25°C for 2 minutes. 1 µL of Superscript II enzyme (200 U) was added and incubated at 25°C for 10 minutes with a longer incubation at 42°C for 50 minutes to allow cDNA synthesis. The superscript II enzyme was heat inactivated to stop the reaction at 70°C for 15 minutes. cDNAs were diluted 1:20 to give a final

concentration of 10 ng/µL. Oligo(dT)$_{15}$ Primer is unsuitable for use as a primer for first-strand cDNA synthesis in *X. laevis* as the primer hybridises to the poly(A) tail of mRNA which *X. laevis* mRNA does not have.

4.3.7. Real-time PCR procedure

Real-time PCR was performed on cDNA extracted from whole embryo (*n*=10) lysates treated with DMSO ± leflunomide (batch #012M4002V, L-5025, Sigma) with samples loaded into plates in triplicate. Brightwhite 96-well plates (BW-FAST) and high quality optical plate seals (BW-ADVSEAL) were used (PrimerDesign Ltd, Southampton, UK). Gene-specific nucleotide sequences were detected using Precision™ FAST-LR 2x mastermix (PrimerDesign Ltd, Southampton, UK). Real-time PCR was performed in a final volume of 20 µL (10 µL 2 x master mix / 1 µL primer [0.25 µMol; 0.25 x 10^{-6} mol/dm^{-3}] / 5 µL cDNA [5 ng / µL; 300 nmol] / 4 µL RNase free water) using a 7500 FAST real-time PCR instrument (Roche) under the following cycling conditions: 95°C for 20 s, 40 cycles at 95°C for 3 s, 60°C for 30 s. After cycling, a melting curve was recorded between 60°C and 95°C under the following conditions: 95°C for 15 s, 60°C for 1 min, 95°C for 15 s, 60°C for 15 s with a ramp rate of 0.11°C•s^{-1}.

4.3.8. Primer design

Detection primers were designed using Primer3 software (http://biotools.umassmed.edu/bioapps/primer3_www.cgi) (Untergasser *et al.*, 2012) and custom designed by PrimerDesign Ltd, UK where indicated in table 4.2. Their oligonucleotide sequences are provided in Table 4.2. In-house designed primers were synthesised by eurofins (Norwich, UK) and custom primers were designed by and purchased from PrimerDesign Ltd (PrimerDesign Ltd, Southampton,

UK). The primers used in this thesis produce low Ct scores and a single peak in the derivative of the melting curve, and did not amplify non-template controls (NTC) and no reverse transcriptase (-RT).

Nucleotide sequences for genes of interest were generated from the NCBI website (http://www.ncbi.nlm.nih.gov/pubmed) and for those genes that were not available on NCBI their nucleotide sequences were downloaded from the *Xenopus* genome browser available from Simon Moxon (TGAC, The Genome Analysis Centre, Norwich) that were held on the servers at the University of Yale, USA. The downloaded *Xenopus* genome browser sequences are given a CUFF link identification number.

For NCBI and CUFF link sequences that were input through the Primer3 algorithm a list of parameters were set in order to generate adequate real-time PCR primers. The following set of parameters was used to design in house primers (Untergasser *et al.*, 2012):

- pair towards 3' end to increase specificity of primers
- pair separated by an exon-exon boundary e.g. last exon & penultimate
- amplified region around 200 bp
- GC content: 50-60%
- minimum length: 18 nt , max length 24 nt (best: 20 nt)
- melting temperature: min 60°C, max 63°C, best 60°C
- maximum Tm difference: 10°C (shouldn't be more than 1°C in final pair)
- maximum 3' self complementary: 1
- maximum poly-x: 3

The primers that were chosen using these parameters were verified by "blasting" the primers sequences (Altschul *et al.*, 1990). The gene of interest should come out with the lowest expected (E) value and no other gene should be detected. The E-value is a parameter that

describes the number of hits that can occur by chance when searching a database of a particular size. The lower the E-value, or the closer it is to zero, the more "significant" the match is (Untergasser *et al.*, 2012).

4.3.9. PCR product purification for sequencing reaction

Real-time PCR product was purified using the QIAquick™ PCR purification kit (Qiagen, 28104) according to manufacturers instructions in another laboratory to prevent sample contamination. The primers used to generate PCR product were sent with purified product to Source Bioscience Ltd, Cambridge, UK. Source Bioscience performed was Sanger Sequencing to identify the sequence of the PCR product.

4.3.10. geNORM analysis – suitable reference genes

geNORM is an algorithm used to determine the most stable reference genes from a set of tested candidate reference genes in a given sample panel. A gene expression normalisation factor can be calculated for each sample based on the geometric mean of a user-defined number of reference genes. The geNORM kit was purchased from PrimerDesign Ltd, UK. This kit provided primers for some of the genes listed in table 4.3.

Xenopus laevis gene name	Gene symbol	Accession number/ XL genome browser CUFF	Sequence length (bp)	Product length (bp)	Tm (°C)	Sense primer	Anti-sense primer	References
XL SRY (sex determining region Y)-box 10	Sox10	NM_001088889	3,324	115	71.5	GATGAAGAAGAAGAAGAAAACAAAA	TCCAGTCGTAGCCATTTAACAC	Primer Design Custom *X. laevis* design
XL twist basic helix-loop-helix transcription factor 1	Twist1-a	NM_001085883	1,379	109	76.3	GAGTAACAGCGAGGAAGAGC	CTTCACTGAGATCGGACTGTC	Primer Design Custom *X. laevis* design
XL snail family zince finger 2	Snail2-a	NM_001086282	1,785	114	71.2	CCCTATTTCCTTGTTGCGTTTAA	CTTCGTAAAGCACCTGAGAATG	Primer Design Custom *X. laevis* design
XL Zic family member 3	Zic3	NM_001087619	2,364	107	68.2	TTGAACCAAGGCGGAAATG	CTTTGTTAGTCTGTAGCCATCT	Primer Design Custom *X. laevis* design
XL SRY (Sex determining region Y)-box 2	Sox2	NM_001088222	1,190	87	75.7	CGGGCATGTCTCTGGGATC	GCGAATGGGAAGAAGAGGTG	Primer Design Custom *X. laevis* design
XL SRY (sex determining region Y)-box 9	Sox9-a	NM_001090807	3,071	130	75.8	CACACATCAAGACCGAGCAA	CGGGTGATAGTTGGGTATGAAG	Primer Design Custom *X. laevis* design
XL paired box 3	Pax3-a	NM_001095524	3,109	123	77.1	GGCTCTGATATTGACTCCGAAC	CGGGTAGTGGGTTCTCTCG	Primer Design Custom *X. laevis* design
XL proto-oncogene c-myc II	Myc	NM_001090653	2,487	93	73.8	GAAACACCACCCATCAGCAG	CTCTTCCTCGTCGCAGTCT	Primer Design Custom *X. laevis* design
XL Zic family member 1	Zic1	CUFF.8063.1	2,435	140	81.6	GCACGTTCATACATCGGACA	TGGACCTTCATGTGCTTCCT	Christopher Ford
XL distal-less homeobox 5	DLX5	CUFF.15807.1	1,301	142	82.9	GAGAGCTGCCTCCAGAACAC	GTTCCCACACCACTGGAGAC	Christopher Ford
XL homeobox containing peptide Xhox 7.1	MSX1b	BC081101	1,619	145	84.3	AAAGCCCAAGCTTCTCACCT	TGCTTCTGCCTGAACTTCCT	Christopher Ford
XL forkhead box D3	FoxD3b	NM_001085609	1,756	148	85.7	GATGCAGAGGGTAAGGGTGA	TCAGGGTGAGCTTCTTCTGG	Christopher Ford
XL snail family zinc finger 1	Snail1	CUFF.39257.1	1,917	151	80.5	CCTCTTGTCTGGGACACTGG	AAGGGCTGATGGGAGACTTT	Christopher Ford
XL AP-2 alpha (activating enhancer binding protein 2 alpha) (tfap2a-a)	AP2a	NM_001087569	1,936	132	81.6	GAGCAAGTAACGCGGAAGAA	CTGTATCCCAGGCTCCAGAA	Christopher Ford
XL gastrulation brain homeobox 2, gene 2	GBX2.2	CUFF.32795.1	2,310	130	81.1	TGCTGCCTTCTCTGCTTCT	GCTTCCTTCCCAGACTCCTC	Christopher Ford
XL inhibitor of DNA binding 3, dominant negative helix-loop-helix protein	ID3	CUFF.8787.1	1,788	154	81.9	CAAGGGACCAGGTATGGATG	CCTGGCACCAACTCTTTCAG	Christopher Ford
XL basic-helix-loop-helix transcription factor hairy2	Hairy2	AF139914	1,804	138	86.6	GCCATGAATTACCAGCAACC	GCCTCCCTGGAATACCTTTG	Christopher Ford

Table 4.2: Neural crest primers

***Xenopus laevis* gene name**	**Gene symbol**	**Accession number/ XL genome browser CUFF**	**Sequence length (bp)**	**Product length (bp)**	**Tm (°C)**	**Sense primer**	**Anti-sense primer**	**References**
XL Actin, beta	actb	NM_001088953	1,662	139	77.1	**PRIMER SEQUENCES PROTECTED BY INTERNATIONAL COPYRIGHT LAW**		Primer Design *X. laevis* GeNORM kit
XL Eukaryotic translation elongation factor 1 alpha 1	eef1a1	NM_001087442	1,730	149	79.1	**PRIMER SEQUENCES PROTECTED BY INTERNATIONAL COPYRIGHT LAW**		Primer Design *X. laevis* GeNORM kit
XL Ornithine decarboxylase 1	odc1	NM_001086698	1,973	151	77.6	**PRIMER SEQUENCES PROTECTED BY INTERNATIONAL COPYRIGHT LAW**		Primer Design *X. laevis* GeNORM kit
XL Glyceraldehyde-3-phosphate dehydrogenase	gapdh	NM_001087098	1,183	106	71.4	**PRIMER SEQUENCES PROTECTED BY INTERNATIONAL COPYRIGHT LAW**		Primer Design *X. laevis* GeNORM kit
XL Succinate dehydrogenase complex, subunit A, flavoprotein	sdha	NM_001087301	2,349	166	78.1	**PRIMER SEQUENCES PROTECTED BY INTERNATIONAL COPYRIGHT LAW**		Primer Design *X. laevis* GeNORM kit

Table 4.3: Reference gene primers

4.4. Statistics

4.4.1. Statistical analysis

The data for real-time PCR experiments was analysed using the 7500 FAST software. Measured C_t values for real-time PCR technical and biological replicates for each gene of interest were analysed using the NORMA-gene algorithm (Heckmann *et al.*, 2011). NORMA-gene reduces systematic and artificial between-replicate bias utilising the entire data set of the target genes being studied. NORMA-gene is applicable to small data sets greater than five genes of interest and is used as my primary analysis tool as it produces equal or better normalisation compared to delta-delta C_t method (Heckmann *et al.*, 2011). NORMA-gene reduces systematic (e.g. general effects of sample preparation such as RNA extraction) variance and does not change relative differences between treatments. A difference in relative normalised expression of the target genes between leflunomide -treated and -control samples was assessed using the student's *t-test*. leflunomide affects gene transcription, thus impacting upon both metabolic and neural crest pathways making reference gene normalisation unreliable using the delta-delta C_t method (Smith and Hall, 1990).

5. Results

5.1. Real-time PCR primer design and optimisation

For this study novel primers were designed and optimised for *Xenopus laevis* to quantitatively validate changes in gene expression profiles due to leflunomide treatment. Genes involved in neural crest formation that are sensitive to leflunomide treatment were confirmed by real-time PCR in order to validate *in situ* hybridisation data and RNA deep sequencing data from my host laboratory. The real-time PCR results generated in this thesis complements other data generated within my host laboratory.

The final primers can be seen in methodologies Table 4.2 with corresponding amplification plots and melt curves for each primer set in figures 5.2 & 5.3. Each individual primer set satisfies the characteristics essential for excellent primer design as outlined by Apte & Daniel and Dieffenbach (Heanue and Pachnis, 2007; Le Lievre and Le Douarin, 1975) that were used to create the primers in this thesis. In table 4.2, it can be seen that each of the primers were within the 18 to 22 bp range with the exception of some primers that had additional adenine (A) bases at the 3' end to aid oligonucleotide annealing. Primers that had similar melting temperatures (T_m) within 5°C of one another were run on the same plate. The guanine (G) and cytosine (C) ratio for each primer was within the range of 50 to 60 %. Ideally, the G and C content is optimal in the range of 45 to 50 %, however, primers that had a GC content outside of this range performed as expected. Ten primer sets were novel designs to the study and have not been previously published, these include: Zic1, Dlx5, Msx1b, FoxD3, Snail2, Ap2a, GBX2.2, Id3a and Hairy2. An external company named PrimerDesign Ltd designed nine primers that were also novel and these include: Sox10, Sox2, Sox9a, Twist1a, Snail2, Zic3, Pax3a and cMyc.

PrimerDesign Ltd designed primers that were unable to be generated by myself as they failed to amplify sequence specific transcript from target cDNA. Gene accession numbers and cufflink ID's for those primers designed from the *Xenopus* Genome Browser (available from Dr Simon Moxon) are listed in table 4.2. An average of five primer sets were generated for each gene of interest and only those that met the criteria outlined in figure 5.1 were used to create a putative bank of *Xenopus laevis* neural crest primers.

A strategy including criteria described in the method 4.3.9 was devised during optimisation of the real-time PCR set-up. This strategy was adapted and altered from Apte & Daniel and Dieffenbach to fit the requirements for using real-time PCR to detect gene expression within *Xenopus laevis* samples (Figure 5.1.) (Heanue and Pachnis, 2007; Le Lievre and Le Douarin, 1975).

For the evaluation of each primer set, both specificity and sensitivity tests were performed. The basic local alignment search tool (BLAST) (Altschul *et al.*, 1990) was used to compare sequences of interest against various gene and genome databases, such as Ensembl (http://www.ensmbl.org) and NCBI (http://www.ncbi.nlm.nih.gov). Initial BLAST homology searches discovered that the newly designed primers were specific to the gene of interest. This was also confirmed experimentally, when the amplicons were identified at specific stages of *Xenopus* development with their known temperature signatures. Primer specificity was observed by melt curve analysis as tall sharp melt curves were observed for all validated primer sets. Genes of interest were unamplified in the presence of genomic DNA to test the specificity of the primers that were synthesised from genes that have only one exon. The occurrence of false positives generated in the method outlined previously as a result of specificity issues would thus be limited or extant. The amplification plots and melt curves for the neural

plate border genes are shown in figure 5.2, the neural crest specifier plots are shown in figure 5.3 and for the reference genes (table 4.3) used in the geNORM analysis are shown in figure 5.4.

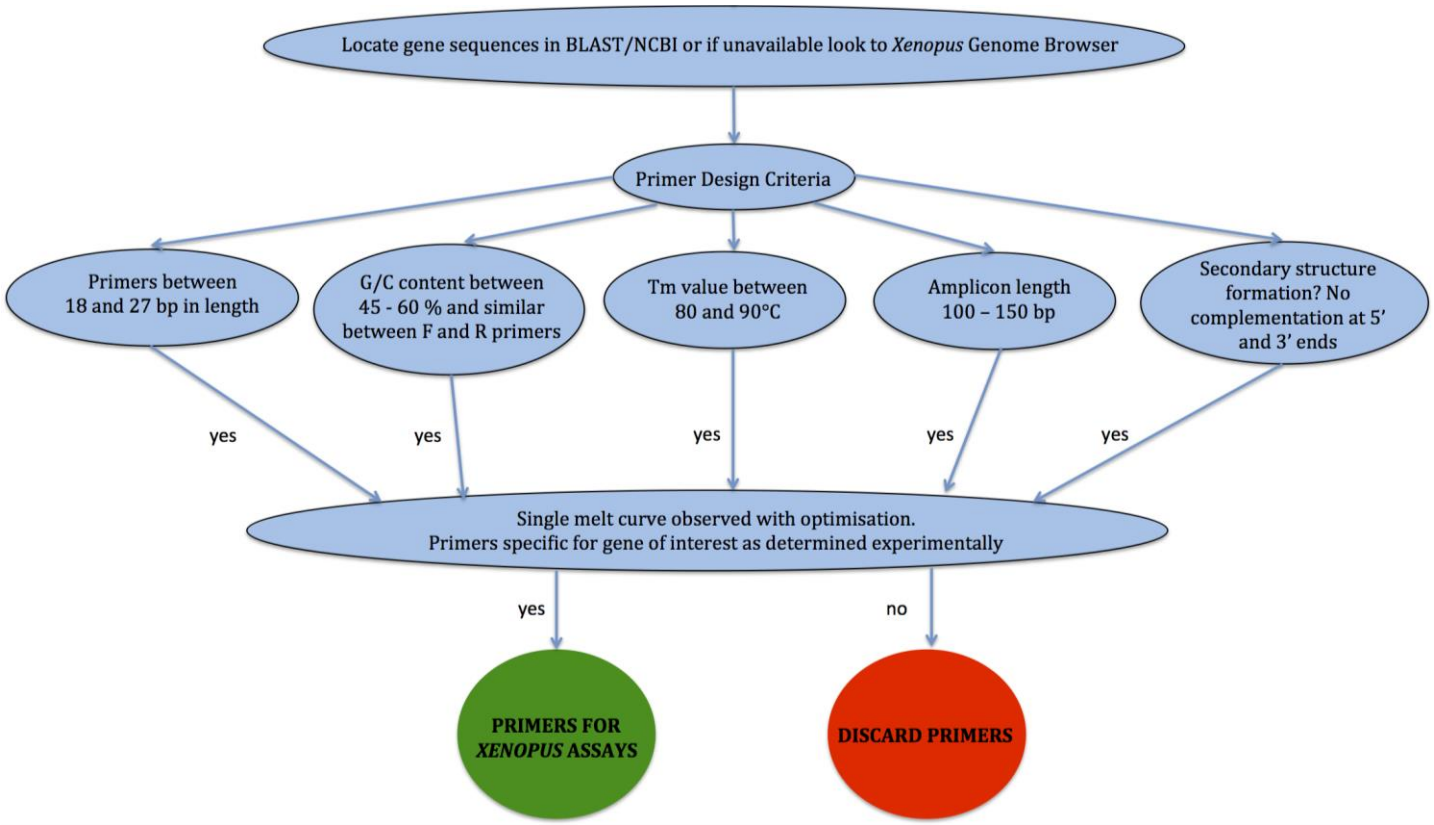

Figure 5.1: Primer design and optimisation workflow chart
An illustration of the management strategy used to outline the minimal criteria for the primer design/selection process.

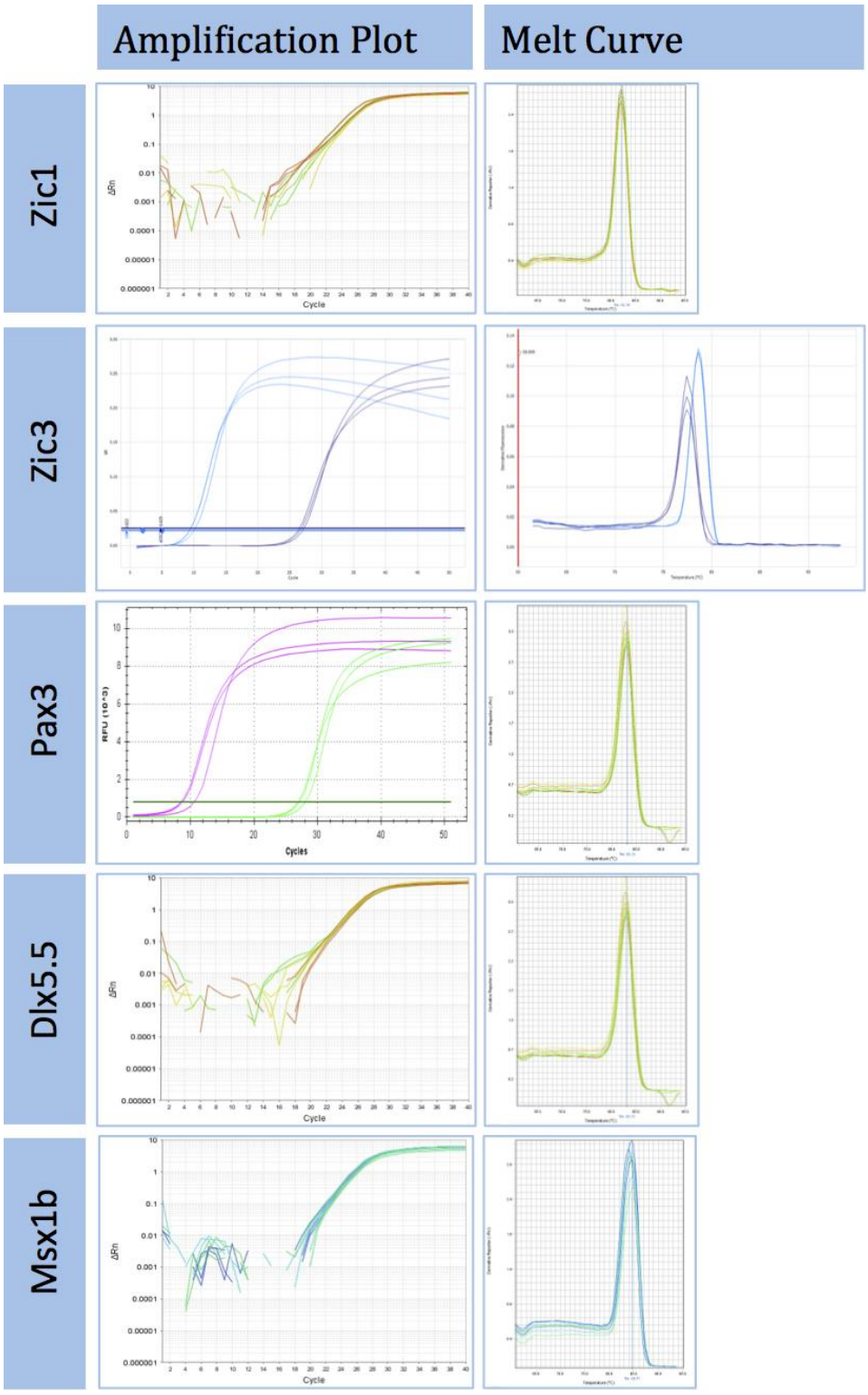
Amplification Plot
Melt Curve
Zic1
Zic3
Pax3
Dlx5.5
Msx1b
Cycle
Cycles
RFU (10^-3)

Figure 5.2: Neural plate border amplification plots and melt curve analysis.
The neural plate border genes Zic1, Zic3, Pax3, Dlx5.5 and Msx1b were amplified from stage 18 template cDNA synthesised using SuperScriptII and detected using SYBR FAST. The primer sets for genes Zic1, Dlx5.5 and Msx1b were designed in house and PrimerDesign Ltd designed mixed primers sets for Zic3 and Pax3. Zic3 and Pax3 were amplified with 18s RNA control (Light blue and pink, respectively). Fluorescence signals from FAST SYBR measured in channel 1 (520 nm) for amplification plots and melt curves. Amplification plot axis labels: cycle number (x-axis), ΔRn (y-axis). ΔRn is the reporter signal normalised to the fluorescence signal of ROX (an inert dye in SYBR reagents). Melt curve axis labels: Temperature (°C) (x-axis), Change in rate of relative fluorescence units (-d(RFU)T/dT) (y-axis).

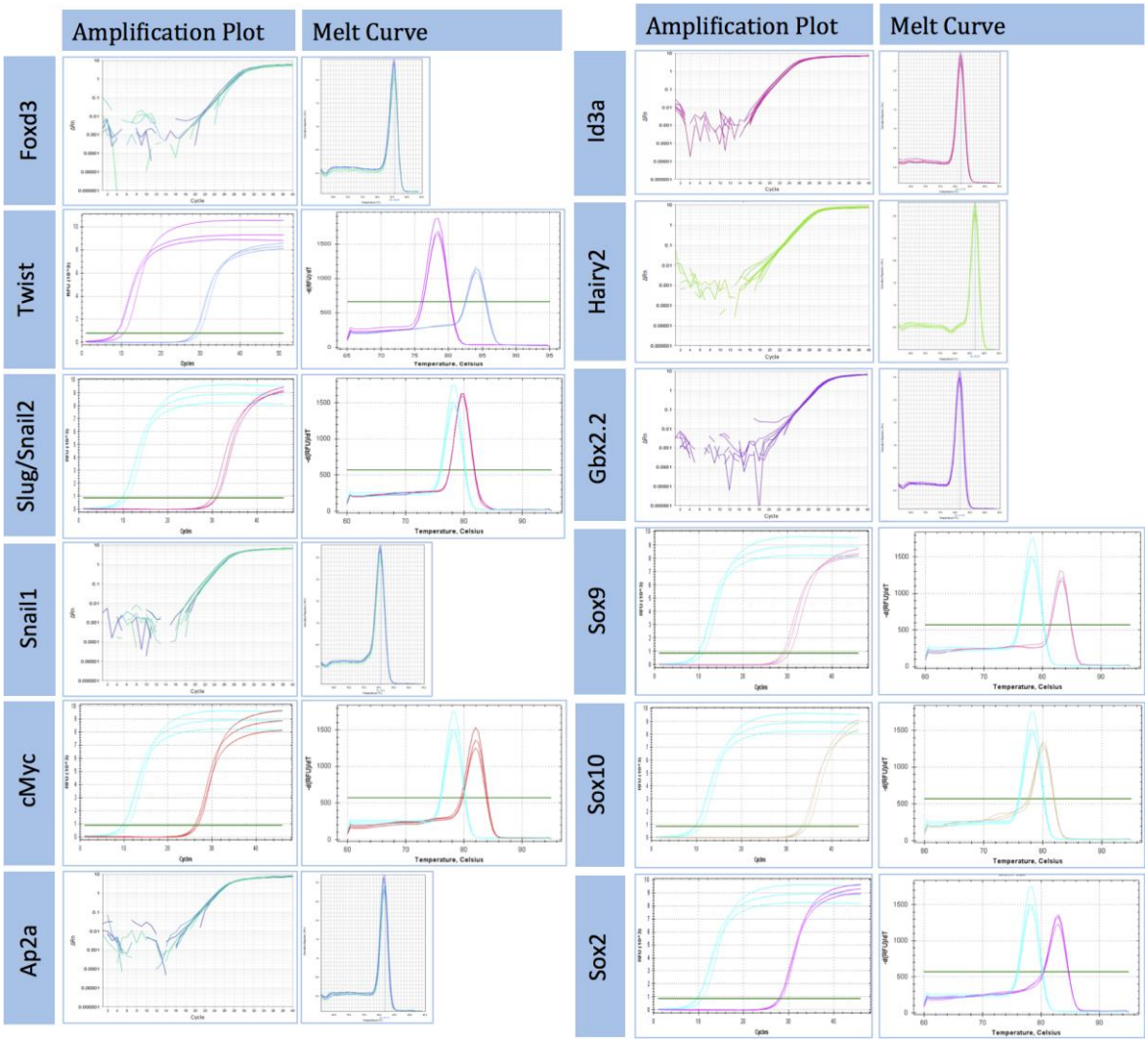

Figure 5.3: Neural crest specifier amplification plots and melt curve analysis including the pan neural marker Sox2.
The neural crest specier genes FoxD3, Id3a, Twist, Hairy2, Slug/Snail2, Gbx2.2, Snail1, Sox9, cMyc, Sox10, Ap2a and the pan neural marker Sox2 were amplified from stage 18 template cDNA synthesised using SuperScriptII and detected using SYBR FAST. The primer sets for genes FoxD3, Id3a, Hairy2, Gbx2.2, Snail1 and Ap2a were designed in house and PrimerDesign Ltd designed mixed primers sets for Twist, Slug/Snail2, Sox9, cMyc, Sox10 and Sox2. Twist, Slug/Snail2, cMyc, Sox9, Sox10 and Sox2 were amplified with 18s RNA control (pink, red, blue and pink, respectively). Amplification plot axis labels: cycle number (x-axis), ΔRn (y-axis). ΔRn is the reporter signal normalised to the fluorescence signal of ROX (an inert dye in SYBR reagents). Melt curve axis labels: Temperature (°C) (x-axis), Change in rate of relative fluorescence units (-d(RFU)T/dT) (y-axis).

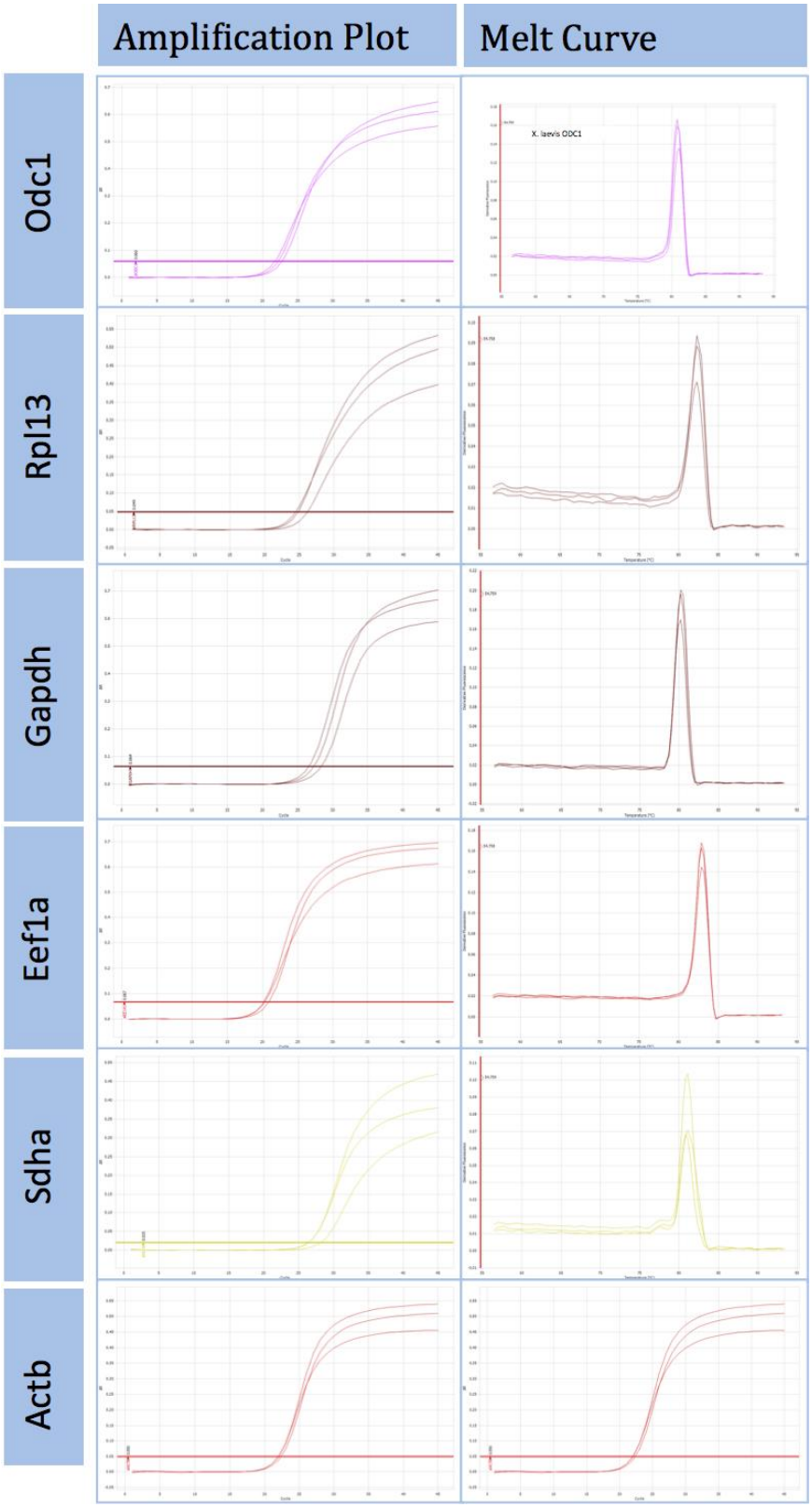
Amplification Plot
Melt Curve
Odc1
Rpl13
Gapdh
Eef1a
Sdha
Actb
X. laevis ODC1

Figure 5.4: Reference genes used for geNORM analysis amplification plots and melt curve analysis
The reference genes for geNORM analysis ornithine decarboxylase 1 (Odc1), ribosomal protein L13 (Rpl13), glyceraldehyde 3-phosphate dehydrogenase (Gapdh), eukaryotic translation elongation factor 1A (Eef1a), Succinate dehydrogenase complex, subunit A (Sdha) and beta actin (Actb) were amplified from stage 18 template cDNA synthesised using SuperScriptII and detected using SYBR FAST. PrimerDesign Ltd designed the mixed primer sets for these reference genes. Amplification plot axis labels: cycle number (x-axis), ΔRn (y-axis). ΔRn is the reporter signal normalised to the fluorescence signal of ROX (an inert dye in SYBR reagents). Melt curve axis labels: Temperature (°C) (x-axis), Change in rate of relative fluorescence units (-d(RFU)T/dT) (y-axis).

5.2. Confirming leflunomide batch inhibits Sox10 expression by *in situ* hybridisation and that Sox10 primers are specific by sequencing

In order to validate that the effect of leflunomide observed in the real-time PCR assays is genuine, whole mount *in situ* hybridisation was performed to detect Sox10 expression. Sox10 is a neural crest cell gene specifically expressed in the neural crest region of early embryonic stage embryos. Leflunomide specifically affects Sox10 gene expression at 60 μM where loss of expression is observed. The effect of leflunomide at 60 μM was quantified by assigning embryos into separate divisions of no effect, partial loss and complete loss (figure 5.5). Sox10 expression in control embryos (n=51) displayed a wild type phenotype in the neural crest region. Leflunomide treated embryos (n_{total}=61) displayed a wild type phenotype of 14.7 % (n=9), a partial loss phenotype of 9.84 % (n=6) and a complete loss of expression in 75.41 % (n=46) of all embryos treated. These results confirmed the batch of leflunomide used to treat embryos elicits the expected efficacy as seen in other studies (unpublished data, Wheeler laboratory).

To confirm that the oligonucleotide primers designed are specific, sequencing was performed to validate the Sox10 amplicon generated by real-time PCR. Sox10 was chosen to validate primer specificity as it is only expressed in neural crest cells at stage 12 and leflunomide

specifically affects its expression. The oligonucleotide sequence identified in figure 5.6 has 100 % sequence homology to that of Sox10 identified under the accession number NM_001088889.1 in the NCBI database.

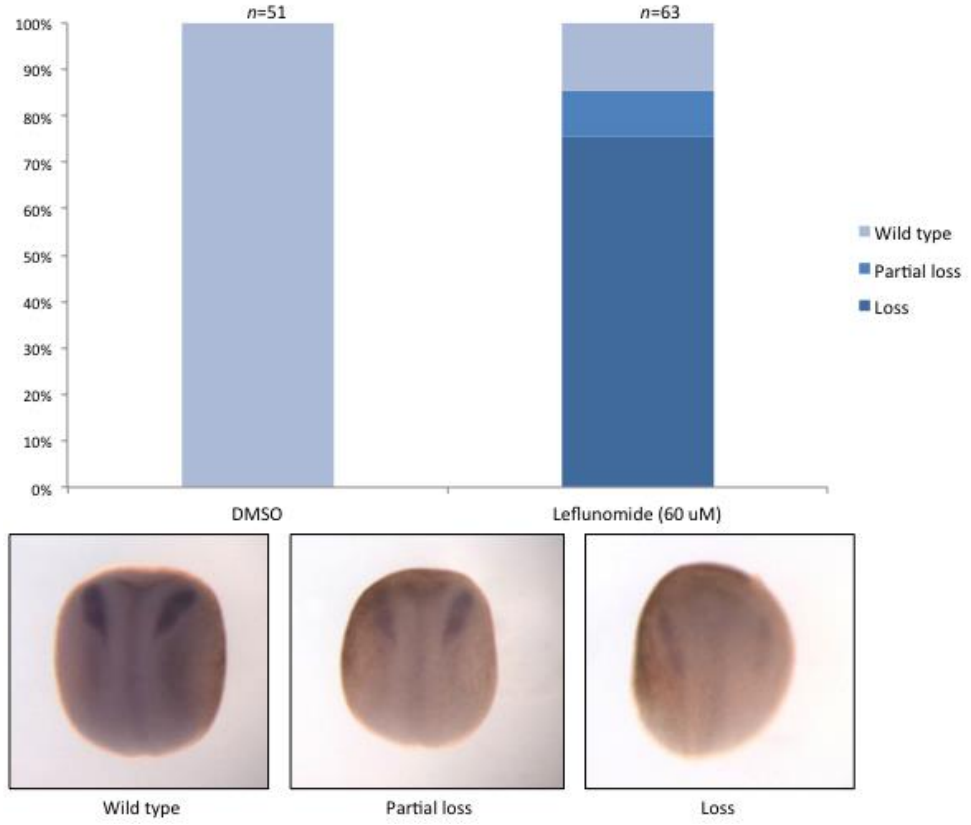

Figure 5.5: Quantification of Sox10 *in situ* hybridisation to confirm leflunomide batch efficacy
The expression of Sox10 was quantified by counting the number of observed wild type, partial loss and loss phenotypes observed after leflunomide treatment. [DMSO treated embryos showed no loss of expression and show wild type Sox10 expression in the neural crest (*n*=51).] The leflunomide treated embryos displayed a wild type phenotype of 14.7 % (*n*=9), a partial loss phenotype 9.84 (*n*=6) and loss of expression in 75.41 % (*n*=46) of the total number of leflunomide treated embryos (*n*=61).

TGTAATGTAACGGGTCTNTNACCTCCGTAGTAGGCATATACTGTCGAATG

CACGTTCTACACATGTGTGGTTCAATATTGTGCTACTGTACTGCGACA

Figure 5.6: Sox10 amplicon generated using Sox10 primers

5.3. Genomic averaging of multiple internal reference genes (geNORM)

To reveal the most stably expressed reference genes, genomic averaging of multiple internal reference genes (geNORM) was conducted. The geNORM algorithm determines the most stable reference genes from a set of six tested candidate reference genes in wild type *Xenopus laevis* samples. From this, it is possible to calculate a gene expression normalisation factor for each sample based on the geometric mean of six reference genes. The experimental layout was determined "perfect" by geNORM analysis. Results gained were from the same run to maximise experimental power.

geNORM calculates the gene expression stability measure (M) for a reference gene as the average pairwise variation (V) for that gene with all other tested reference genes. Stepwise exclusion of the gene with the highest M value allows ranking of the tested genes according to their expression stability (figure 5.7a) (Vandesompele *et al.*, 2002).

geNORM analysis revealed the optimal number of reference targets to be two (geNORM V<0.15 when comparing a normalisation factor based on the 2 or 3 most stable reference genes). As such, the optimal normalisation factor can be calculated as the geometric mean of reference targets rpl13 and odc1. High reference gene stability was observed (average geNORM M ≤ 0.5). This is observed when evaluating candidate reference targets on a homogenous set of samples (e.g. untreated cultured cells, or blood from normal individuals). The average expression stability of the reference genes are ranked from least stable to most stable in figure 5.7b. The reference genes are ranked least stable to most stable: actb, sdha, eef1a1, gapdh, rpl13 and odc1, respectively. Figure 5.7b summarises the optimal number of reference genes to normalise gene data, too. The two most stable genes revealed by geNORM analysis are odc1 and rpl13. Gapdh was identified

as the most unstable reference gene versus the five other target genes tested; however, Gapdh was determined stable for normalisation. In summary, *Xenopus laevis* provides a very stable system for gene expression assays using real-time PCR and all reference genes studied are suitable targets for normalisation.

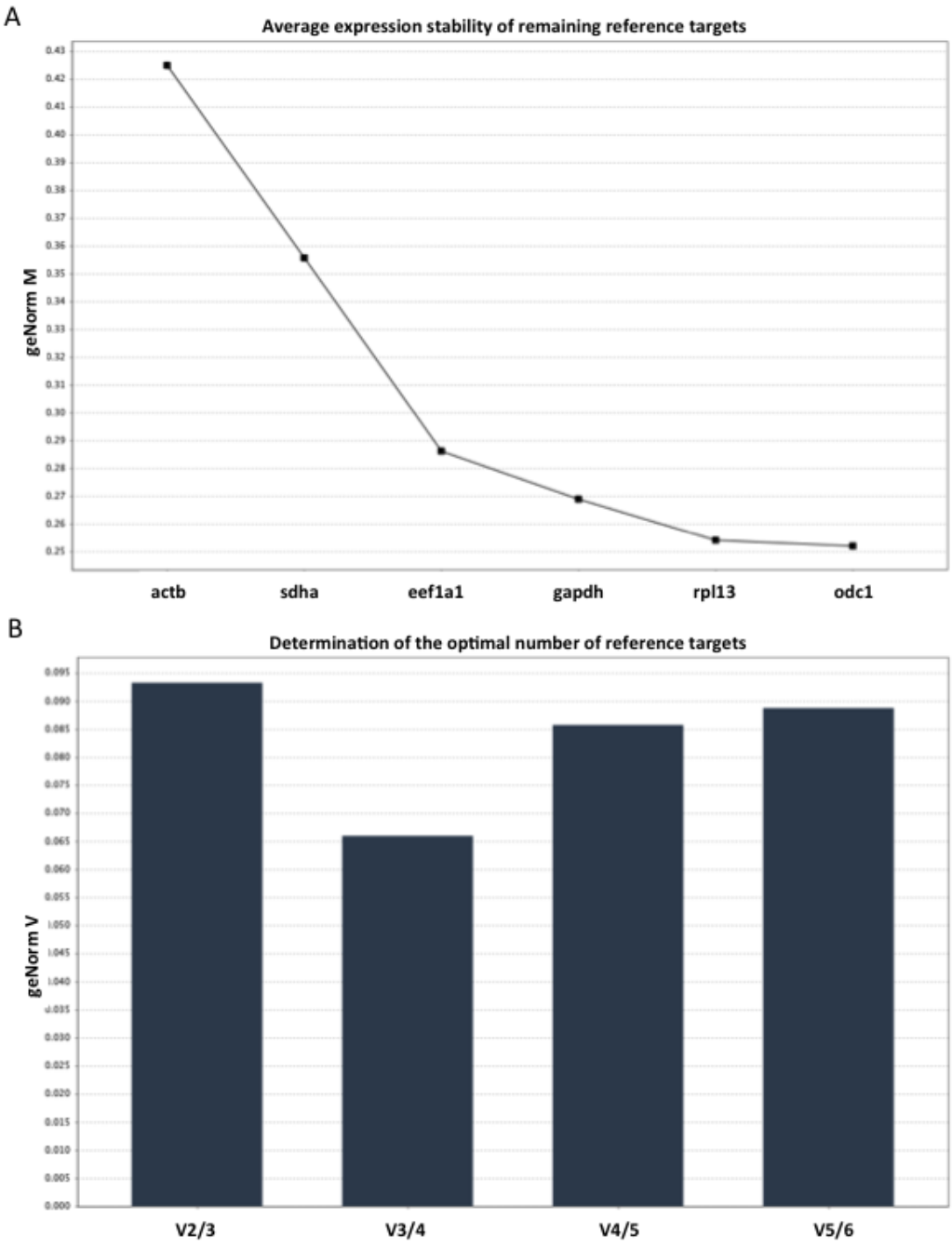

Figure 5.7: geNORM analysis of reference gene stability and the number of reference genes required for normalisation
GeNORM analysis was performed to establish how stable reference gene expression is in *Xenopus laevis* and the required number of reference genes to generate reliable data. (A) Average expression stability of remaining reference targets. (B) Determination of the optimal number of reference genes.

5.4. Leflunomide affects reference gene expression

In order to quantify the effect of leflunomide on reference gene expression without bias, cDNA was synthesised using two different reverse transcriptase kits purchased from different manufacturers. Assessing the ability of leflunomide to alter reference gene expression was analysed by comparing the cycle threshold value (C_t) of DMSO-treated samples against leflunomide-treated samples. Secondly, in order to optimise real-time PCR sensitivity by observing low cycle thresholds, it was necessary to compare different reverse transcriptase kits. The first reverse transcriptase kit used was SuperScript® II reverse transcriptase that has been genetically engineered by the introduction of point mutations in the RNase H active center to reduce RNase H activity. This structural modification eliminates degradation of RNA molecules during first-strand cDNA synthesis and can generate real-time PCR products up to 12 kb and enzymatic activity is optimal at 42°C. The SuperScript® II Reverse Transcriptase kit can use total or poly(A)$^+$ RNA. The second reverse transcriptase kit tested was PrimerDesign precision nanoScript. Precision nanoscript is a novel, mutated form of the Moloney Murine Leukemia Virus enzyme (M-MLV) enzyme. The enzyme contains multiple point mutations and has been engineered to enhance its processing power and versatility in a reverse transcription reaction. Principally, the enzyme retains greater activity over a wider range of temperatures than other modified MMLV enzymes and has greater thermo-stability. Reactions performed at higher temperatures are faster and increase the total cDNA yield. Higher temperature reactions also produce longer transcripts and are more reproducible

due to lower levels of secondary structure in the template. The enzyme also has an enhanced affinity for primer template complexes enabling efficient transcription of very low concentrations of RNA.

Leflunomide has been identified to regulate neural crest cell gene transcription and has been shown previously by RNA-sequencing in the Wheeler group to affect global gene expression in *Xenopus* animal cap assays. I have confirmed by real-time PCR that leflunomide affects the expression of the reference genes used in this thesis. The reference genes identified by geNORM analysis are highly expressed genes and are not co-regulated. Several conclusions can be drawn from data displayed in figure 5.8. Using cDNA synthesised from the superscript II kit, a difference in cycle threshold is observed. Secondly, the superscript II kit performed better than expected when compared to nanoScript as the cycle threshold for each reference gene was significantly reduced for superscript II versus nanoScript. The cycle thresholds observed for cDNA synthesised from precision nanoscript are close to the limit of detection. Lastly, an increase of transcript is observed in all leflunomide treated samples versus non-treated samples across all the reference genes assayed. To conclude, superscript II performed better than nanoScript and is therefore the chosen reverse transcriptase kit used in this thesis. The most significant conclusion that can be drawn from this data is that leflunomide affects all genes; therefore, reference genes are very difficult to find and use.

A) Invitrogen Ltd

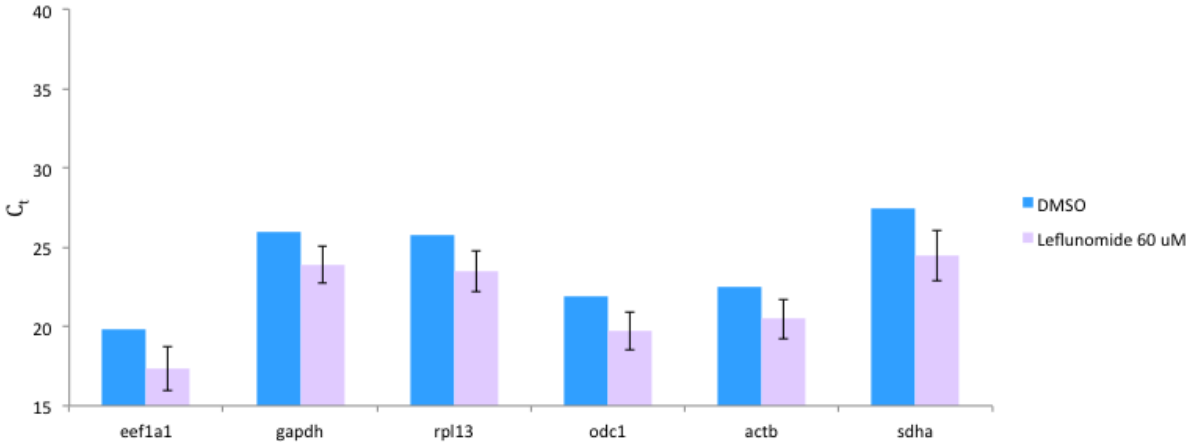

B) PrimerDesign Ltd

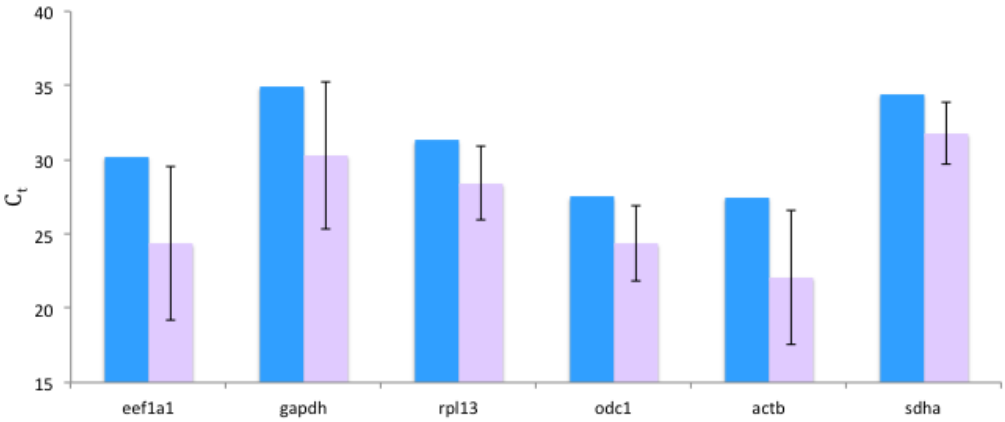

Figure 5.8: Identifying the optimal reverse transcriptase kit and analysis of the effect of leflunomide on reference genes
Graph A: Invitrogen superScriptII kit using Applied Biosystems SYBR reporter. Graph B: PrimerDesign nanoScript kit using Applied Biosystems SYBR reporter. Real-time PCR showing level of mRNA expression after 60 µM leflunomide treatment at stage 4 compared to DMSO-treated whole embryos. From graph A showing the level of expression of stage 18 reference genes from cDNA synthesised using the superScript kit are Eef1a1 (17.33 ± 1.37, p= 0.00014), Gapdh (23.89 ± 1.16, p= 0.00015), Rpl13 (23.46 ± 1.27, p= 0.00026), Odc1 (19.70 ± 1.20, p= 6.53x10-5), Actb (20.47 ± 1.24, p= 0.00746), Sdha (24.47 ± 1.60, p= 3.37x10-6). *= $p \leq 0.05$ to $p > 0.0000001$. From graph B showing the level of expression of stage 18 reference genes from cDNA synthesised using the nanoScript kit are Eef1a1 (24.36 ± 5.17, p= 0.11), Gapdh (30.31 ± 4.96, p= 0.21), Rpl13 (28.40 ± 2.48, p= 0.09), Odc1 (24.37 ± 2.52, p= 0.07), Actb (22.09 ± 4.52, p= 0.09), Sdha (31.77 ± 2.07, p= 0.06). NS = not significant. *= $p \leq 0.05$ to $p > 0.0000001$. Error bars are of the st.dev.

5.5. Testing reporter dyes in real-time PCR

In order to increase amplicon detection in reporter dye-based real-time PCR, two SYBR intercalating dyes were tested. SYBR reporter dye Applied Biosystems SYBR was compared with PrimerDesign FAST SYBR by plotting the cycle threshold for amplicons generated from primers that amplify reference gene rpl13 cDNA from stage 18 embryos (figure 5.9). PrimerDesigns' FAST SYBR has a more efficient enzyme than Applied Biosystems' SYBR green as a difference of two cycle thresholds is observed. To reduce the cycle thresholds of the genes of interest in this thesis it was necessary from this result to switch to using PrimerDesigns' FAST sybr.

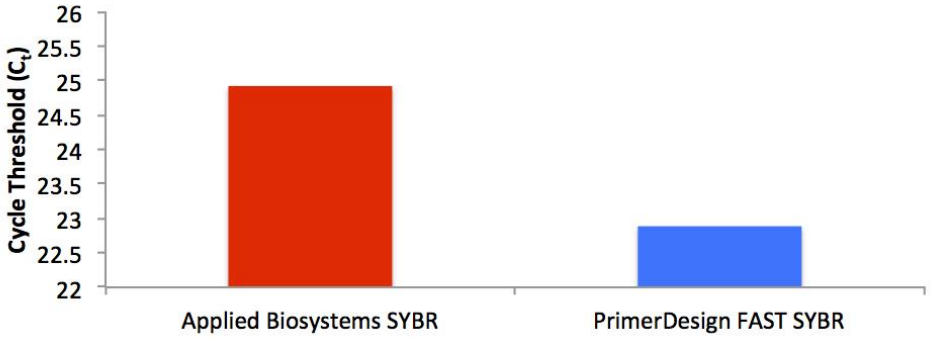

Figure 5.9: Testing SYBR reporter dyes to increase amplicon detection
Applied Biosystems SYBR green and PrimerDesign FAST SYBR were tested on cDNA from stage 18 wild type embryos using primers to amplify rpl13. PrimerDesign FAST SYBR detects rpl13 two cycle thresholds earlier than Applied Biosystems SYBR. PrimerDesign FAST SYBR is a more sensitive reporter.

5.6. Analysis of neural crest cell genes by real-time PCR

5.6.1 Neural plate and neural plate border specifiers

Previous experiments carried out in my host laboratory have shown that treatment of 60 µM leflunomide causes *Xenopus* embryos to display a loss of neural crest derivatives such as melanophores, cranio-facial cartilage and sensory neurons (unpublished data). The reduction in this

variety of derivatives suggests that the neural crest cells themselves are not forming or are not being specified into neural crest cells and consequently not undergoing differentiation into the different cell types they are able to form. Neural crest cells are initially induced at the neural plate border at stage 12 due to the upregulation of neural plate border specific genes such as Zic1, Zic3, Pax3, Dlx5 and Msx1. To explore the stage of neural crest development in that transcriptional elongation is important during early neural crest formation it was necessary to treat embryos at an early stage. Stage 4 embryos were treated with 60 μM leflunomide and allowed to develop until stage 12 where they underwent Trizol treatment to isolate total RNA and subsequent real-time PCR to identify neural plate border markers expression. Embryos were analysed by real-time PCR at stage 15 to investigate any possible effect leflunomide might have on general neural plate development by carrying out real-time PCR for the pan neural plate marker Sox2.

Real time PCR cycle thresholds for the neural plate border markers Zic1, Zic3, Pax3, Dlx5 and Msx1 after DMSO treatment are representative of wild type expression cycle thresholds of the neural plate border genes assayed in stage 12 and stage 15 embryos (figure 5.10). Post leflunomide treatment there appears to be no change in the expression of these neural plate border genes and their expression resembles that of the wild type expression when normalised to the DMSO treated embryos. However, Msx1b (0.54 ± 0.017666 s.dev, p=0.01) at stage 12 in response to 60 μM leflunomide is downregulated by 1.8 fold. These results suggest that leflunomide is not having an effect on early neural crest induction at the neural plate border. Comparably, the neural plate marker Sox2 (figure 5.11l) shows wild type expression in both the DMSO-treated and leflunomide-treated embryos by indicating that leflunomide has no effect on general neural development as confirmed by *in situ* hybridisation (summary figure 5.12). Real-time PCR data for

the neural crest border genes is shown in table 5.1. Validation of real-time PCR data was confirmed by a screen of neural plate border specifiers by *in situ* hybridisations (figure 5.12).

A

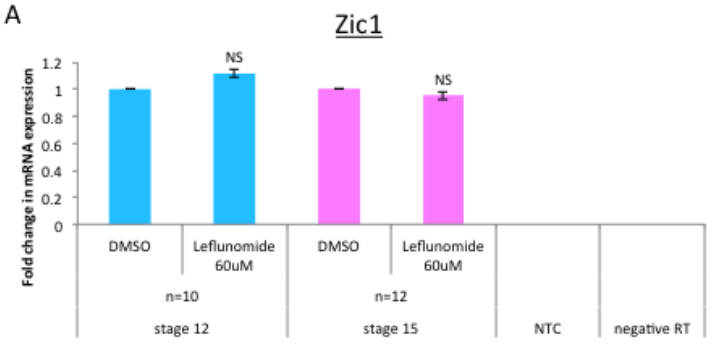
Zic1
Fold change in mRNA expression
1.2
1
0.8
0.6
0.4
0.2
0
NS
NS
DMSO
Leflunomide 60uM
DMSO
Leflunomide 60uM
n=10
n=12
stage 12
stage 15
NTC
negative RT

B

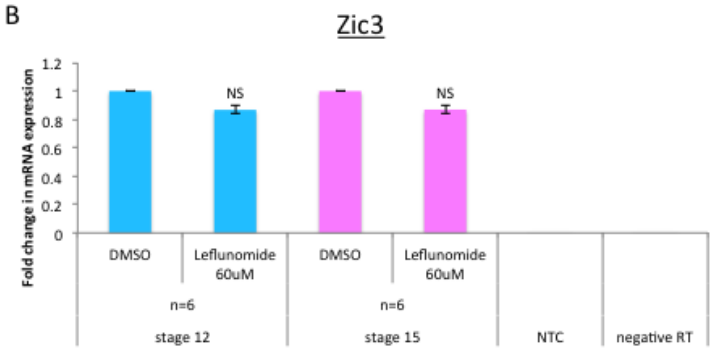
Zic3
Fold change in mRNA expression
1.2
1
0.8
0.6
0.4
0.2
0
NS
NS
DMSO
Leflunomide 60uM
DMSO
Leflunomide 60uM
n=6
n=6
stage 12
stage 15
NTC
negative RT

C

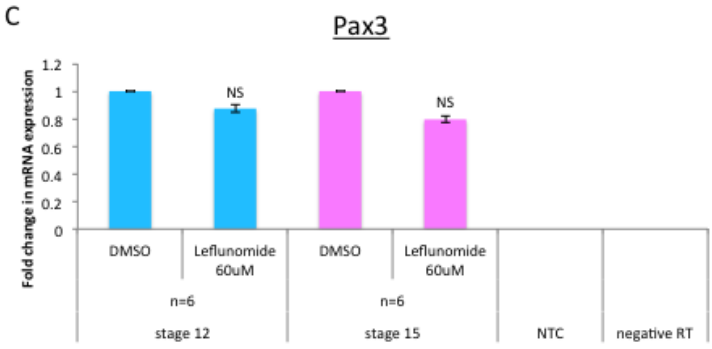
Pax3
Fold change in mRNA expression
1.2
1
0.8
0.6
0.4
0.2
0
NS
NS
DMSO
Leflunomide 60uM
DMSO
Leflunomide 60uM
n=6
n=6
stage 12
stage 15
NTC
negative RT

D

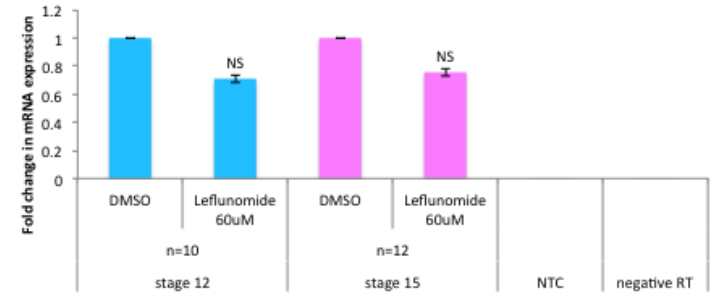
Dlx5
Fold change in mRNA expression
1.2
1
0.8
0.6
0.4
0.2
0
NS
NS
DMSO
Leflunomide 60uM
DMSO
Leflunomide 60uM
n=10
n=12
stage 12
stage 15
NTC
negative RT

E

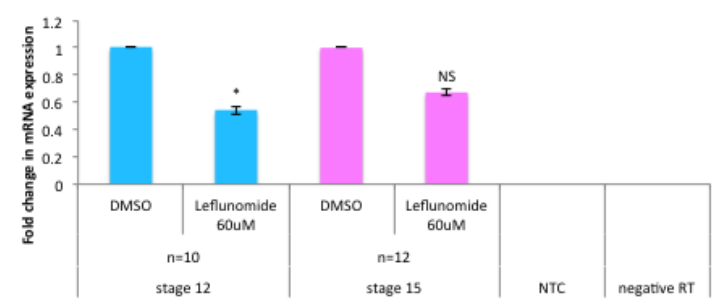
Msx1b
Fold change in mRNA expression
1.2
1
0.8
0.6
0.4
0.2
0
*
NS
DMSO
Leflunomide 60uM
DMSO
Leflunomide 60uM
n=10
n=12
stage 12
stage 15
NTC
negative RT

Figure 5.10: Neural plate border specifiers treated with 60 μM leflunomide

Real-time PCR showing level of mRNA expression after 60 μM leflunomide treatment at stage 4 compared to DMSO-treated whole embryos. Panel A to E show the level of expression of stage 12 neural crest border specifers: Zic1 (A), Zic3 (B), Pax3 (C), Dlx5 (D) and Msx1b (E) and a negative reverse transcription (RT) control and no target control (NTC) for each assay. No significant change in expression was seen for any of these genes NS = not significant. Msx1b at stage 12 was significantly downregulated. *= $p \leq 0.05$ to $p > 0.0000001$. Error bars are st.dev and the *n* number represents the number of technical replicates including two biological controls.

	Stage 12			Stage 15		
***Xenopus laevis* gene**	No. of real-time PCR runs with 3 technical replicates	Fold change ± s.d. (6*dp*)	Two-tailed Student's t-test	No. of real-time PCR runs with 3 technical replicates	Fold change ± s.d. (6*dp*)	Two-tailed Student's t-test
Zic1	10	1.12 ± 0.016723	*p*= 0.250	12	0.95 ± 0.023535	*p*= 0.97
Zic3	6	0.87 ± 0.017819	*p*= 0.215	6	0.87 ± 0.027121	*p*= 0.55
Pax3	6	0.87 ± 0.017694	*p*= 0.810	6	0.80 ± 0.026572	*p*= 0.07
DLX5	10	0.71 ± 0.016742	*p*= 0.222	12	0.76 ± 0.024595	*p*= 0.73
MSX1b	10	0.54 ± 0.017666	*p*= 0.010	12	0.67 ± 0.023532	*p*= 0.57

Table 5.1: Neural plate and neural plate border specifier real-time PCR data
Tabulated real-time PCR results for neural plate and neural plate border genes showing fold change plus/minus standard deviation and t-test to shown significance of gene expression on stage 12 and stage 15 embryos treated with 60 μM leflunomide.

5.3.2 Neural crest specifiers

Following induction at the neural plate border the neural crest cells then undergo specification. A number of genes have been shown to be involved in this process. To analyse the effect of leflunomide on neural crest specification, real-time PCR experiments were carried out using a range of neural crest specifying genes. Embryos were treated with 60 μM leflunomide and left to develop until stage 12 and stage 15 where they then underwent processing for real-time PCR of neural crest specifier genes.

The most obvious downregulation for these neural crest specifiers was seen after real-time PCR analysis of Slug and Sox10. The real-time PCR results showed that Slug/Snail2 levels in the 60 μM leflunomide-treated embryos at stage 12 and stage 15 were downregulated by 1.9 fold (0.51 ± 0.017883 st.dev, p= 1.03 x 10^{-08}) and 2.5 fold (0.40 ± 0.026547 st.dev, p= 2.99 x 10^{-07}), respectively (figure 5.11e). Likewise, Sox10 levels of 60 μM leflunomide-treated embryos at stage 12 and stage 15 were downregulated by 2.4 fold (0.42 ± 0.017662 st.dev, p= 3.38 x 10^{-13}) and 1.7 fold (0.60 ± 0.027310 st.dev, p= 8.02 x 10^{-08}), respectively (figure 5.11j). Other neural crest specifiers showed some downregulation of expression but not as striking as Slug and Sox10 at both stage 12 and stage 15. cMyc expression in the neural crest region shown by *in situ* hybridisation (figure 5.12c) was shown to be obliterated, however, real-time PCR could not reflect this as cMyc is expressed in neural tissue where leflunomide does not alter its expression (Hatch and Wheeler, unpublished). cMyc is an early neural crest specifier and starts to be expressed in the neural crest at stage 12 as detected by real-time PCR. DMSO treated embryos showing wild type cMyc expression (figure 5.12) show expression in the early neural crest cells in the anterior of the embryo and also dorsal neural tissues. cMyc is not specific for neural crest and plays a role in determining other tissue types. Real-

time PCR revealed cMyc to be downregulated by 1.5 fold (0.68 ± 0.017355 st.dev, p= 0.0002) in stage 12 embryos treated with 60 μM leflunomide. Sox10 wild type expression shown in figure 5.5j is specific for the neural crest cells at stage 15 and continues to be expressed in migrating neural crest cells where its expression is crucial for neural crest cell differentiation. Along with cMyc this neural crest specifier showed a striking downregulation of expression after leflunomide treatment that was detected by real-time PCR.

Additional neural crest specifier genes that were assayed at stage 12 and stage 15 include FoxD3, Gbx2.2, Twist, Id3, Slug/Snail2, Hairy2, Snail1, Sox9, cMyc, Sox10, and Ap2a. These data are represented in table 5.2. These all show specific expression in the neural crest cells by *in situ* hybridisation (Hatch and Wheeler, unpublished data). Post leflunomide treatment these neural crest specifiers show some downregulation of expression (figure 5.11) with the exception of FoxD3 (figure 5.11a), Hairy2 (figure 5.11f), Sox9 (figure 5.11h) and Ap2a (figure 5.11k), which are unaffected or are upregulated by 60 μM leflunomide treatment. Sox2 is a neural marker and leflunomide does not affect its expression. FoxD3 expression is seen to increase at stage 12 and Hairy2 expression is seen to increase at stage 12 and stage 15 which may be due to their expression in neural tissue and not due to leflunomide treatment directly. *In situ* hybridisation is poor at reflecting overexpression of genes, which may be a reason why the overexpression of these genes has only been reported in this thesis. However, RNA-sequencing has shown FoxD3 expression in *wnt* + *noggin* injected animal caps (neural crest samples) at stage 15 to be downregulated. This has been confirmed by *in situ* hybridisation. In the same samples RNA-sequencing has shown Hairy 2 to remain unaffected by leflunomide treatment, however, real-time PCR has revealed their expression to increase significantly at stage 12 and stage 15. Taken as a whole, these results suggest that leflunomide is acting on neural crest

cells during their specification to selectively inhibit their specification.

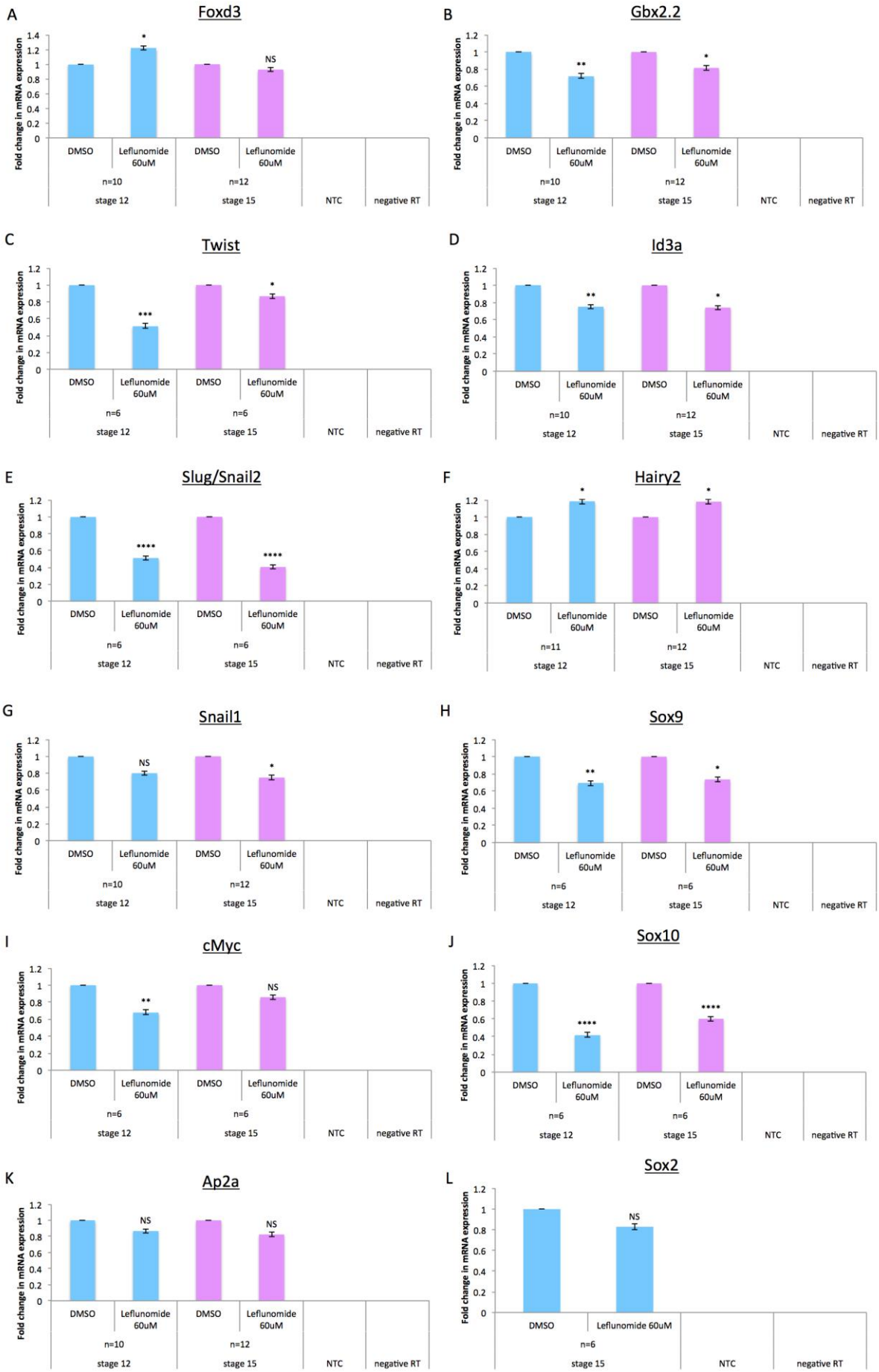
A
Foxd3
B
Gbx2.2
C
Twist
D
Id3a
E
Slug/Snail2
F
Hairy2
G
Snail1
H
Sox9
I
cMyc
J
Sox10
K
Ap2a
L
Sox2
Fold change in mRNA expression
DMSO
Leflunomide 60uM
n=10
n=12
n=6
n=11
stage 12
stage 15
NTC
negative RT
NS

Figure 5.11: Neural crest specifiers treated with 60 µM leflunomide

Real-time PCR showing level of mRNA expression after 60 µM leflunomide treatment at stage 4 compared to DMSO-treated whole embryos. Panels from A to K show the level of gene expression of neural crest specifiers: FoxD3 (A), Gbx2.2 (B), Twist (C), Id3a (D), Slug/Snail2 (E), Hairy2 (F), Snail1 (G), Sox9 (H), cMyc (I), Sox10 (J), Ap2a (K) and the pan neural marker Sox2 (L). All assays were performed alongside a negative reverse transcription (RT) control and no target control (NTC). The genes that show significance are indicated with *= $p \leq 0.05$ to $p > 0.0000001$,**=$p \leq 0.0000001$ to >0.0000000001 and ***= $p \leq 0.0000000001$ to ∞. NS = not significant. Error bars are of the st.dev and the *n* number represents the number of technical replicates including two biological controls.

	Stage 12			Stage 15		
***Xenopus laevis* gene**	No. of real-time PCR runs with 3 technical replicates	Fold change ± s.d. (6*dp*)	Two-tailed Student's t-test	No. of real-time PCR runs with 3 technical replicates	Fold change ± s.d. (6*dp*)	Two-tailed Student's t-test
FoxD3b	10	1.22 ± 0.016202	$p = 0.023$	12	0.93 ± 0.024376	$p = 0.49$
Twist	6	0.51 ± 0.016805	$p = 0.0001$	6	0.87 ± 0.027037	$p = 0.003$
Slug	6	0.51 ± 0.017883	$p = 1.03 \times 10^{-08}$	6	0.40 ± 0.026547	$p = 2.99 \times 10^{-07}$
Snail1	10	0.80 ± 0.017508	$p = 0.389$	12	0.75 ± 0.023267	$p = 0.02$
cmyc	6	0.68 ± 0.017355	$p = 0.0002$	6	0.86 ± 0.027141	$p = 0.09$
AP2a	10	0.87 ± 0.017618	$p = 0.292$	12	0.82 ± 0.023894	$p = 0.21$
GBX2.2	10	0.72 ± 0.016652	$p = 0.0002$	12	0.81 ± 0.023839	$p = 0.02$
ID3	10	0.75 ± 0.016638	$p = 0.0003$	12	0.74 ± 0.023482	$p = 0.03$
Hairy2	11	1.18 ± 0.017502	$p = 0.002$	12	1.18 ± 0.027018	$p = 0.03$
Sox9	6	0.69 ± 0.018026	$p = 0.0002$	6	0.74 ± 0.027283	$p = 4.64 \times 10^{-07}$
Sox10	6	0.42 ± 0.017662	$p = 3.38 \times 10^{-13}$	6	0.60 ± 0.027310	$p = 8.02 \times 10^{-08}$
Sox2 (NPB)	**NOT EXPRESSED**			6	0.83 ± 0.026703	$p = 0.14$

Table 5.2: Neural crest specifier genes and neural plate border specifier sox2 gene real-time PCR data
Tabulated real-time PCR results for neural crest specifier genes and neural plate border Sox2 gene showing fold change plus/minus standard devidation and t-test to shown significance of gene expression on stage 12 and stage 15 embryos treated with 60 μM leflunomide.

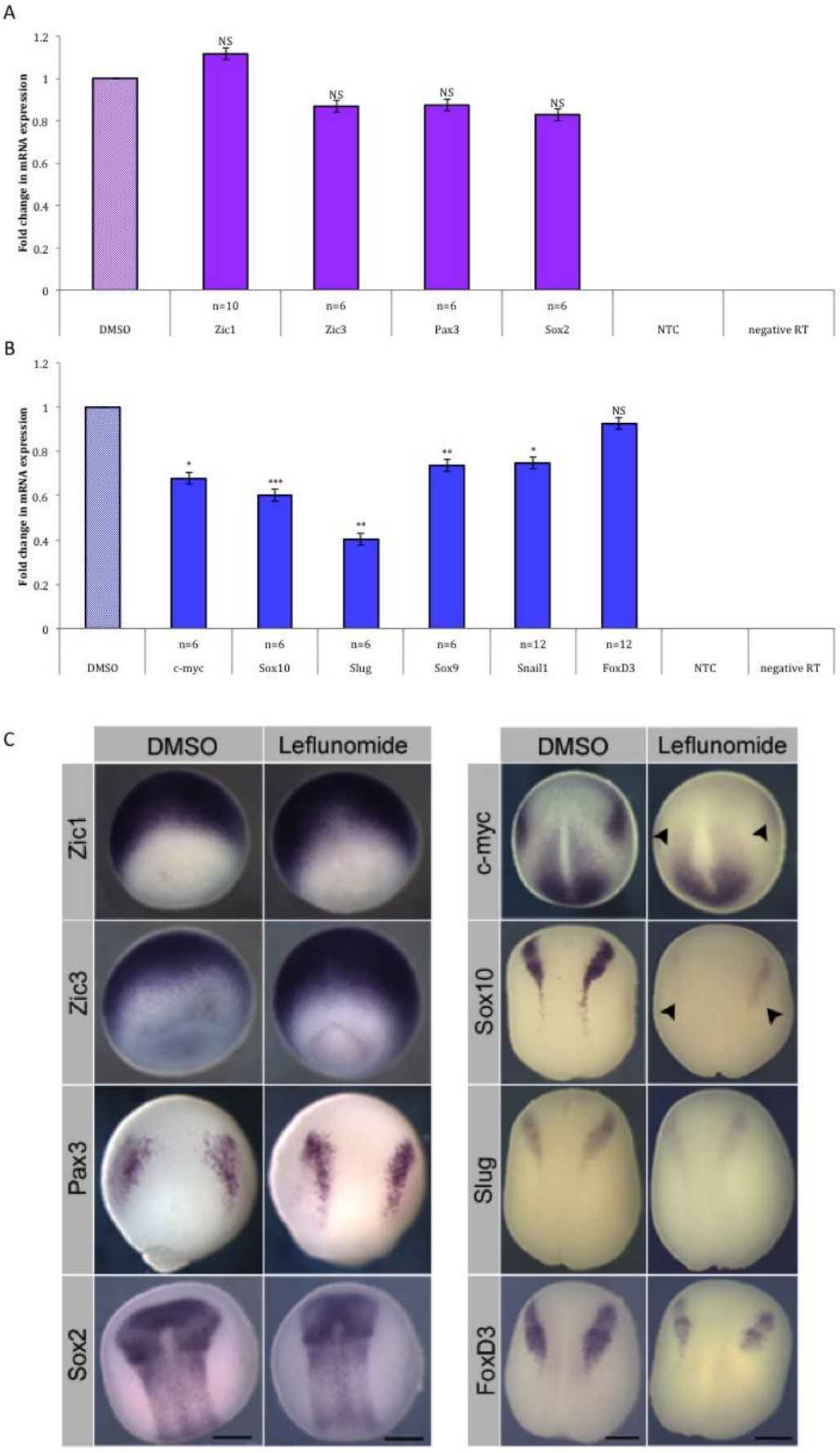
A
Fold change in mRNA expression
1.2
1
0.8
0.6
0.4
0.2
0
NS
NS
NS
NS
DMSO
n=10
Zic1
n=6
Zic3
n=6
Pax3
n=6
Sox2
NTC
negative RT
B
Fold change in mRNA expression
1.2
1
0.8
0.6
0.4
0.2
0
*
***
**
**
*
NS
DMSO
n=6
c-myc
n=6
Sox10
n=6
Slug
n=6
Sox9
n=12
Snail1
n=12
FoxD3
NTC
negative RT
C
DMSO
Leflunomide
Zic1
Zic3
Pax3
Sox2
DMSO
Leflunomide
c-myc
Sox10
Slug
FoxD3

Figure 5.12: Leflunomide inhibits the transcription of neural crest specifier genes.
(A) Whole mount *in situ* hybridisation carried out on embryos treated with either DMSO or 60 μM leflunomide from stage 4 until stage 13 (Zic1, Zic3 and Pax3) or stage 15 (Sox2). Neural plate border markers Zic1, Zic3 and Pax3 show no change in expression. Likewise, no change is seen for neural plate marker Sox2. (B) Whole mount *in situ* hybridisation carried out on embryos treated with either DMSO or 60 μM leflunomide from stage 4 until stage 13 (cMyc) or stage 15 (Sox10, Slug and FoxD3). Neural crest tissue-specific loss of cMyc expression is seen in the anterior region of the embryo (black arrows) and no loss of expression is seen in the posterior neural tissue. Loss of Sox10 expression (black arrows) and some loss or alteration of expression on Slug and FoxD3 can be seen. Scale bar represents 0.5 mm. (C) Real-time PCR showing level of mRNA expression after 60 μM leflunomide treatment at stage 4 compared to DMSO-treated whole embryos. Top panel shows the level of expression of stage 12 neural crest border specifers: Zic1, Zic3, Pax3, Sox2 and a negative reverse transcription (RT) control and no target control (NTC). No significant change in expression was seen for any of these genes (NS = not significant). Bottom panel shows the level of expression of neural crest specifiers cMyc at stage 12 (n=6) others at stage 15; Sox10, Slug, Sox9, Snail1 and a negative reverse transcription (RT) control and no target control. All of these show a significant decrease in expression level. *= $p \leq 0.05$ to $p > 0.0000001$,**=$p \leq 0.0000001$ to >0.0000000001 and ***= $p \leq 0.0000000001$ to ∞. Error bars are st.dev and the n number represents the number of technical replicates including two biological controls. Copyright authorisation: *In situ hybridisation* images courtesy of Dr Victoria Hatch for reproduction in this thesis to support real-time PCR data and for reference purposes only.

6. Discussion

6.1. The importance and relevance of studying the neural crest cells

Appearing synchronously alongside the vertebrate lineage, neural crest cells were principally responsible for the development of the "new head" and "new neck" of vertebrate animals. The neural crest was also responsible for the predatory behaviors that follow from these morphological changes (Gans and Northcutt, 1983; Kuratani, 2008). Interestingly, the diversity that we see today not only in humans, but also in Galapagos finches as studied by Charles Darwin (beak shape and size), are due to the governance of neural crest cells that form the cartilage and bones of the face, as well as pigmentation which arises from the neural crest cell derivative, the melanophore. Neural crest cells that form at the neural plate border between the neural and non-neural ectoderm, are unique as these cells migrate over long distances along stereotypical pathways to give rise to derivatives that are highly diverse and specialised (Knecht and Bronner-Fraser, 2002; Le Douarin *et al.*, 2007).

We aimed to study the neural crest in ever-greater detail, to reveal the intricate levels of control that allows this population of cells to succeed in its contribution to the developing embryo and in disease such as neurocristopathies and cancer. Our depth of understanding is not restricted to the potential of these cells to develop, but also allows us to uncover other self-renewing populations such as somatic stem cells and cancers. There are countless pathologies that involve the neural crest, due to their ability to proliferate, metastasise and their resilience against therapeutics. The potential for translational advances is enormous, as the genes that govern the neural crest may potentially represent therapeutic targets. A wealth of knowledge has been gained

from studying the neural crest and related pathologies, however, many questions still remain.

6.2. Primer design and selection process

In the present study, the objective was to quantitatively analyse the effect of leflunomide on neural crest cell gene regulation during early embryonic development. For this study, oligonucleotide primers were selected to target five neural plate border genes, eleven neural crest specifier genes and one pan neural plate marker gene Sox2. To further strengthen our hypothesis that leflunomide can specifically affect neural crest specification genes other neural plate markers such as Nestin, NeuroD1 and Sox1 are needed for real-time PCR analysis. These genes all have been identified as playing an important role in neural crest development in *Xenopus laevis* and other vertebrate species. To date, no single study has examined the simultaneous detection of these neural crest genes in *Xenopus* or any other species. The primers designed for *Xenopus laevis* are entirely novel and have not been previously published making this study useful for researchers to refer to for neural crest real time PCR primers.

Careful primer design was essential for progression of this present study, since the selection of non-optimal primers may incorrectly amplify unwanted DNA and cause problems further downstream. The primer characteristics of optimal primers for the purpose of identifying neural crest cell genes sensitive to leflunomide were that they would have high target specificity, are robust to reduce the occurrence of mispriming and that they detect amplicons with lower cycle thresholds. To ensure that the most suitable primers were synthesised, stringent design criteria were met (Bustin *et al.*, 2009).

Molecular biologists have conflicting views on the considerations for the most optimal primer design conditions. To illustrate this, Apte & Daniel and Dieffenbach (Heanue and Pachnis, 2007; Le Lievre and Le Douarin, 1975) suggests that the T_m between the forward and reverse primer should be similar; conversely, SantaLucia Jr. advocates the opposite methodology (Jiang *et al.*, 2002). The software that designs primers also has a role in these conflicting arguments as no two design programmes will generate primers that are identical for the same DNA sequence because matches are calculated by different algorithms. When primers are designed, the literature will only make reference to the primer design software used. Primer3 has been used in this thesis to design in-house primers, as Primer3 has been previously demonstrated to be exceptional for designing primers for sequences with both AT-and GC-rich regions and has a high success rate (Chavali *et al.*, 2005).

While computer software was used to enhance the selection of the most optimal target regions on the gene of interest, certain parameters were user-specified. User-specified selection of desired annealing temperatures and both the oligo and final amplicon sizes were defined to select primer sets. User-specified settings were then used by the design software to generate primers with defined criteria. User input was further needed to select the most ideal primer set from the top five matches generated algorithmically. A high degree of skill and primer design knowledge was required to then select the best of those five primer sets chosen for testing on cDNA. The chosen primers were considered suitable because of the fulfillment of essential primer design parameters: the closeness in T_m for sense and anti-sense primers, the GC content and marginal secondary structure formation. Disparity in T_m between the sense and antisense primer of each set was determined to be within a 1 – 2 °C range. The significance of satisfying these parameters is closely linked with primer specificity. Commonly seen in primer design is that specificity is lost when primer pairs are

inadequately matched for both T_m and GC content (Heanue and Pachnis, 2007). Primers that met these estimations were deemed to have a theoretically high efficiency for annealing and a reduced chance of miss-priming.

6.3. The importance of correct data analysis

Real-time PCR is the current state-of-the-art approach used to measure gene expression. This method can be applied in biological and biomedical research. Leflunomide was found to affect all the reference genes used in this thesis. Two reference genes that were included on plate runs were Rpl13 and Odc1, these genes were determined to be the most stably expressed genes in *Xenopus laevis*. Using the 2–[delta][delta]Ct method, where [delta][delta]Ct = [delta]Ct,sample - [delta]Ct,reference. I found that genes such as Sox10 and Slug where upregulated or remained unchanged due to leflunomide treatment at either stage 12 or stage 15 depending upon normalisation to Rpl13 or Odc1 (supplementary data). Normalisation in some instances gave conflicting results and did not agree with RNA-sequencing data and *in situ* hybridisation data already generated in our laboratory. The real-time PCR data generally agreed that neural plate marker genes were not affected by leflunomide, conversely, of all the neural crest specification genes analysed, all tended to upregulate their expression in response to treatment. These results were confusing and contradicted our working hypothesis that neural crest specification is affected by leflunomide. This data is available in the supplementary section of this thesis. In order to prove that my real-time PCR data did reflect the expected result and that using the comparative C_t method was unsuitable, another analytical approach was needed. The NORMA-gene method was employed and was found to correctly analyse my data, discussed next.

6.4. Drawbacks and solutions in real-time PCR data analysis

Real-time PCR is a robust technique, however, results can vary depending upon factors such as RNA integrity, reverse transcriptase efficiencies, sample-to-sample variations in amplification efficiency, and variation in cDNA sample loading. It is essential for the experimenter to reduce these variations are far as is possible (Heckmann *et al.*, 2011). Normalisation to an internal control is a sure way to reduce sample-to-sample variations in real-time PCR. The widely used internal control is attained using reference genes or better a normalisation factor derived from several reference genes using algorithms such as geNORM (Vandesompele *et al.*, 2002). Conversely, the use of reference genes suffer from a circular argument. For example, analysts normalise gene of interest expression data to exclude the systematic variation by using reference gene expression data gathered by the same method as the data that is required to be normalised. Therefore, we assume that reference genes are unaffected by experimental treatment(s). These assumptions are often logically valid because if the premises are true, the conclusion must be true. In many studies, reference genes are chosen at random and have not been validated for the particular experimental conditions. In my case leflunomide was found to affect all my reference genes that were validated for my model system (*Xenopus laevis*). These reference genes were validated in untreated embryos using geNORM, an approach used to find the most stably expressed reference genes. Searching for and validating reference genes is time consuming and very expensive and may not be successful or practical. Samples that are heterogeneous i.e. 10 embryos treated with leflunomide; requires a comprehensive normalisation approach. Conventional normalisation using reference genes can introduce unintentional random variation to the mean expression of genes of interest if the reference gene(s) being used are poor or are affected by treatment i.e. leflunomide. This inadvertently will result in invalid

conclusions being drawn from the data, which increases the risk of type I and type II statistical errors being made (supplementary data). I report the use of an algorithm, NORMAgene, which is a data driven normalisation approach that does not require the use of reference genes. This has allowed me to focus my research effort on studying neural crest cell genes to quantitate how sensitive these genes are to leflunomide treatment at different stages of development.

6.5. cMyc is sensitive to leflunomide treatment during early development

To identify which genes were sensitive to leflunomide treatment real-time PCR was performed to identify these genes. cMyc is sensitive to leflunomide treatment in the whole embryo, which has also been shown by *in situ* hybridisation and morpholino knockdown of neural crest markers. These experiments showed that leflunomide has no effect on the development of early neural plate border markers such as Zic1, Zic3, Pax3 at stage 12 and 15 and Msx1b at stage 15. The changes in gene expression were seen in genes involved in neural crest specification and differentiation such as Sox10. The two genes demonstrating the greatest level of knockdown by real-time PCR were Sox10, a neural crest specifier also expressed in the migrating neural crest, and Slug/Snail2, an early neural crest specifier. cMyc, which is also an early neural crest specifier, did not give the strongest knockdown in expression as it is not affected when expressed in neural tissue. Because these experiments were performed on whole embryos there was a homogenous mix of neural and neural crest cMyc transcript. By *in situ* hybridisation cMyc expression is lost completely in the neural crest region but remains unaffected in the neural folds.

Accumulating evidence indicates that neural crest formation is a complex, multistep process. cMyc has been shown to be an early neural

crest specifier. Studies in *Xenopus* have shown that myc is required for downstream neural crest specifiers such as Sox10 to be expressed. The expression of neural crest specifiers is important for the development of neural crest derivatives such as craniofacial cartilage, melanophores and sensory neurons (Bellmeyer *et al.*, 2003). Bellmeyer also reported that by knocking down cMyc expression in *Xenopus* results in the loss of expression of trigeminal placode markers such as Six1. A loss of expression of Sox10 was also observed in the trigeminal, seventh (VII), ninth (IX), and tenth (X) cranial ganglia (Bellmeyer *et al.*, 2003). I would hypothesise that if cMyc is the direct primary target of inhibiting transcriptional elongation in the neural crest then a loss of trigeminal placode markers would be observed after the knockdown of p-TEFb components using morpholinos. The same study showed this to be true by *in situ* hybridisation that tbx2, elrd and NeuroD after knock down of CyclinT1 and Cdk9 (Bellmeyer *et al.*, 2003). This provides convincing evidence that myc may undergo RNA polymerase pausing and transcriptional elongation.

It is a logical assumption for myc to be the direct primary target for gene regulation by transcriptional elongation and RNA polymerase pausing in the neural crest. Takahashi has recently shown that cMyc can undergo RNA polymerase pausing when Med26, a component of the super elongation complex is knocked out in stem cells (Adams *et al.*, 2008). Looking at all the evidence to date in conjunction with its role in neural crest cell specification a convincing argument can be made for cMyc to be a master regulator of gene regulation. To confirm that Sox10 was not also a direct target and that its downregulation is a consequence of the loss of myc expression, it is necessary to rescue myc expression using a myc construct after knockdown of the p-TEFb components CyclinT1 and Cdk9. Sox10 expression was rescued by the myc expressing construct which strongly supports the argument that Sox10 is not itself a target of p-TEFb but must be lost due to the loss of

cMyc signals from further upstream (Hatch and Wheeler, unpublished). This is illustrated in figure 6.1 to show the position of p-TEFb in neural crest specification for neural crest cell development.

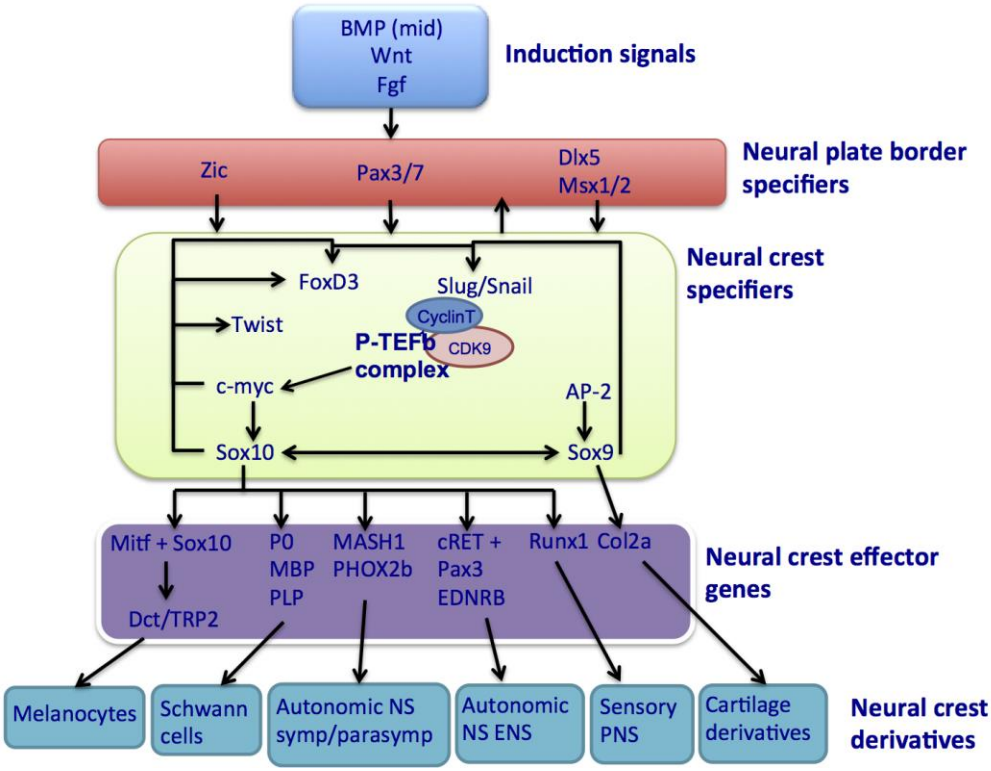

Figure 6.1: Schematic illustration of the position of p-TEFb in neural crest development
P-TEFb may target cMyc directly as loss of p-TEFb results in a downregulation of cMyc, Sox10 and other neural crest specification genes shown in this illustration. This hypothesis suggests that cMyc is the master regulator of Sox10 and that the changes in gene expression of other neural crest specifiers may be due to loss of Sox10. Shown here is an oversimplified gene regulatory network depicting the levels of gene regulation. Shown in this illustration from top to bottom are the inductive signals, neural plate border specifiers, neural crest specifiers, neural crest effectors and neural crest derivatives.

Wnt and BMP signalling play an important role in embryonic development but this relationship between these signalling cascades and cMyc is poorly understood. Myc has been shown in studies conducted in colon cancer to position itself downstream of Wnt signalling (Myant and Sansom, 2011). Conversely, an upregulation of Wnt is observed with a downregulation of cMyc in RNA-sequencing data of neural crest animal caps in the Wheeler laboratory. The

downregulation we observe in our data is not as extreme as our oberservations in *in situ* hybridisation data. We hypothesise that Wnt is upregulated in order to maintain myc in an equilibrated state, after downregulation of myc through inhibition of transcriptional elongation during early neural crest specification in stage 12 *Xenopus* embryos. Wnt expression must be upregulated in order to increase the amount of myc level to their endogenous level. There is also uncertainty to why BMP is upregulated in neural crest animal caps post leflunomide treatment as observed in our laboratories RNA-sequencing data. Follistatin is BMP antagonist that is also downregulated in this data. It may be that different levels of crosstalk are at play between Wnt and BMP in a tissue dependent manner and for these signals to have a mutual target in the same cell or tissue (Itasaki and Hoppler, 2010). To expand on this further it has been found that in the developing mouse kidney elevated levels of BMP signals caused an increase in canonical Wnt signalling which results in the formation of a phospo-Smad1/tcf4/ β-catenin complex. This complex is able to upregulate the expression of cMyc, which may provide an argument that there is a level of synergy between BMP and Wnt in order to increase cMyc expression (Hu and Rosenblum, 2005).

6.6. Melanoma and cMyc expression

cMyc is a proto-oncogene that does not require to be mutated to contribute to neoplastic transformation. Deregulated expression of cMyc at low levels is sufficient to initiate this process. The transforming ability of cMyc may be due to its ability to modulate gene expression and therefore, promote genes involved in oncogenesis and metastasis. cMyc is a protein with many functions that can affect genome stability and thereby, promote cancer cell development (Mai and Mushinski, 2003). In many cancers such as melanoma cMyc is found to be overexpressed resulting in enhanced cell proliferation and

differentiation. The expression of cMyc protein is tightly regulated by mitogens (Amati *et al.*, 1993), and both cMyc protein and mRNA have very short half-lives enabling finely tuned regulation of cMyc activity (Schlagbauer-Wadl *et al.*, 1999). cMyc is a neural crest cell gene that is closely regulated in migratory neural crest cells by transcriptional pause-release by recruitment of the p-TEFb complex (Hatch and Wheeler, unpublished). I hypothesis that by knocking out components of the p-TEFb complex in melanoma cells then cMyc expression can be knocked down which may result in real therapeutic benefits for melanoma patients. Small molecule compounds such as Cyclin and CDK inhibitors that specifically block the recruitment of p-TEFb components such as CyclinT and CDK9 in melanoma cell metastasis may have some therapeutic potential in the clinic. The proposed mechanism for the recruitment of p-TEFb to regulate the expression of cMyc is shown in figure 6.1.

6.7. Conclusions and future work

The work presented in this thesis shows that neural crest cell specifiers are sensitive to leflunomide treatment at early stages of development. This work has quantified the expression patterns of neural crest cell genes shown by *in situ* hybridisation experiments. I have also strengthened the argument that the regulation of transcriptional elongation is important for the development of neural crest cells. By inhibiting transcriptional elongation, a decrease in the expression of the neural crest specifier genes cMyc and Sox10 and other neural crest markers leads to developmental defects in the normal development of neural crest derivatives that include cranio-facial cartilage, sensory neurons and melanophores. cMyc has been shown here in stage 12 embryos to be sensitive to inhibition of transcription elongation and so it is likely that cMyc is a primary target of RNA polymerase pausing. Inhibition of cMyc has been shown by unpublished work in my host

laboratory to cause developmental defects. We also see a significant downregulation of Sox10 and Snail2/Slug expression during early development in response to leflunomide treatment. We know that Sox10 is not a primary target of RNA polymerase pausing as loss of Sox10 expression can be rescued by injection of cMyc RNA (Hatch and Wheeler, unpublished data).

To further validate these results it would be good to perform these experiments in animal cap tissue. By moving these leflunomide assays into animal caps the hope would be to see a more drastic downregulation of cMyc and other neural crest specifier genes. To confirm that cMyc is a primary target of transcriptional regulation, valuable data would be generated if loss of Sox10 expression was rescued with injected cMyc but a loss of endogenous cMyc was still observed. This may be performed using ChIP-PCR or ChIP-sequencing with specific antibodies against RNA pol II to elucidate at which location along the exon of the gene the polymerase is not generally located i.e absent at position Ser2 or Ser5. cMyc in other cell types has been shown to be paused, however, it would be developmentally relevant to reveal this in the *Xenopus* whole embryo or in neural crest animal caps by injection of wnt and noggin. The hypothesis that we would generate from this is that RNA pol II is normally found at the promoter region of cMyc revealing that if it is found 50 bases downstream of its promoter then it is held in a poised state. RNA polymerase pausing is known to be crucial in other cell types such as stem cells and it may be suggested that it is also specific for neural crest cells. Our laboratory will continue to unravel the developmental processes in neural crest regulation and reveal further the mechanisms that govern neural crest cell fates.

7. Appendix (supplementary material)

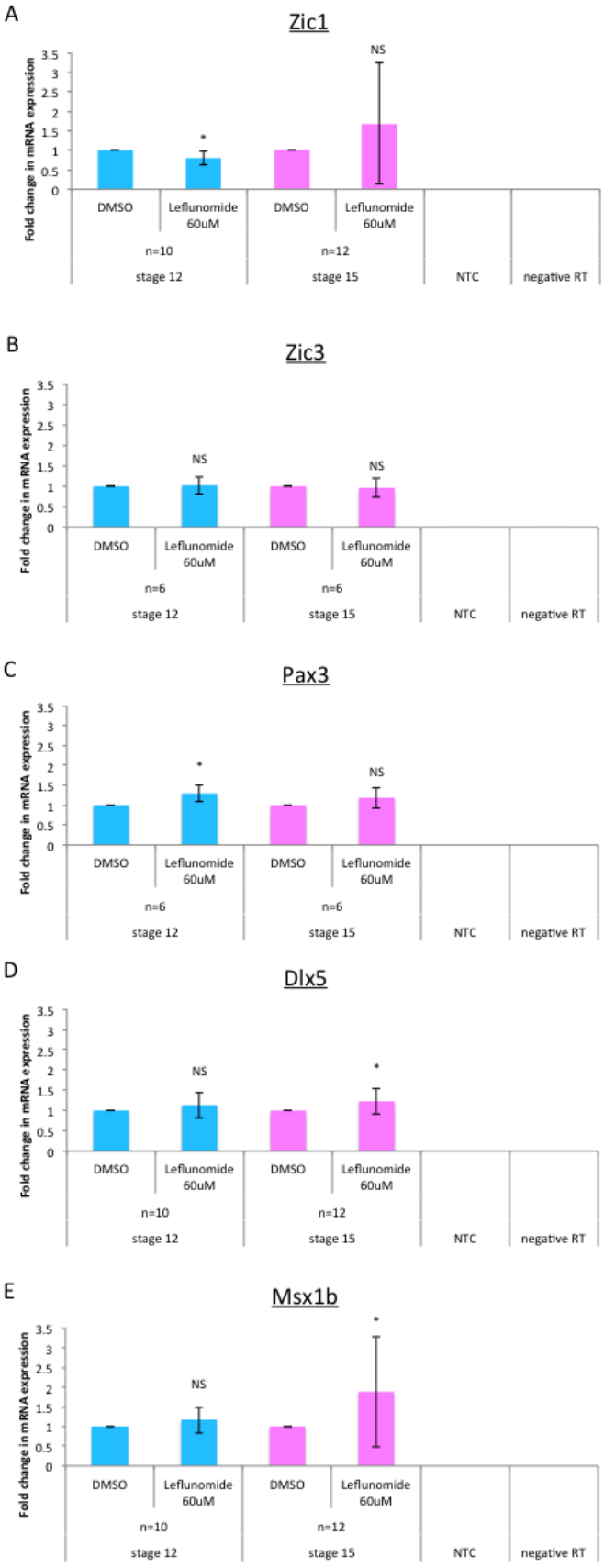

Supplementary Figure 7.1: Neural plate border specifiers treated with 60 µM leflunomide normalised to ODC1

Real-time PCR showing level of mRNA expression after 60 µM leflunomide treatment at stage 4 compared to DMSO-treated whole embryos. Panel A to E show the level of expression of stage 12 neural crest border specifers: Zic1 (A), Zic3 (B), Pax3 (C), Dlx5 (D) and Msx1b (E) and a negative reverse transcription (RT) control and no target control (NTC) for each assay. No significant change in expression was seen for Zic3, Dlx5 and Msx1b at stage 12. No significant change in expression was seen for Zic1, Zic3, Pax3 and Msx1b at stage 15. NS = not significant. Zic1 and Pax3 at stage 12 and Dlx5 at stage 15 were significantly up or downregulated. *= $p \leq 0.05$ to $p > 0.0000001$. Error bars are st.dev and the *n* number represents the number of technical replicates including two biological controls.

	Stage 12			Stage 15		
***Xenopus laevis* gene**	No. of real-time PCR runs with 3 technical replicates	Fold change ± s.d. (6*dp*)	Two-tailed Student's t-test	No. of real-time PCR runs with 3 technical replicates	Fold change ± s.d. (6*dp*)	Two-tailed Student's t-test
Zic1	12	0.80 ± 0.18	*p= 0.008*	12	1.70 ± 1.56	*p= 0.158*
Zic3	6	1.02 ± 0.21	*p= 0.807*	6	0.96 ± 0.23	*p= 0.682*
Pax3	6	1.30 ± 0.21	*p= 0.005*	6	1.19 ± 0.26	*p= 0.109*
DLX5	12	1.13 ± 0.31	*p= 0.251*	12	1.23 ± 0.31	*p= 0.019*
MSX1b	12	1.16 ± 0.33	*p= 0.190*	12	1.88 ± 1.41	*p= 0.042*

Supplementary Table 7.1: Neural plate and neural plate border specifier real-time PCR data normalised to ODC1
Tabulated real-time PCR results for neural plate and neural plate border genes showing fold change plus/minus standard deviation and t-test to shown significance of gene expression on stage 12 and stage 15 embryos treated with 60 μM leflunomide. Data has been normalised to ODC1.

A

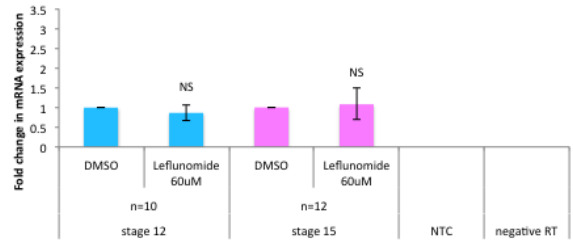

B

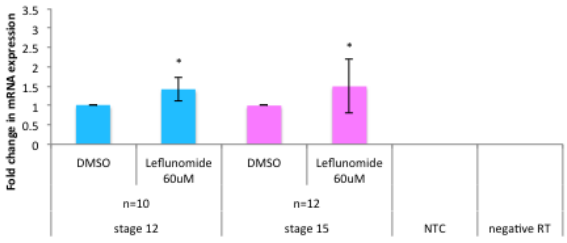

C

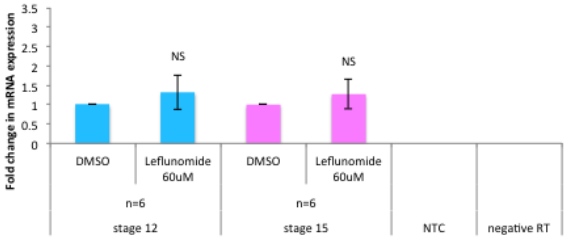

D

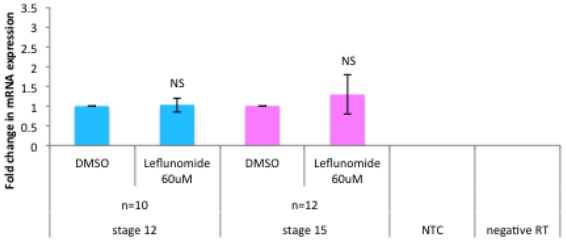

E

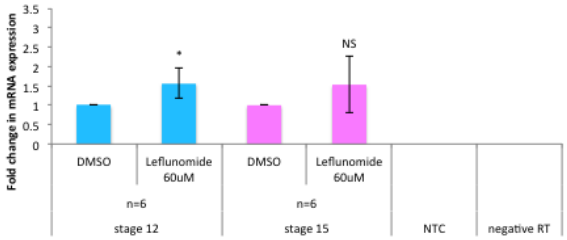

F

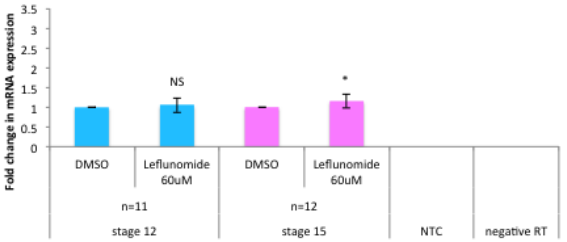

G

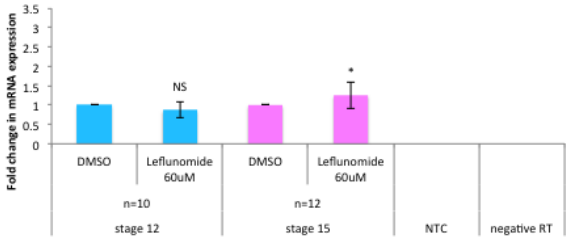

H

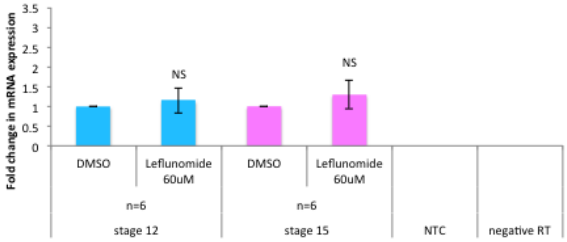

I

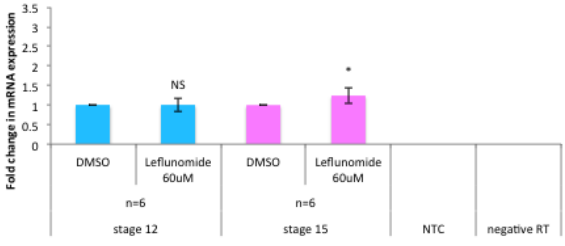

J

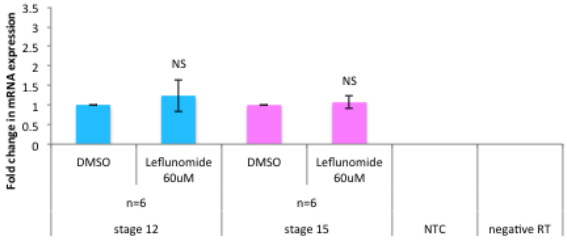

K

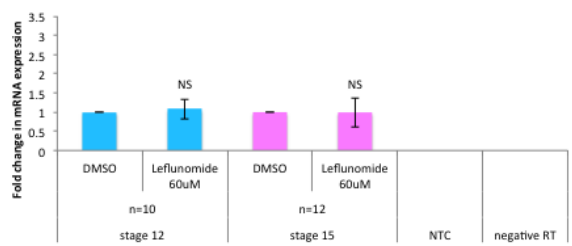

L

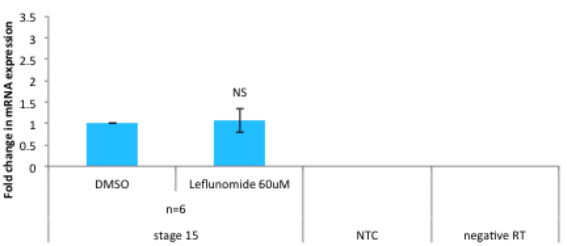

Supplementary Figure 7.2: Neural crest specifiers treated with 60 µM leflunomide normalised to ODC1

Real-time PCR showing level of mRNA expression after 60 µM leflunomide treatment at stage 4 compared to DMSO-treated whole embryos. Panels from A to K show the level of gene expression of neural crest specifiers: FoxD3 (A), Gbx2.2 (B), Twist (C), Id3a (D), Slug/Snail2 (E), Hairy2 (F), Snail1 (G), Sox9 (H), cMyc (I), Sox10 (J), Ap2a (K) and the pan neural marker Sox2 (L). All assays were performed alongside a negative reverse transcription (RT) control and no target control (NTC). The genes that show significance are indicated with *= $p \leq 0.05$ to $p > 0.0000001$. NS = not significant. Error bars are of the st.dev and the *n* number represents the number of technical replicates including two biological controls.

	Stage 12			Stage 15		
***Xenopus laevis* gene**	No. of real-time PCR runs with 3 technical replicates	Fold change ± s.d. (6*dp*)	Two-tailed Student's t-test	No. of real-time PCR runs with 3 technical replicates	Fold change ± s.d. (6*dp*)	Two-tailed Student's t-test
FoxD3b	12	0.87 ± 0.20	*p= 0.086*	12	1.08 ± 0.40	*p= 0.514*
Twist	6	1.32 ± 0.44	*p= 0.108*	6	1.27 ± 0.38	*p= 0.109*
Slug	6	1.57 ± 0.39	*p= 0.005*	6	1.53 ± 0.72	*p= 0.102*
Snail1	12	0.87 ± 0.20	*p= 0.090*	12	1.25 ± 0.35	*p= 0.027*
cmyc	6	1.01 ± 0.18	*p= 0.935*	6	1.24 ± 0.20	*p= 0.014*
AP2a	12	1.08 ± 0.26	*p= 0.396*	12	0.99 ± 0.38	*p= 0.948*
GBX2.2	12	1.42 ± 0.29	*p= 0.001*	12	1.50 ± 0.69	*p= 0.016*
ID3	12	1.02 ± 0.17	*p= 0.782*	12	1.29 ± 0.50	*p= 0.056*
Hairy2	12	1.05 ± 0.18	*p= 0.454*	12	1.15 ± 0.18	*p= 0.006*
Sox9	6	1.15 ± 0.32	*p= 0.283*	6	1.29 ± 0.36	*p= 0.071*
Sox10	6	1.23 ± 0.41	*p= 0.192*	6	1.07 ± 0.15	*p= 0.301*
Sox2 (NPB)	**NOT EXPRESSED**			6	1.07 ± 0.28	*p= 0.541*

Supplementary Table 7.2: Neural crest specifier genes and neural plate border specifier sox2 gene real-time PCR data normalised to ODC1

Tabulated real-time PCR results for neural crest specifier genes and neural plate border Sox2 gene showing fold change plus/minus standard deviation and t-test to shown significance of gene expression on stage 12 and stage 15 embryos treated with 60 μM leflunomide. Data has been normalised to ODC1.

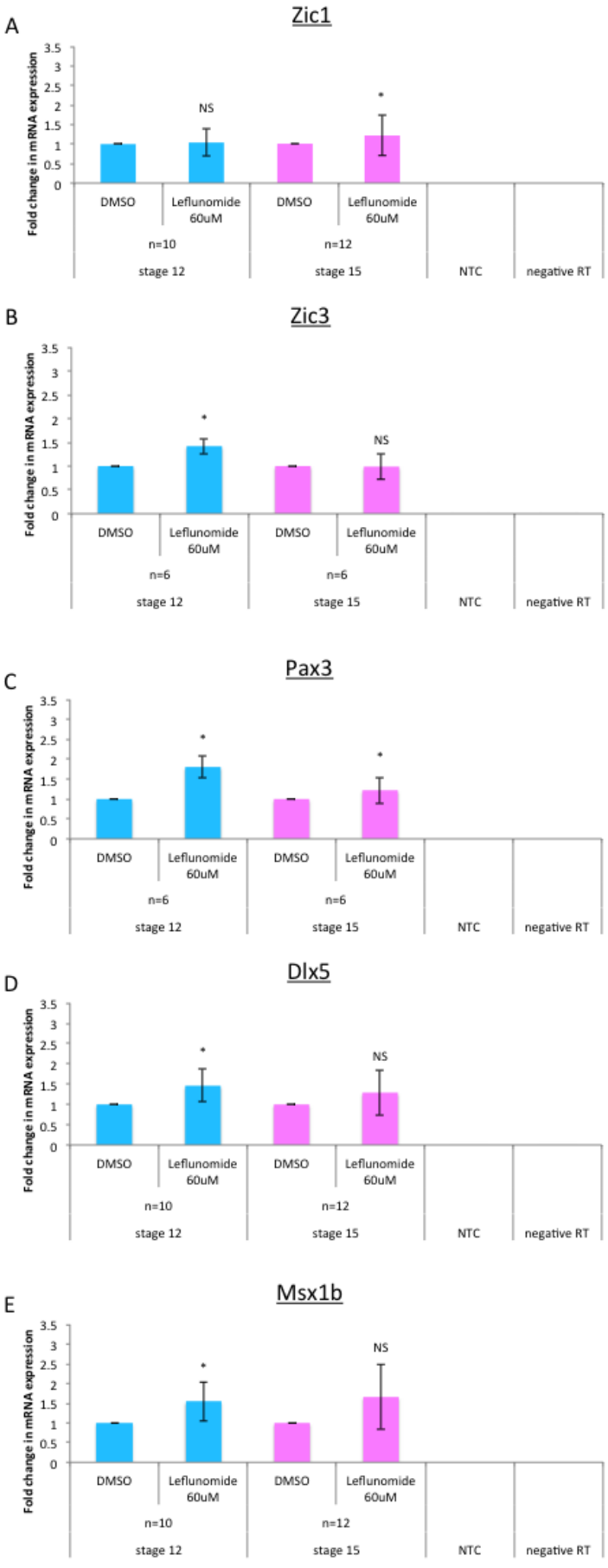
A
Zic1
Fold change in mRNA expression
3.5
3
2.5
2
1.5
1
0.5
0
NS
*
DMSO
Leflunomide 60uM
DMSO
Leflunomide 60uM
n=10
n=12
stage 12
stage 15
NTC
negative RT
B
Zic3
Fold change in mRNA expression
*
NS
DMSO
Leflunomide 60uM
DMSO
Leflunomide 60uM
n=6
n=6
stage 12
stage 15
NTC
negative RT
C
Pax3
Fold change in mRNA expression
*
*
DMSO
Leflunomide 60uM
DMSO
Leflunomide 60uM
n=6
n=6
stage 12
stage 15
NTC
negative RT
D
Dlx5
Fold change in mRNA expression
*
NS
DMSO
Leflunomide 60uM
DMSO
Leflunomide 60uM
n=10
n=12
stage 12
stage 15
NTC
negative RT
E
Msx1b
Fold change in mRNA expression
*
NS
DMSO
Leflunomide 60uM
DMSO
Leflunomide 60uM
n=10
n=12
stage 12
stage 15
NTC
negative RT

Supplementary Figure 7.3: Neural plate border specifiers treated with 60 µM leflunomide normalised to Rpl13

Real-time PCR showing level of mRNA expression after 60 µM leflunomide treatment at stage 4 compared to DMSO-treated whole embryos. Panel A to E show the level of expression of stage 12 neural crest border specifers: Zic1 (A), Zic3 (B), Pax3 (C), Dlx5 (D) and Msx1b (E) and a negative reverse transcription (RT) control and no target control (NTC) for each assay. No significant change in expression was seen for Zic1 at stage 12 and for Zic3, Dlx5 and Msx1b at stage 15. NS = not significant. Zic3, Pax3, Dlx5 and Msx1b at stage 12 and Zic1 and Pax3 at were significantly upregulated. *= $p \leq 0.05$ to $p > 0.0000001$. Error bars are st.dev and the *n* number represents the number of technical replicates including two biological controls.

	Stage 12			Stage 15		
***Xenopus laevis* gene**	No. of real-time PCR runs with 3 technical replicates	Fold change ± s.d. (6*dp*)	Two-tailed Student's t-test	No. of real-time PCR runs with 3 technical replicates	Fold change ± s.d. (6*dp*)	Two-tailed Student's t-test
Zic1	10	1.04 ± 0.35	*p= 0.750*	12	1.22 ± 0.52	*p= 0.168*
Zic3	6	1.42 ± 0.16	*p= 9.356 x* 10^{-05}	6	0.99 ± 0.27	*p= 0.929*
Pax3	6	1.81 ± 0.28	*p= 2.978* x 10^{-05}	6	1.22 ± 0.33	*p= 0.132*
DLX5	10	1.46 ± 0.40	*p= 0.006*	12	1.29 ± 0.56	*p= 0.085*
MSX1b	10	1.54 ± 0.49	*p= 0.008*	12	1.66 ± 0.82	*p= 0.011*

Supplementary Table 7.3: Neural plate and neural plate border specifier real-time PCR data normalised to Rpl13
Tabulated real-time PCR results for neural plate and neural plate border genes showing fold change plus/minus standard deviation and t-test to shown significance of gene expression on stage 12 and stage 15 embryos treated with 60 μM leflunomide. Data has been normalised to Rpl13.

A

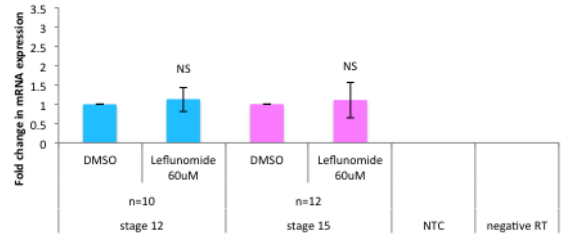

B

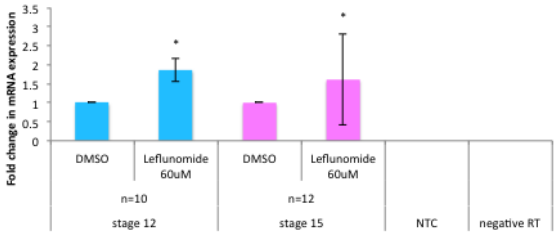

C

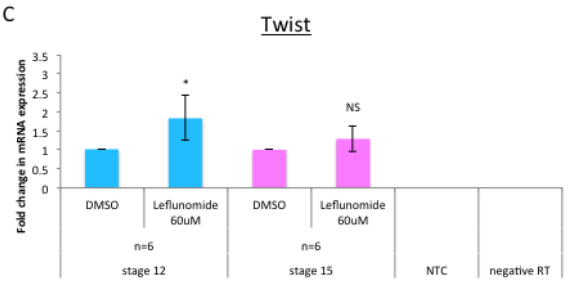

D

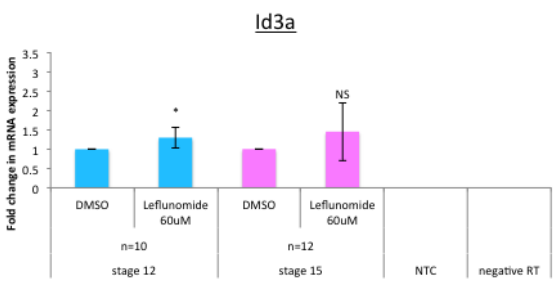

E

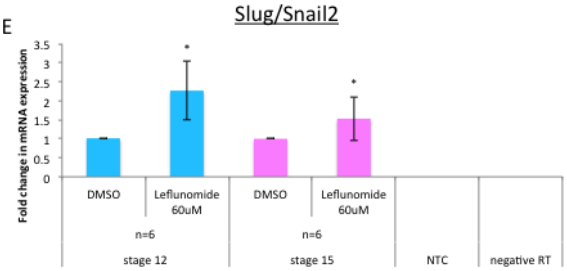

F

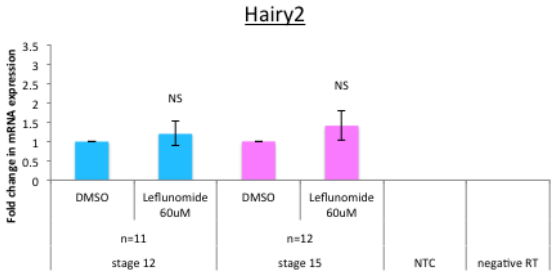

G

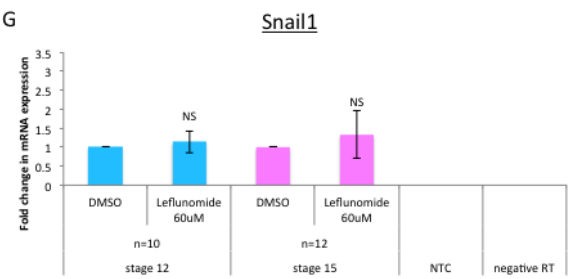

H

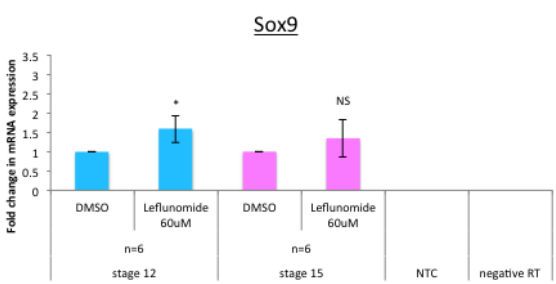

I

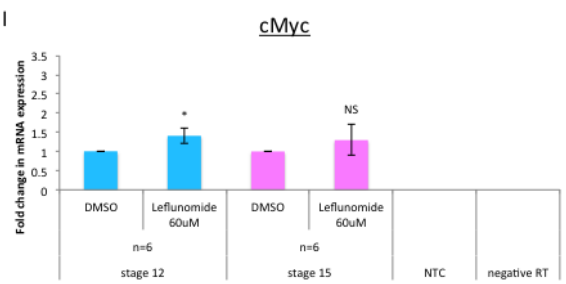

J

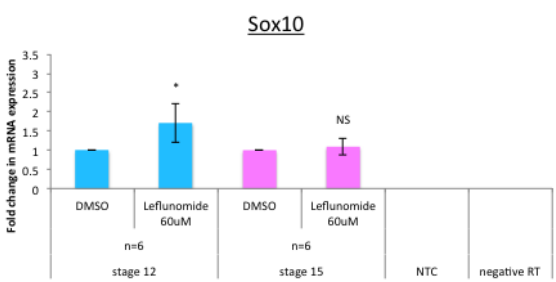

K

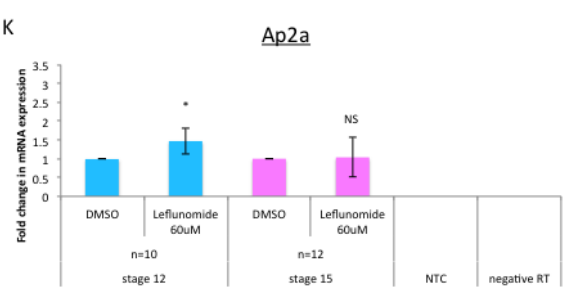

L

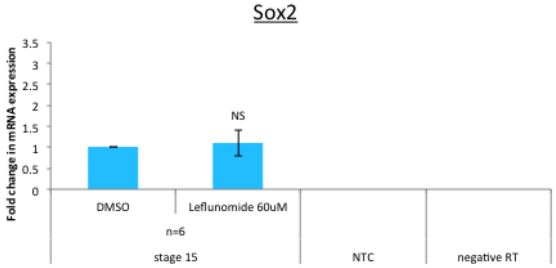

Supplementary Figure 7.4: Neural crest specifiers treated with 60 µM leflunomide normalised to Rpl13

Real-time PCR showing level of mRNA expression after 60 µM leflunomide treatment at stage 4 compared to DMSO-treated whole embryos. Panels from A to K show the level of gene expression of neural crest specifiers: FoxD3 (A), Gbx2.2 (B), Twist (C), Id3a (D), Slug/Snail2 (E), Hairy2 (F), Snail1 (G), Sox9 (H), cMyc (I), Sox10 (J), Ap2a (K) and the pan neural marker Sox2 (L). All assays were performed alongside a negative reverse transcription (RT) control and no target control (NTC). The genes that show significance are indicated with *= $p \leq 0.05$ to $p > 0.0000001$. NS = not significant. Error bars are of the st.dev and the *n* number represents the number of technical replicates including two biological controls.

	Stage 12			Stage 15		
***Xenopus laevis* gene**	No. of real-time PCR runs with 3 technical replicates	Fold change ± s.d. (6*dp*)	Two-tailed Student's t-test	No. of real-time PCR runs with 3 technical replicates	Fold change ± s.d. (6*dp*)	Two-tailed Student's t-test
FoxD3b	10	1.13 ± 0.32	*p= 0.278*	12	1.11 ± 0.46	*p= 0.456*
Twist	6	1.84 ± 0.58	*p= 0.006*	6	1.29 ± 0.33	*p= 0.059*
Slug	6	2.27 ± 0.77	*p= 0.002*	6	1.53 ± 0.57	*p= 0.047*
Snail1	10	1.14 ± 0.29	*p= 0.182*	12	1.33 ± 0.62	*p= 0.081*
cmyc	6	1.41 ± 0.20	*p= 0.001*	6	1.30 ± 0.40	*p= 0.101*
AP2a	10	1.47 ± 0.35	*p= 0.002*	12	1.04 ± 0.52	*p= 0.807*
GBX2.2	10	1.87 ± 0.31	*p= 1.433* x 10^{-06}	12	1.61 ± 1.19	*p= 0.090*
ID3	10	1.29 ± 0.27	*p= 0.009*	12	1.45 ± 0.75	*p= 0.049*
Hairy2	11	1.21 ± 0.32	*p= 0.068*	12	1.41 ± 0.37	*p= 0.001*
Sox9	6	1.59 ± 0.35	*p= 0.002*	6	1.35 ± 0.49	*p= 0.117*
Sox10	6	1.71 ± 0.52	*p= 0.007*	6	1.09 ± 0.21	*p= 0.322*
Sox2 (NPB)	**NOT EXPRESSED**			6	1.10 ± 0.30	*p= 0.450*

Supplementary Table 7.4: Neural crest specifier genes and neural plate border specifier sox2 gene real-time PCR data normalised to Rpl13

Tabulated real-time PCR results for neural crest specifier genes and neural plate border Sox2 gene showing fold change plus/minus standard deviation and t-test to shown significance of gene expression on stage 12 and stage 15 embryos treated with 60 μM leflunomide. Data has been normalised to Rpl13.

8. References

Adams, M.S., Gammill, L.S., Bronner-Fraser, M., 2008. Discovery of transcription factors and other candidate regulators of neural crest development. Developmental Dynamics 237, 1021-1033.

Altschul, S.F., Gish, W., Miller, W., Myers, E.W., Lipman, D.J., 1990. Basic local alignment search tool. Journal of molecular biology 215, 403-410.

Amati, B., Littlewood, T.D., Evan, G.I., Land, H., 1993. The c-Myc protein induces cell cycle progression and apoptosis through dimerisation with Max. EMBO J 12, 5083-5087.

Anderson, D.J., 1993. Molecular control of cell fate in the neural crest: the sympathoadrenal lineage. Annual review of neuroscience 16, 129-158.

Badner, J.A., Sieber, W.K., Garver, K.L., Chakravarti, A., 1990. A genetic study of Hirschsprung disease. American journal of human genetics 46, 568-580.

Bagnato, A., Rosano, L., Spinella, F., Di Castro, V., Tecce, R., Natali, P.G., 2004. Endothelin B receptor blockade inhibits dynamics of cell interactions and communications in melanoma cell progression. Cancer research 64, 1436-1443.

Baker, C.V., Bronner-Fraser, M., 1997. The origins of the neural crest. Part I: embryonic induction. Mechanisms of development 69, 3-11.

Bakos, R.M., Maier, T., Besch, R., Mestel, D.S., Ruzicka, T., Sturm, R.A., Berking, C., 2010. Nestin and SOX9 and SOX10 transcription factors are coexpressed in melanoma. Experimental dermatology 19, e89-94.

Barboric, M., Kohoutek, J., Price, J.P., Blazek, D., Price, D.H., Peterlin, B.M., 2005. Interplay between 7SK snRNA and oppositely charged regions in HEXIM1 direct the inhibition of P-TEFb. The EMBO Journal 24, 4291-4303.

Bellmeyer, A., Krase, J., Lindgren, J., LaBonne, C., 2003. The protooncogene c-myc is an essential regulator of neural crest formation in *Xenopus*. Developmental cell 4, 827-839.

Biswas, D., Milne, T.A., Basrur, V., Kim, J., Elenitoba-Johnson, K.S., Allis, C.D., Roeder, R.G., 2011. Function of leukemogenic mixed lineage leukemia 1 (MLL) fusion proteins through distinct partner protein complexes. Proceedings of the National Academy of Sciences of the United States of America 108, 15751-15756.

Boettiger, A.N., Levine, M., 2009. Synchronous and stochastic patterns of gene activation in the *Drosophila* embryo. Science (New York, N.Y.) 325, 471-473.

Bondurand, N., Dastot-Le Moal, F., Stanchina, L., Collot, N., Baral, V., Marlin, S., Attie-Bitach, T., Giurgea, I., Skopinski, L., Reardon, W., Toutain, A., Sarda, P., Echaieb, A., Lackmy-Port-Lis, M., Touraine, R., Amiel, J., Goossens, M., Pingault, V., 2007. Deletions at the SOX10 gene locus cause Waardenburg syndrome types 2 and 4. American journal of human genetics 81, 1169-1185.

Bonstein, L., Elias, S., Frank, D., 1998. Paraxial-fated mesoderm is required for neural crest induction in *Xenopus* embryos. Dev Biol 193, 156-168.

Brannan, K., Kim, H., Erickson, B., Glover-Cutter, K., Kim, S., Fong, N., Kiemele, L., Hansen, K., Davis, R., Lykke-Andersen, J., Bentley, D.L., 2012. mRNA decapping factors and the exonuclease Xrn2 function in widespread premature termination of RNA polymerase II transcription. Molecular cell 46, 311-324.

Bres, V., Yoh, S.M., Jones, K.A., 2008. The multi-tasking P-TEFb complex. Current opinion in cell biology 20, 334-340.

Briggs, S.D., Xiao, T., Sun, Z.W., Caldwell, J.A., Shabanowitz, J., Hunt, D.F., Allis, C.D., Strahl, B.D., 2002. Gene silencing: trans-histone regulatory pathway in chromatin. Nature 418, 498.

Bustin, S.A., Benes, V., Garson, J.A., Hellemans, J., Huggett, J., Kubista, M., Mueller, R., Nolan, T., Pfaffl, M.W., Shipley, G.L., Vandesompele, J., Wittwer, C.T., 2009. The MIQE guidelines: minimum information for publication of quantitative real-time PCR experiments. Clinical chemistry 55, 611-622.

Byers, S.A., Price, J.P., Cooper, J.J., Li, Q., Price, D.H., 2005. HEXIM2, a HEXIM1-related Protein, Regulates Positive Transcription Elongation Factor b through Association with 7SK. Journal of Biological Chemistry 280, 16360-16367.

Cai, D.H., Vollberg, T.M., Sr., Hahn-Dantona, E., Quigley, J.P., Brauer, P.R., 2000. MMP-2 expression during early avian cardiac and neural crest morphogenesis. The Anatomical record 259, 168-179.

Cano, A., Perez-Moreno, M.A., Rodrigo, I., Locascio, A., Blanco, M.J., del Barrio, M.G., Portillo, F., Nieto, M.A., 2000. The transcription factor snail controls epithelial-mesenchymal transitions by repressing E-cadherin expression. Nature cell biology 2, 76-83.

Cebra-Thomas, J.A., Betters, E., Yin, M., Plafkin, C., McDow, K., Gilbert, S.F., 2007. Evidence that a late-emerging population of trunk neural crest cells forms the plastron bones in the turtle Trachemys scripta. Evolution & development 9, 267-277.

Chang, C., Werb, Z., 2001. The many faces of metalloproteases: cell growth, invasion, angiogenesis and metastasis. Trends in cell biology 11, S37-43.

Chavali, S., Mahajan, A., Tabassum, R., Maiti, S., Bharadwaj, D., 2005. Oligonucleotide properties determination and primer designing: a critical examination of predictions. Bioinformatics (Oxford, England) 21, 3918-3925.

Chen, Y., Yamaguchi, Y., Tsugeno, Y., Yamamoto, J., Yamada, T., Nakamura, M., Hisatake, K., Handa, H., 2009. DSIF, the Paf1 complex, and Tat-SF1 have nonredundant, cooperative roles in RNA polymerase II elongation. Genes & development 23, 2765-2777.

Clark, K., Bender, G., Murray, B.P., Panfilio, K., Cook, S., Davis, R., Murnen, K., Tuan, R.S., Gilbert, S.F., 2001. Evidence for the neural crest origin of turtle plastron bones. Genesis (New York, N.Y. : 2000) 31, 111-117.

Cooper, C.D., Raible, D.W., 2009. Mechanisms for reaching the differentiated state: Insights from neural crest-derived melanocytes. Seminars in cell & developmental biology 20, 105-110.

Core, L.J., Lis, J.T., 2008. Transcription regulation through promoter-proximal pausing of RNA polymerase II. Science (New York, N.Y.) 319, 1791-1792.

Dover, J., Schneider, J., Tawiah-Boateng, M.A., Wood, A., Dean, K., Johnston, M., Shilatifard, A., 2002. Methylation of histone H3 by COMPASS requires ubiquitination of histone H2B by Rad6. The Journal of biological chemistry 277, 28368-28371.

Edery, P., Attie, T., Amiel, J., Pelet, A., Eng, C., Hofstra, R.M., Martelli, H., Bidaud, C., Munnich, A., Lyonnet, S., 1996. Mutation of the endothelin-3 gene in the Waardenburg-Hirschsprung disease (Shah-Waardenburg syndrome). Nature genetics 12, 442-444.

Elworthy, S., Lister, J.A., Carney, T.J., Raible, D.W., Kelsh, R.N., 2003. Transcriptional regulation of mitfa accounts for the sox10 requirement in *zebrafish* melanophore development. Development 130, 2809-2818.

Endo, Y., Osumi, N., Wakamatsu, Y., 2002. Bimodal functions of Notch-mediated signaling are involved in neural crest formation during avian ectoderm development. Development 129, 863-873.

Fish, R.N., Kane, C.M., 2002. Promoting elongation with transcript cleavage stimulatory factors. Biochimica et biophysica acta 1577, 287-307.

Freitas, R., Zhang, G., Albert, J.S., Evans, D.H., Cohn, M.J., 2006. Developmental origin of shark electrosensory organs. Evolution & development 8, 74-80.

Fuda, N.J., Ardehali, M.B., Lis, J.T., 2009. Defining mechanisms that regulate RNA polymerase II transcription *in vivo*. Nature 461, 186-192.

Fujita, T., Piuz, I., Schlegel, W., 2009. The transcription elongation factors NELF, DSIF and P-TEFb control constitutive transcription in a gene-specific manner. FEBS letters 583, 2893-2898.

Gans, C., Northcutt, R.G., 1983. Neural crest and the origin of vertebrates: a new head. Science (New York, N.Y.) 220, 268-273.

Gargano, B., Amente, S., Majello, B., Lania, L., 2007. P-TEFb is a crucial co-factor for Myc transactivation. Cell cycle (Georgetown, Tex.) 6, 2031-2037.

Garraway, L.A., Widlund, H.R., Rubin, M.A., Getz, G., Berger, A.J., Ramaswamy, S., Beroukhim, R., Milner, D.A., Granter, S.R., Du, J., Lee, C., Wagner, S.N., Li, C., Golub, T.R., Rimm, D.L., Meyerson, M.L., Fisher, D.E., Sellers, W.R., 2005. Integrative genomic analyses identify MITF as a lineage survival oncogene amplified in malignant melanoma. Nature 436, 117-122.

Gilchrist, D.A., Fromm, G., dos Santos, G., Pham, L.N., McDaniel, I.E., Burkholder, A., Fargo, D.C., Adelman, K., 2012. Regulating the regulators: the pervasive effects of Pol II pausing on stimulus-responsive gene networks. Genes & development 26, 933-944.

Glavic A Fau - Silva, F., Silva F Fau - Aybar, M.J., Aybar Mj Fau - Bastidas, F., Bastidas F Fau - Mayor, R., Mayor, R., 2004. Interplay between Notch signaling and the homeoprotein Xiro1 is required for neural crest induction in *Xenopus* embryos.

Graveson, A.C., Smith, M.M., Hall, B.K., 1997. Neural crest potential for tooth development in a urodele amphibian: developmental and evolutionary significance. Dev Biol 188, 34-42.

Groves, A.K., Labonne, C., 2014. Setting appropriate boundaries: Fate, patterning and competence at the neural plate border. Dev Biol 389, 2-12.

Gupta, P.B., Kuperwasser, C., Brunet, J.P., Ramaswamy, S., Kuo, W.L., Gray, J.W., Naber, S.P., Weinberg, R.A., 2005. The melanocyte differentiation program predisposes to metastasis after neoplastic transformation. Nature genetics 37, 1047-1054.

Hall, B.K., 1999. The neural crest in development and evolution. Springer-Verlag, New York.

Harland, R.M., Grainger, R.M., 2011. *Xenopus* research: metamorphosed by genetics and genomics. Trends in genetics : TIG 27, 507-515.

Harrison, M., Abu-Elmagd, M., Grocott, T., Yates, C., Gavrilovic, J., Wheeler, G.N., 2005. Matrix metalloproteinase genes in Xenopus development. Developmental Dynamics 232, 246-246.

He, N., Chan, C.K., Sobhian, B., Chou, S., Xue, Y., Liu, M., Alber, T., Benkirane, M., Zhou, Q., 2011. Human Polymerase-Associated Factor complex (PAFc) connects the Super Elongation Complex (SEC) to RNA polymerase II on chromatin. Proceedings of the National Academy of Sciences of the United States of America 108, E636-645.

He, N., Jahchan, N.S., Hong, E., Li, Q., Bayfield, M.A., Maraia, R.J., Luo, K., Zhou, Q., 2008. A La-related protein modulates 7SK snRNP integrity to suppress P-TEFb-dependent transcriptional elongation and tumorigenesis. Molecular cell 29, 588-599.

Heanue, T.A., Pachnis, V., 2007. Enteric nervous system development and Hirschsprung's disease: advances in genetic and stem cell studies. Nature reviews. Neuroscience 8, 466-479.

H**eckmann, L.H., Sorensen, P.B., Krogh, P.H., Sorensen, J.G., 2011.** NORMA-Gene: a simple and robust method for qPCR normalization based on target gene data. BMC bioinformatics 12, 250.

Hochheimer, A., Tjian, R., 2003. Diversified transcription initiation complexes expand promoter selectivity and tissue-specific gene expression. Genes & development 17, 1309-1320.

Hong, S.K., Tsang, M., Dawid, I.B., 2008. The mych gene is required for neural crest survival during *zebrafish* development. PloS one 3, e2029.

Honore, S.M., Aybar, M.J., Mayor, R., 2003. Sox10 is required for the early development of the prospective neural crest in *Xenopus* embryos. Dev Biol 260, 79-96.

Hu, M.C., Rosenblum, N.D., 2005. Smad1, beta-catenin and Tcf4 associate in a molecular complex with the Myc promoter in dysplastic renal tissue and cooperate to control Myc transcription. Development 132, 215-225.

Huang, X., Saint-Jeannet, J.P., 2004. Induction of the neural crest and the opportunities of life on the edge. Dev Biol 275, 1-11.

Itasaki, N., Hoppler, S., 2010. Crosstalk between Wnt and bone morphogenic protein signaling: a turbulent relationship. Developmental dynamics : an official publication of the American Association of Anatomists 239, 16-33.

Iyengar, B., Singh, A.V., 2010. Patterns of neural differentiation in melanomas. Journal of biomedical science 17, 87.

Jiang, X., Choudhary, B., Merki, E., Chien, K.R., Maxson, R.E., Sucov, H.M., 2002. Normal fate and altered function of the cardiac neural crest cell lineage in retinoic acid receptor mutant embryos. Mechanisms of development 117, 115-122.

Kanazawa, S., Soucek, L., Evan, G., Okamoto, T., Peterlin, B.M., 2003. c-Myc recruits P-TEFb for transcription, cellular proliferation and apoptosis. Oncogene 22, 5707-5711.

Kee, Y., Bronner-Fraser, M., 2005. To proliferate or to die: role of Id3 in cell cycle progression and survival of neural crest progenitors. Genes & development 19, 744-755.

Keegan, B.R., Feldman, J.L., Lee, D.H., Koos, D.S., Ho, R.K., Stainier, D.Y., Yelon, D., 2002. The elongation factors Pandora/Spt6 and Foggy/Spt5 promote transcription in the *zebrafish* embryo. Development 129, 1623-1632.

Kim, J., Guermah, M., Roeder, R.G., 2010. The human PAF1 complex acts in chromatin transcription elongation both independently and cooperatively with SII/TFIIS. Cell 140, 491-503.

Knecht, A.K., Bronner-Fraser, M., 2002. Induction of the neural crest: a multigene process. Nature reviews. Genetics 3, 453-461.

Kohoutek, J., 2009. P-TEFb- the final frontier. Cell division 4, 19.

Krogan, N.J., Dover, J., Wood, A., Schneider, J., Heidt, J., Boateng, M.A., Dean, K., Ryan, O.W., Golshani, A., Johnston, M., Greenblatt, J.F., Shilatifard, A., 2003a. The Paf1 complex is required for histone H3 methylation by COMPASS and Dot1p: linking transcriptional elongation to histone methylation. Molecular cell 11, 721-729.

Krogan, N.J., Kim, M., Ahn, S.H., Zhong, G., Kobor, M.S., Cagney, G., Emili, A., Shilatifard, A., Buratowski, S., Greenblatt, J.F., 2002. RNA polymerase II elongation factors of *Saccharomyces cerevisiae*: a targeted proteomics approach. Molecular and cellular biology 22, 6979-6992.

Krogan, N.J., Kim, M., Tong, A., Golshani, A., Cagney, G., Canadien, V., Richards, D.P., Beattie, B.K., Emili, A., Boone, C., Shilatifard, A., Buratowski, S., Greenblatt, J., 2003b. Methylation of histone H3 by Set2 in *Saccharomyces cerevisiae* is linked to transcriptional elongation by RNA polymerase II. Molecular and cellular biology 23, 4207-4218.

Krueger, B.J., Jeronimo, C., Roy, B.B., Bouchard, A., Barrandon, C., Byers, S.A., Searcey, C.E., Cooper, J.J., Bensaude, O., Cohen, E.A., Coulombe, B., Price, D.H., 2008. LARP7 is a stable component of the 7SK snRNP while P-TEFb, HEXIM1 and hnRNP A1 are reversibly associated. Nucleic acids research 36, 2219-2229.

Kuhlbrodt, K., Schmidt, C., Sock, E., Pingault, V., Bondurand, N., Goossens, M., Wegner, M., 1998. Functional analysis of Sox10 mutations found in human Waardenburg-Hirschsprung patients. The Journal of biological chemistry 273, 23033-23038.

Kuratani, S., 2008. Evolutionary developmental studies of cyclostomes and the origin of the vertebrate neck. Development, growth & differentiation 50 Suppl 1, S189-194.

LaBonne, C., Bronner-Fraser, M., 1998. Neural crest induction in *Xenopus*: evidence for a two-signal model. Development 125, 2403-2414.

Le Douarin, N.M., Brito, J.M., Creuzet, S., 2007. Role of the neural crest in face and brain development. Brain research reviews 55, 237-247.

Le Douarin, N.M., Teillet, M.A., 1974. Experimental analysis of the migration and differentiation of neuroblasts of the autonomic nervous system and of neurectodermal mesenchymal derivatives, using a biological cell marking technique. Dev Biol 41, 162-184.

Le Lievre, C.S., Le Douarin, N.M., 1975. Mesenchymal derivatives of the neural crest: analysis of chimaeric quail and chick embryos. Journal of embryology and experimental morphology 34, 125-154.

Lecoin, L., Sakurai, T., Ngo, M.T., Abe, Y., Yanagisawa, M., Le Douarin, N.M., 1998. Cloning and characterisation of a novel endothelin receptor subtype in the avian class. Proceedings of the National Academy of Sciences of the United States of America 95, 3024-3029.

Li, B., Kuriyama, S., Moreno, M., Mayor, R., 2009. The posteriorising gene Gbx2 is a direct target of Wnt signalling and the earliest factor in neural crest induction. Development 136, 3267-3278.

Li, Q., Price, J.P., Byers, S.A., Cheng, D., Peng, J., Price, D.H., 2005. Analysis of the large inactive P-TEFb complex indicates that it contains one 7SK molecule, a dimer of HEXIM1 or HEXIM2, and two P-TEFb molecules containing Cdk9 phosphorylated at threonine 186. The Journal of biological chemistry 280, 28819-28826.

Light, W., Vernon, A.E., Lasorella, A., Iavarone, A., LaBonne, C., 2005. *Xenopus* Id3 is required downstream of Myc for the formation of multipotent neural crest progenitor cells. Development 132, 1831-1841.

Lin, C., Garrett, A.S., De Kumar, B., Smith, E.R., Gogol, M., Seidel, C., Krumlauf, R., Shilatifard, A., 2011. Dynamic transcriptional events in embryonic stem cells mediated by the super elongation complex (SEC). Genes & development 25, 1486-1498.

Lin, C., Smith, E.R., Takahashi, H., Lai, K.C., Martin-Brown, S., Florens, L., Washburn, M.P., Conaway, J.W., Conaway, R.C., Shilatifard, A., 2010. AFF4, a component of the ELL/P-TEFb elongation complex and a shared subunit of MLL chimeras, can link transcription elongation to leukemia. Molecular cell 37, 429-437.

Loffler, M., Jockel, J., Schuster, G., Becker, C., 1997. Dihydroorotat-ubiquinone oxidoreductase links mitochondria in the biosynthesis of pyrimidine nucleotides. Molecular and cellular biochemistry 174, 125-129.

Lumsden, A.G., 1988. Spatial organisation of the epithelium and the role of neural crest cells in the initiation of the mammalian tooth germ. Development 103 Suppl, 155-169.

Luo, Z., Lin, C., Guest, E., Garrett, A.S., Mohaghegh, N., Swanson, S., Marshall, S., Florens, L., Washburn, M.P., Shilatifard, A., 2012. The super elongation complex family of RNA polymerase II elongation factors: gene target specificity and transcriptional output. Molecular and cellular biology 32, 2608-2617.

Mai, S., Mushinski, J.F., 2003. c-Myc-induced genomic instability. Journal of environmental pathology, toxicology and oncology : official organ of the International Society for Environmental Toxicology and Cancer 22, 179-199.

Marchant, L., Linker, C., Ruiz, P., Guerrero, N., Mayor, R., 1998. The inductive properties of mesoderm suggest that the neural crest cells are specified by a BMP gradient. Dev Biol 198, 319-329.

Mayanil, C.S., 2013. Transcriptional and Epigenetic Regulation of Neural Crest Induction during Neurulation. Developmental Neuroscience 35, 361-372.

Mayor, R., Guerrero, N., Martinez, C., 1997. Role of FGF and noggin in neural crest induction. Dev Biol 189, 1-12.

Mayor, R., Theveneau, E., 2013. The neural crest. Development 140, 2247-2251.

Medic, S., Ziman, M., 2010. PAX3 Expression in Normal Skin Melanocytes and Melanocytic Lesions (Naevi and Melanomas). PloS one 5, e9977.

Meulemans, D., Bronner-Fraser, M., 2004. Gene-regulatory interactions in neural crest evolution and development. Developmental cell 7, 291-299.

Meulemans, D., Bronner-Fraser, M., 2005. Central role of gene cooption in neural crest evolution. Journal of experimental zoology. Part B, Molecular and developmental evolution 304, 298-303.

Michels, A.A., Fraldi, A., Li, Q., Adamson, T.E., Bonnet, F., Nguyen, V.T., Sedore, S.C., Price, J.P., Price, D.H., Lania, L., Bensaude, O., 2004. Binding of the 7SK snRNA turns the HEXIM1 protein into a P-TEFb (CDK9/cyclin T) inhibitor. The EMBO Journal 23, 2608-2619.

Milet, C., Monsoro-Burq, A.H., 2012. Embryonic stem cell strategies to explore neural crest development in human embryos. Dev Biol 366, 96-99.

Missra, A., Gilmour, D.S., 2010. Interactions between DSIF (DRB sensitivity inducing factor), NELF (negative elongation factor), and the Drosophila RNA polymerase II transcription elongation complex. Proceedings of the National Academy of Sciences of the United States of America 107, 11301-11306.

Monsoro-Burq, A.H., Fletcher, R.B., Harland, R.M., 2003. Neural crest induction by paraxial mesoderm in *Xenopus* embryos requires FGF signals. Development 130, 3111-3124.

Monsoro-Burq, A.H., Wang, E., Harland, R., 2005. Msx1 and Pax3 cooperate to mediate FGF8 and WNT signals during *Xenopus* neural crest induction. Developmental cell 8, 167-178.

Myant, K., Sansom, O.J., 2011. Wnt/Myc interactions in intestinal cancer: partners in crime. Experimental cell research 317, 2725-2731.

Nguyen, V.T., Kiss, T., Michels, A.A., Bensaude, O., 2001. 7SK small nuclear RNA binds to and inhibits the activity of CDK9/cyclin T complexes. Nature 414, 322-325.

Nieuwkoop, P., Faber, J., 1967. Normal Table of *Xenopus Laevis*. North Holland Publishing Co, Amsterdam, The Netherlands.

Omenn, G.S., McKusick, V.A., 1979. The association of Waardenburg syndrome and Hirschsprung megacolon. American journal of medical genetics 3, 217-223.

Patton, E.E., Widlund, H.R., Kutok, J.L., Kopani, K.R., Amatruda, J.F., Murphey, R.D., Berghmans, S., Mayhall, E.A., Traver, D., Fletcher, C.D., Aster, J.C., Granter, S.R., Look, A.T., Lee, C., Fisher, D.E., Zon, L.I., 2005. BRAF mutations are sufficient to promote nevi formation and cooperate with p53 in the genesis of melanoma. Current biology : CB 15, 249-254.

Pegoraro, C., Monsoro-Burq, A.H., 2013. Signaling and transcriptional regulation in neural crest specification and migration: lessons from *Xenopus* embryos. Wiley Interdisciplinary Reviews: Developmental Biology 2, 247-259.

Peterlin, B.M., Price, D.H., 2006. Controlling the elongation phase of transcription with P-TEFb. Molecular cell 23, 297-305.

Polak, J.M., Pearse, A.G., Le Lievre, C., Fontaine, J., Le Douarin, N.M., 1974. Immunocytochemical confirmation of the neural crest origin of avian calcitonin-producing cells. Histochemistry 40, 209-214.

Potterf, S.B., Mollaaghababa, R., Hou, L., Southard-Smith, E.M., Hornyak, T.J., Arnheiter, H., Pavan, W.J., 2001. Analysis of SOX10 function in neural crest-derived melanocyte development: SOX10-dependent transcriptional control of dopachrome tautomerase. Dev Biol 237, 245-257.

Rahl, P.B., Lin, C.Y., Seila, A.C., Flynn, R.A., McCuine, S., Burge, C.B., Sharp, P.A., Young, R.A., 2010. c-Myc Regulates Transcriptional Pause Release. Cell 141, 432-445.

Read, A.P., Newton, V.E., 1997. Waardenburg syndrome. Journal of medical genetics 34, 656-665.

Romeo, G., Ronchetto, P., Luo, Y., Barone, V., Seri, M., Ceccherini, I., Pasini, B., Bocciardi, R., Lerone, M., Kaariainen, H., et al., 1994. Point mutations affecting the tyrosine kinase domain of the RET proto-oncogene in Hirschsprung's disease. Nature 367, 377-378.

Sanchez-Martin, M., Rodriguez-Garcia, A., Perez-Losada, J., Sagrera, A., Read, A.P., Sanchez-Garcia, I., 2002. SLUG (SNAIL2) deletions in patients with Waardenburg disease. Human molecular genetics 11, 3231-3236.

Sato, S., Ikeda, K., Shioi, G., Ochi, H., Ogino, H., Yajima, H., Kawakami, K., 2010. Conserved expression of mouse Six1 in the pre-placodal region (PPR) and identification of an enhancer for the rostral PPR. Dev Biol 344, 158-171.

Sato, T., Sasai, N., Sasai, Y., 2005. Neural crest determination by co-activation of Pax3 and Zic1 genes in *Xenopus* ectoderm. Development 132, 2355-2363.

Sauka-Spengler, T., Bronner-Fraser, M., 2006. Development and evolution of the migratory neural crest: a gene regulatory perspective. Current opinion in genetics & development 16, 360-366.

Sauka-Spengler, T., Bronner-Fraser, M., 2008a. A gene regulatory network orchestrates neural crest formation. Nat Rev Mol Cell Biol.

Sauka-Spengler, T., Bronner-Fraser, M., 2008b. Insights from a sea lamprey into the evolution of neural crest gene regulatory network. The Biological bulletin 214, 303-314.

Sauka-Spengler, T., Meulemans, D., Jones, M., Bronner-Fraser, M., 2007. Ancient Evolutionary Origin of the Neural Crest Gene Regulatory Network. Developmental cell 13, 405-420.

Schlagbauer-Wadl, H., Griffioen, M., van Elsas, A., Schrier, P.I., Pustelnik, T., Eichler, H.G., Wolff, K., Pehamberger, H., Jansen, B., 1999. Influence of increased c-Myc expression on the growth characteristics of human melanoma. The Journal of investigative dermatology 112, 332-336.

Schmitt, S.M., Gull, M., Brandli, A.W., 2014. Engineering *Xenopus* embryos for phenotypic drug discovery screening. Advanced drug delivery reviews.

Schneider, M., Schambony, A., Wedlich, D., 2010. Prohibitin1 acts as a neural crest specifier in *Xenopus* development by repressing the transcription factor E2F1. Development 137, 4073-4081.

Seila, A.C., Calabrese, J.M., Levine, S.S., Yeo, G.W., Rahl, P.B., Flynn, R.A., Young, R.A., Sharp, P.A., 2008. Divergent transcription from active promoters. Science (New York, N.Y.) 322, 1849-1851.

Shin, M.K., Levorse, J.M., Ingram, R.S., Tilghman, S.M., 1999. The temporal requirement for endothelin receptor-B signalling during neural crest development. Nature 402, 496-501.

Sieber-Blum, M., Schnell, L., Grim, M., Hu, Y.F., Schneider, R., Schwab, M.E., 2006. Characterisation of epidermal neural crest stem cell (EPI-NCSC) grafts in the lesioned spinal cord. Molecular and cellular neurosciences 32, 67-81.

Sims, R.J., 3rd, Belotserkovskaya, R., Reinberg, D., 2004. Elongation by RNA polymerase II: the short and long of it. Genes & development 18, 2437-2468.

Smith, M.M., Hall, B.K., 1990. Development and evolutionary origins of vertebrate skeletogenic and odontogenic tissues. Biological reviews of the Cambridge Philosophical Society 65, 277-373.

Smith, S.H., Murray, R.G., Hall, M., 1994. The surface structure of *Leptotrichia buccalis*. Canadian journal of microbiology 40, 90-98.

Song, Y.S., Lee, H.J., Park, I.H., Lim, I.S., Ku, J.H., Kim, S.U., 2008. Human neural crest stem cells transplanted in rat penile corpus cavernosum to repair erectile dysfunction. BJU international 102, 220-224; discussion 224.

Steventon, B., Araya, C., Linker, C., Kuriyama, S., Mayor, R., 2009. Differential requirements of BMP and Wnt signalling during gastrulation and neurulation define two steps in neural crest induction. Development 136, 771-779.

Tachibana, M., 2000. MITF: a stream flowing for pigment cells. Pigment cell research / sponsored by the European Society for Pigment Cell Research and the International Pigment Cell Society 13, 230-240.

Takahashi, H., Parmely, T.J., Sato, S., Tomomori-Sato, C., Banks, C.A., Kong, S.E., Szutorisz, H., Swanson, S.K., Martin-Brown, S., Washburn, M.P., Florens, L., Seidel, C.W., Lin, C., Smith, E.R., Shilatifard, A., Conaway, R.C., Conaway, J.W., 2011. Human mediator subunit MED26 functions as a docking site for transcription elongation factors. Cell 146, 92-104.

Tassabehji, M., Newton, V.E., Read, A.P., 1994. Waardenburg syndrome type 2 caused by mutations in the human microphthalmia (MITF) gene. Nature genetics 8, 251-255.

Tassabehji, M., Read, A.P., Newton, V.E., Harris, R., Balling, R., Gruss, P., Strachan, T., 1992. Waardenburg's syndrome patients have mutations in the human homologue of the Pax-3 paired box gene. Nature 355, 635-636.

Thiery, J.P., Sleeman, J.P., 2006. Complex networks orchestrate epithelial-mesenchymal transitions. Nat Rev Mol Cell Biol 7, 131-142.

Thomas, A.J., Erickson, C.A., 2008. The making of a melanocyte: the specification of melanoblasts from the neural crest. Pigment cell & melanoma research 21, 598-610.

Thomas, A.J., Erickson, C.A., 2009. FOXD3 regulates the lineage switch between neural crest-derived glial cells and pigment cells by repressing MITF through a non-canonical mechanism. Development 136, 1849-1858.

Tomlinson, M.L., Field, R.A., Wheeler, G.N., 2005. *Xenopus* as a model organism in developmental chemical genetic screens. Molecular bioSystems 1, 223-228.

Tomlinson, M.L., Guan, P., Morris, R.J., Fidock, M.D., Rejzek, M., Garcia-Morales, C., Field, R.A., Wheeler, G.N., 2009. A Chemical Genomic Approach Identifies Matrix Metalloproteinases as Playing an Essential and Specific Role in *Xenopus* Melanophore Migration. Chemistry & Biology 16, 93-104.

Unsicker, K., 1993. The chromaffin cell: paradigm in cell, developmental and growth factor biology. Journal of anatomy 183 (Pt 2), 207-221.

Untergasser, A., Cutcutache, I., Koressaar, T., Ye, J., Faircloth, B.C., Remm, M., Rozen, S.G., 2012. Primer3 new capabilities and interfaces. Nucleic acids research 40, e115.

Uong, A., Zon, L.I., 2010. Melanocytes in development and cancer. Journal of cellular physiology 222, 38-41.

Vandesompele, J., De Preter, K., Pattyn, F., Poppe, B., Van Roy, N., De Paepe, A., Speleman, F., 2002. Accurate normalisation of real-time quantitative RT-PCR data by geometric averaging of multiple internal control genes. Genome Biol 3.

Wada, T., Takagi, T., Yamaguchi, Y., Ferdous, A., Imai, T., Hirose, S., Sugimoto, S., Yano, K., Hartzog, G.A., Winston, F., Buratowski, S., Handa, H., 1998. DSIF, a novel transcription elongation factor that regulates RNA polymerase II processivity, is composed of human Spt4 and Spt5 homologs. Genes & development 12, 343-356.

Wheeler, G.N., Brandli, A.W., 2009. Simple vertebrate models for chemical genetics and drug discovery screens: lessons from *zebrafish* and *Xenopus*. Developmental dynamics : an official publication of the American Association of Anatomists 238, 1287-1308.

White, R.M., Cech, J., Ratanasirintrawoot, S., Lin, C.Y., Rahl, P.B., Burke, C.J., Langdon, E., Tomlinson, M.L., Mosher, J., Kaufman, C., Chen, F., Long, H.K., Kramer, M., Datta, S., Neuberg, D., Granter, S., Young, R.A., Morrison, S., Wheeler, G.N., Zon, L.I., 2011. DHODH modulates transcriptional elongation in the neural crest and melanoma. Nature 471, 518-522.

Wolpert, L., Tickle, C., 2010. Principles of Development, 4th ed, Oxford University Press.

Wood, A., Schneider, J., Dover, J., Johnston, M., Shilatifard, A., 2003. The Paf1 complex is essential for histone monoubiquitination by the Rad6-Bre1 complex, which signals for histone methylation by COMPASS and Dot1p. The Journal of biological chemistry 278, 34739-34742.

Xue, Y., Yang, Z., Chen, R., Zhou, Q., 2010. A capping-independent function of MePCE in stabilizing 7SK snRNA and facilitating the assembly of 7SK snRNP. Nucleic acids research 38, 360-369.

Yamaguchi, Y., Takagi, T., Wada, T., Yano, K., Furuya, A., Sugimoto, S., Hasegawa, J., Handa, H., 1999. NELF, a multisubunit complex containing RD, cooperates with DSIF to repress RNA polymerase II elongation. Cell 97, 41-51.

Yik, J.H.N., Chen, R., Pezda, A.C., Zhou, Q., 2005. Compensatory Contributions of HEXIM1 and HEXIM2 in Maintaining the Balance of Active and Inactive Positive Transcription Elongation Factor b Complexes for Control of Transcription. Journal of Biological Chemistry 280, 16368-16376.

Yokoyama, A., Lin, M., Naresh, A., Kitabayashi, I., Cleary, M.L., 2010. A higher-order complex containing AF4 and ENL family proteins with P-TEFb facilitates oncogenic and physiologic MLL-dependent transcription. Cancer cell 17, 198-212.

Zhiyuan, Y., Qingwei, Z., Kunxin, L., Qiang, Z., 2001. The 7SK small nuclear RNA inhibits the CDK9/cyclin T1 kinase to control transcription. Nature 414, 317-322.

Zhou, Q., Li, T., Price, D.H., 2012. RNA polymerase II elongation control. Annual review of biochemistry 81, 119-143.

Zito, G., Richiusa, P., Bommarito, A., Carissimi, E., Russo, L., Coppola, A., Zerilli, M., Rodolico, V., Criscimanna, A., Amato, M., Pizzolanti, G., Galluzzo, A., Giordano, C., 2008. *In vitro* identification and characterisation of CD133(pos) cancer stem-like cells in anaplastic thyroid carcinoma cell lines. PloS one 3, e3544.

Zon, L.I., Peterson, R.T., 2005. *In vivo* drug discovery in the *zebrafish*. Nature reviews. Drug discovery 4, 35-44.

Zuber, J., Shi, J., Wang, E., Rappaport, A.R., Herrmann, H., Sison, E.A., Magoon, D., Qi, J., Blatt, K., Wunderlich, M., Taylor, M.J., Johns, C., Chicas, A., Mulloy, J.C., Kogan, S.C., Brown, P., Valent, P., Bradner, J.E., Lowe, S.W., Vakoc, C.R., 2011. RNAi screen identifies Brd4 as a therapeutic target in acute myeloid leukaemia. Nature 478, 524-528.